1,2,4-TRIAZINE BASED ENERGETIC MATERIALS AND IMPROVED NITRO-COMPOUND SYNTHESIS

by

Shannon E. Creegan

A Dissertation

Submitted to the Faculty of Purdue University

In Partial Fulfillment of the Requirements for the degree of

Doctor of Philosophy

School of Materials Engineering

West Lafayette, Indiana

May 2022

THE PURDUE UNIVERSITY GRADUATE SCHOOL

STATEMENT OF COMMITTEE APPROVAL

Dr. Davin G. Piercey, Chair

School of Materials Engineering

Dr. Steven Son

School of Mechanical Engineering

Dr. Jeffrey Youngblood

School of Materials Engineering

Dr. Paul G. Wenthold

Department of Chemistry

Approved by:

Dr. David Bahr

This paper is dedicated to my family.

Most especially to my parents who encouraged me along this path while tolerating many space and time consuming projects for the sake of letting my curiosity bloom.

Special thanks to my grandparents who told me to aim high and supported my endeavors even after passing on.

ACKNOWLEDGMENTS

I want to thank my advisor, Dr. Davin Piercey, for the immense amount of support and encouragement he provided throughout this process in addition to his research related guidance. Also want to thank him for his patience, positivity, and sense of humor; you made it enjoyable to work even when the materials refused to.

Full appreciation is given to the members of Piercey's Research group, past and present, for their persisting enthusiasm and numerous discussions (even the odd ones). Additional thanks to my undergraduates for their help in maintaining the precursor supply.

Special thanks are given to Dr. Matthias Zeller, for countless crystal structure measurements and analyses, and to Dr. Edward F. C. Byrd, for his wizardry with Gaussion09 in the generation computational values.

I acknowledge the Office of Naval Research for financial support of my projects under grant N00014-19-1-2089, the National Science Foundation for the single crystal X-ray diffractometer through the Major Research Instrumentation Program under Grant No. CHE 1625543, and Purdue University and The Army Research Office (ARO) for support of the research lab.

The chapters in this dissertation are reproduced from the journals in which the work was originally published. Licenses have been obtained where required by the journal. In the case of articles under review the most recent draft is used. Listed below are the sources for published articles and the intended publication locations for those in submission.

1. "Nitroacetonitrile as a versatile precursor in energetic materials synthesis" was reprinted with permission from **S. E. Creegan** and D. G. Piercey, *RSC Adv.*, **2020**, 1, 39478. Copyright 2020 Royal Society of Chemistry.

2. "Synthesis and Characterization of the Energetic 3-Azido-5-amino-6-nitro-1,2,4-triazine" was reprinted with permission from **S. E. Creegan**, M. Zeller, E. F. C. Byrd, D. G. Piercey, *Prop., Explos., Pyrotech.* **2021**, 46, 214. License number 5235430668195. Copyright 2021 John Wiley and Sons.

3. “Energetic 1,2,4-Triazines: 3,5-Diamino-6-nitro-1,2,4-triazine and Its Oxide” was reprinted with permission from **S. E. Creegan**, M. Zeller, E. F. C. Byrd, D. G. Piercey, *Cryst. Growth Des.*, **2021**, 21, 7, 3922. Copyright 2021 American Chemical Society.

4. “Energetic Triazinium Salts from *N*-amination of 3,5-diamino-6-nitro-1,2,4-triazine” was reprinted with permission from **S. E. Creegan**, M. Zeller, E. F. C. Byrd, D. G. Piercey. Submitted for publication to *Energetic Materials Frontiers*, **2022**. Copyright 2022 KeAi Publishing.

5. “Titanium Superoxide for the Oxidation of Amines: Synthesis of bis(3-nitro-1H-1,2,4-triazol-5-yl)methane and its Metal Salts” was reprinted with permission from **S. E. Creegan**, M. Zeller, E. F. C. Byrd, D. G. Piercey, *Z. Anorg. Allg. Chem.*, **2022**, e202200007. Copyright 2022 John Wiley and Sons.

TABLE OF CONTENTS

LIST OF TABLES

LIST OF FIGURES

LIST OF SCHEMES

ABSTRACT

The following document is a compilation of four manuscripts which were peer-reviewed and accepted for publication in the following scientific journals: *Propellants, Explosives, Pyrotechniques*, *Crystal Growth & Design*, *Zeitschrift für Anorganische und Allgemeine Chemie ZAAC*, and *Energetic Materials Frontiers*. This work, also, includes excerpts from the author's review of energetic materials synthesized via reactions with nitroacetonitrile published by *RSC Advances*. The research presented is the result of a four-year graduate program in the School of Materials Engineering and as part of the Purdue Energetics Research Center (PERC).

1,2,4-Triazine Based Energetic Materials and Improved Nitro-Compound Synthesis briefly addresses the history of energetic materials, key requirements, and ways to modify materials to meet those requirements before transitioning to the research synthesis and characterization. The discussion sections address the synthesis methods of the heterocyclic 1,2,4-triazine structure and alternative routes for the formation of nitro moieties. Also discussed are the methods for chemical characterization, thermal stability, mechanical sensitivity, and the theoretical calculations used to obtain energetic performances for comparison with traditional known explosive materials.

1. INTRODUCTION

1.1 Energetic Materials Background

1.1.1 A Brief History

The dawn of explosives has been attributed to the accidental creation of blackpowder, a low explosive, by the Chinese during the 9th century. Records indicate blackpowder was used for both fireworks and weapons by the Chinese, Arabs, Greeks, and Romans; though it is unclear if these latter groups invented their own version or obtained access through trade. Around the 13th century, blackpowder was developed by Roger Bacon a European monk [1-3]. The next step in explosive development was the creation of the first high explosive, fulminating gold, later in the 16th century. The brisance of high explosives expanded the understanding of what explosives could do and the number of applications.

Modern explosives begins with nitrocellulose (NC), created in 1846 by Schönbein and Böttger (independent of each other), and nitroglycerine (NG), invented by Ascanio Sobrero in 1847 [2]. Alfred B. Nobel used NG as a base for Dynamite which saw widespread use in the civilian sector [1]. Dynamite was not widely used for military purposes due to its slow leakage of NG, though the alternative picric acid was not much of an improvement, causing corrosion of shells and forming even more sensitive metal salts [1-2]. The World Wars saw the development of trinitrotoluene (TNT), pentaerythritol tetranitrate (PETN), and cyclotrimethylenetrinitramine (RDX).

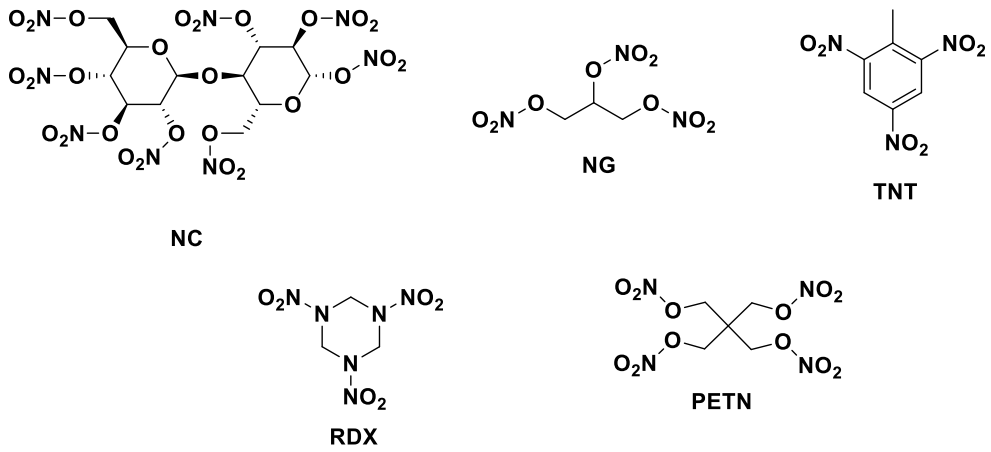

Figure 1. Structures of NC, NG, TNT, PETN, and RDX

Today, energetic materials are used in a multitude of fields from munition to earthworks, space exploration to deep well drilling. Though marked for their destructive prowess these materials have many benefits which should not be overlooked. The development of energetic materials has a immense impact on economy and the chemistry behind them can be found in many treatises [4].

1.1.2 Terminology and Considerations

Terminology

The word 'explosion' refers to the sudden release of energy usually accompanied by a blast wave, propelled debris, or the emission of thermal or ionizing radiation [1]. There are three classes of explosions, physical, atomic, and chemical. Physical explosions occur when compressed substances undergo rapid physical transformations causing the conversion of potential to kinetic energy and an increase in temperature [1]. Atomic explosions are the rapid release of energy from nuclear reactions and produce shockwaves similar to those of chemical explosions, which are caused by sudden rapid reactions or transformation of states [1]. Chemical explosions usually generate heat and exert pressure [5] while releasing energy and gas [1, 6]. Materials capable of generating chemical explosions fall under the term energetic materials, broadly defined as materials possessing high amounts of stored chemical energy [6] which, upon initiation, undergo rapid chemical reactions. Energetic materials can be subdivided, by use, into the categories of propellants, pyrotechnics, and explosives; the primary focus of this dissertation being explosives.

Two classification systems are applied to explosives, the first high/low, is based on a material's performance, and the second, primary/secondary/tertiary is based on sensitivity and can be applied either independently or after the first system [5]. It is noted that these classifications can be applied differently depending on interpretation and intent, commonly high and secondary explosives are taken as equivalent and low explosives the same as propellants. Differentiation between high and low explosives is decided, roughly, by the detonation velocity and propagation mechanism with substantial consideration regarding overall performance [3]. Whereas low explosives mainly undergo deflagration and might explode under confinement, high explosives do not need to be confined and undergo detonation.

Deflagration is a self-propagating surface phenomenon the rate of which increases under confinement [1]. During deflagration the rate of flame propagation through the material is less than the speed of sound and is accompanied by an audible hissing or crackling [1, 3]. Detonation, on the reverse side, proceeds faster than the speed of sound, propagating through the material at supersonic speeds. This event is accompanied by a sharp crack and can be initiated by a deflagration-to-detonation (DDT) or shock-to-detonation transition (SDT). DDT occurs only under confinement conditions, conceivably due to the increase of the burning rate index above unity, which is characteristic of detonating materials [1]. SDT is a straightforward chain of cause and effect. The application of a shockwave compresses particles which, through adiabatic heating, raises the temperature higher than that of decomposition. Leading to exothermic decomposition which, in turn, accelerates the shockwave.

Though primary and secondary explosives are both high explosives, there are distinct differences between the two. Summarized in Table 1 are some common examples of primary and secondary explosives with their respective sensitivities and performances. Primary explosives are readily initiated by a variety of conditions (e.g. heat, static, impact, etc.), will explode without confinement, and can undergo both DDT and SDT easily and on small scale [1]. The general trend for sensitivity in a primary material is friction and impact sensitivities less than 5 N and 5 J, respectively. Secondaries are less sensitive than primaries and require initiators to trigger a SDT within the material. Usually, secondaries have more explosive power than primaries; however, there are exceptions to every trend as seen with the primary K_2DNABT and TNT.

Table 1. Thermal stability, mechanical sensitivity, and detonation parameters of common primary and secondary explosives

	Primary				Secondary			
Explosive	Lead azide[7]	Tetrazene[8]	K_2DNABT[9]	DBX-1[10]	TNT[8]	RDX[11-13]	HMX[14]	PETN[15-16]
Formula	$Pb(N_3)_2$	$C_2H_6N_{10}•H_2O$	$C_2N_{12}O_4K_2$	$C_2Cu_2N_{10}O_4$	$C_7H_5N_3O_6$	$C_3H_6N_6O_6$	$C_4H_8N_8O_8$	$C_5H_8N_4O_{12}$
T_{dec} (K)	315	160	200	302	300	205	265	165
IS (J)	< 5	1	1	< 1	15	7.5	6.1	< 5
FS (N)	< 1	< 5	< 1	< 1	353	120	150	60
P_{CJ} (GPa)	33.8	11.0	31.7	36.7	22.0	33.6	39.0	30.8
$V_{det.}$ ($m\ s^{-1}$)	5920	5900	8330	6734	7300	8801	9110	8429

Research Consideration

Modern energetic materials need to meet heightened requirements for performance, sensitivity, environmental safety, and economic feasibility to be considered for practical use. These requirements can potentially restrict the use of energetics containing heavy metals, nitramines, and aromatic nitro compounds [8]; also under restriction, are compounds with complex multi-step syntheses. Fundamentally, the goal of energetic materials research is to develop high energy systems that are stable, insensitive, and whose final product and subsequent byproducts are environmentally friendly.

Development relies heavily on the judicious selection of synthetic processes and knowledge of applicable building blocks. Energy content within a compound can be imparted by balancing the fuel to oxidizer ratio, inducing ring or cage strain, or invoking a high heat of formation [3, 5, 8]. The inclusion of fuel and oxidizer, within the same compound, ideally allows for the complete oxidation of carbon and hydrogen atoms into CO, CO_2, and H_2O upon detonating, resulting in increased energy. Termed as oxygen balance, it is defined as the ratio of contained oxygen to the amount of total oxygen required for complete oxidation leading to the identification of materials as oxygen rich or deficient [5]. Similarly, a system with a high ring or cage strain will release more energy upon initiation due to the inherent energy these systems contain [17-18]. A consideration not previously listed is the effect of density on energetic performance. Compounds exhibiting larger densities have higher detonation velocities and pressures. Density can be increased by improving molecule planarity and expanding the opportunities for intermolecular bonding. Additional benefits can be gained as increased planarity lessens sensitivity and greater bonding correlates to increased stability [19] .

These conditions lean heavily towards the use of nitrogen-rich heterocyclic backbones, such as, triazoles [11, 20-25], tetrazoles [20, 26-31], triazines [11-12, 14, 32-33], and tetrazines [32, 34-42]. The inclusion of nitrogen is favored due to the lower toxicity of many nitrogen-rich compounds, high stability, and high heats of formation [8] as compared to their metal counterparts. The limitations to utilizing the afore mentioned methods can be circumvented by the creative balancing act of inherent backbone characteristics and applied characteristics from tailored functional groups or salts.

1.2 Investigated Materials Background

1.2.1 1,2,4-Triazines Formation

Arguably some of the most important heterocyclic systems are annulated. Annulated systems often possess higher thermal stabilities, lower sensitivities, and higher densities than the related non-annulated materials [17, 43-44]; examples of this would be annulated 1,2,9,10-tetranitrodipyrazolo[1,5-d:5′,1′-f][1,2,3,4]tetrazine from 4,4′,5,5′-tetranitro-2H,2′H-3,3′-bipyrazole [45] and ,9-dinitro-bis[1,2,4]triazolo[1,5-d:50,10-f][1,2,3,4]tetrazine from 5,5’-dinitro-2H,2’H-3,3’-bi(1,2,4-tri-azole)-2,2’-diamine [46]. However, the syntheses of many annulated heterocyclic systems are complex and consist of many steps rendering them impractical due to expense; examples of this are 2,9-dinitro-bis[1,2,4]triazolo[1,5-*d*:50,10-*f*][1,2,3,4]tetrazine (Scheme 1) [17, 42, 47] and 2,4,8,10-tetranitrobenzo [4′,5′][1,2,3]triazolo[2′,1′:2,3][1,2,3]triazolo[4,5-b]pyridin-6-ium-5-ide (TACOT) (Scheme 2) [48]. As a result, research into simple routes for complex systems has become a necessity.

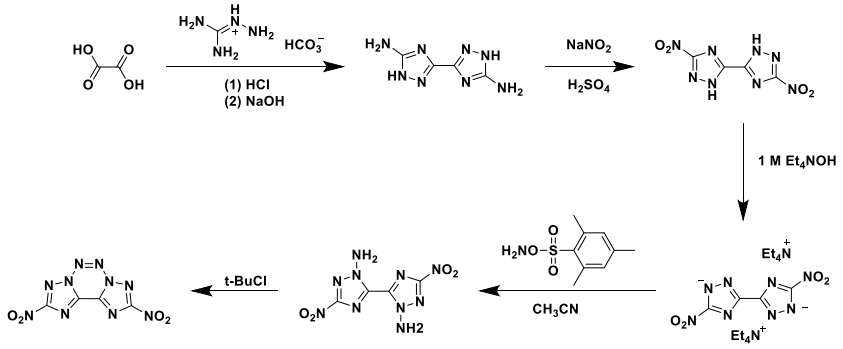

Scheme 1. Synthesis of 2,9-dinitro-bis[1,2,4]triazolo[1,5-d:50,10-f][1,2,3,4]tetrazine

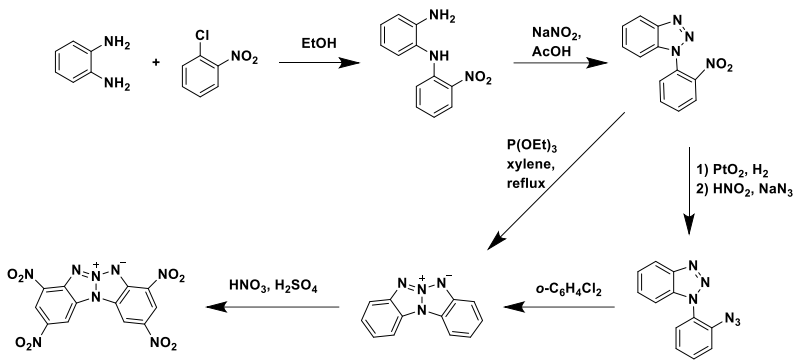

Scheme 2. Synthesis of 2,4,8,10-tetranitrobenzo [4′,5′][1,2,3]triazolo[2′,1′:2,3][1,2,3]triazolo[4,5-b]pyridin-6-ium-5-ide (TACOT)

Reactions utilizing the α-nitronitrile, nitroacetonitrile, possessing two strong electronegative electron-withdrawing groups are simple and straightforward [44]. Traditionally, nitroacetonitrile is utilized as a versatile synthetic precursor in the formation of heterocyclic and polyfunctional aliphatic products [49]. While neutral nitroacetonitrile has drawbacks, including synthesis via low-yield low-purity routes, and chemical instability including the chance of spontaneous explosion [50], stable salts of nitroacetonitrile, such as the potassium salt, can be easily prepared via an indirect route and do not pose a lab hazard [51-52]. Typically nitroacetonitrile based energetic material synthesis proceeds by reacting diazonium salts with nitroacetonitrile, or salt thereof, to produce the nitrocyanohydrazone which can then be cyclized through the nitrile giving a 1,2,4-triazine with vicinal amino and nitro groups. [44] These viscinal groups can stabilize via intra- and intermolecular hydrogen bonding [11, 53] as well as lead to conjugation resulting in a planar structure with π-π stacking interactions serving to increase thermal stability and lessen mechanical sensitivity [44]. Energetic 1,2,4-triazines made via nitroacetonitrile reactions include **7**-amino-2,3,6-trinitropyrazolo[5,1-c][1,2,4]triazine (PTX) [14, 54], 3,8-dinitropyrazolo[5,1-*c*][1,2,4]triazine-4,7-diamine (DNPTDA) [53], 4-amino-3,7-dinitrotriazolo-[5,1-c][1,2,4] triazine (DPX-26) [11], and 4-amino-3-nitro-7-cyanotriazolo-[5,1-c][1,2,4] triazine (ANCTT) [55] (Figure 1).

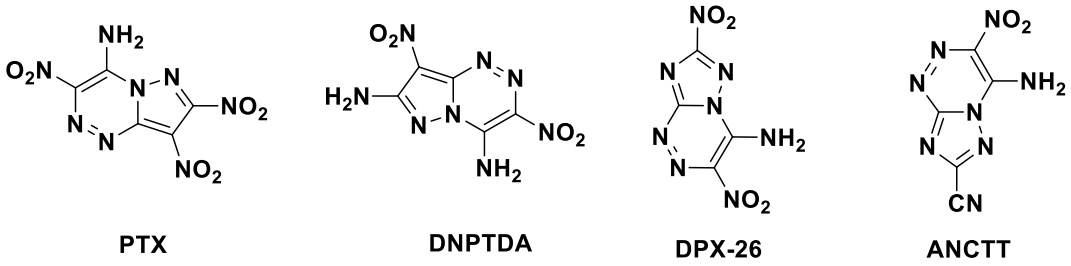

Figure 2. 1,2,4-triazines synthesized by reaction with nitroacetonitrile

1.2.2 Backbone Characteristic Modification

Two ways to modify the characteristics of an energetic backbone structure are functional group modification and salt formation. The purpose behind most modifications is to improve performance while maintaining, or improving, the material's stability and resistance to stimuli. Commonly, the first change is increasing the molecule's oxygen content by attaching an oxygen containing functional group (i.e. a nitro or oxide) or ion (i.e. nitrate or perchlorate). Nitro group addition can be done a multitude of ways, though usually done via nitration or oxidation using mixed acids, a modified Sandmeyer reaction, or oxidation (Refer to Chap. 4). Oxides, usually as *N*-oxide, can be formed through oxidation with reagents such as HOF and Oxone®. Introducing additional oxygen serves to increase the amount of energy released upon detonation by acting as an oxidizer, reacting with carbon and hydrogen, driving the formation of detonation products. The oxide and nitro groups are expected to stabilize through inter- and intramolecular bonding, though the result is not guaranteed (Refer Chap. 3).

Beyond increasing oxygen content, higher performing energetics can be made by combining ions that are of themselves energetic with charged backbones. The same principle applies for improving thermal stability and lessening sensitivity. As the majority of charged energetic material are anionic, they are commonly paired with nitrogen rich cations such as ammonium, hydroxylammonium, and hydrazinium. Metal ions are another common component of energetic salts (e.g. lead styphnate). Their presence, while usually increasing sensitivity, can be used to impart the distinct colors favored in pyrotechnics (e.g. flares).

1.3 Material Characterization

1.3.1 Chemical and Structural

Chemical characterization is necessary for the accurate confirmation of synthesis success, determination of molecular structure, and material purity. Each technique provides distinct data corresponding to molecular details which are combined to form a complete and accurate description of the resulting material. Crystallographic analysis of formed crystal structures definitively confirms molecular structure and provides insight to the interaction between molecules.

Spectroscopy & Elemental Analysis

Electrospray ionization mass spectroscopy is used to monitor reaction progress as well as confirm the formation of the targeted molecule and provide a rough indication of product purity. Low-resolution spectra were obtained using an Agilent 1260 Infinity II Quaternary LC instrument and high-resolution spectra with a Thermo Fisher Scientific LTQ Orbitrap. A sampling of the reaction mixture, or resulting solid, is dissolved in an inert carrier solution and ionized before passing through a mass analyzer and arriving at the instruments detector. The generated spectra display the relative intensity of at each mass/charge (m/z) ratio. These values of m/z correspond the mass of the charged material ions, commonly observed as the material mass plus one, [M+H], or the mass minus one, [M-H]. Exceptions to this are previously charged materials such as oxides or *N*-amines which display at their mass. The m/z is also affected by adducts which can adhere the material changing the related m/z by the mass of the adduct (e.g. $[M+NH_4]$ and [2M+H]).

Subsequent to confirming the presence of the targeted compound and obtaining a rough estimate on material purity by mass spectrometry, ^{1}H and ^{13}C NMR spectra are obtained via the Bruker AV-III-500-HD and Bruker Avance-III-800 (5mm QCI Z-gradient cryoprobe) nuclear magnetic resonance (NMR) spectrometers. This process involves dissolving a sampling of the material in non-reactive deuterated solvent and placing it in the instrument which proceeds to apply a magnetic field that resonates with the carbon or hydrogen isotope. This resonance results in a transference of energy with the final result of the process being a measurable signal that is converted into a spectrum of peaks which correlate to each distinct atom in the material sample. Determination of sample purity is done by correlating the number of atoms and peak values to

what is expected for the material. While capable of verifying the presence of additional hydrogen or carbon atoms, NMR is limited in the differentiation of salts as it does not indicate the presence of metals or ion groups such as perchlorates.

Elemental analysis can be used to determine which salt is present and acts as a good indicator for material purity. This technique can also be used to identify the number of hydrate units contained within a material. The Elementar vario EL cube elemental analyzer determines elemental percent by comparison with the known reference sample, acetanilide. The experimentally determined percentages of carbon, nitrogen, and hydrogen content are compared to the theoretical values generated from the material's molecular formula.

Once compound composition and purity completely defined, infrared spectroscopy (IR) is run to obtain further information on bond structure, utilizing a PerkinElmer Spectrum Two spectrometer with UATR (Universal Attenuated Total Reflectance) accessory. As IR radiation passes through the material it initiates excitation vibrations in the bonding structure. The absorbance at a given wavenumber is reported and categorized as weak, medium, or strong. Specific bond types can be determined by comparing correlated peak strength and wavenumbers with those listed in reference materials. While aspects of a material's structure can be determined using the methods discussed, when possible, the structure was confirmed by crystallography.

Crystal

Single-crystal X-ray crystallography was used, when applicable, to analyze crystal structure and obtain room temperature densities of the materials. These analyses were performed and compiled by Dr. Matthias Zeller. Complete crystallographic data, in CIF format, have been deposited with the Cambridge Crystallographic Data Centre. CCDC 2004613 – 2004612, 2057283 – 2057287, 2132933 – 2132935, and 2157067 – 2157073 contain the supplementary crystallographic data for this paper. These data can be obtained free of charge from The Cambridge Crystallographic Data Centre via www.ccdc.cam.ac.uk/data_request/cif.

1.3.2 Computational

The research addressed in this dissertation utilized the computational software packages EXPLO5v6.05 and Gaussian09. All Gaussian09 calculations were performed by Dr. Edward F. C.

Byrd and the results of which were used in the running of EXPLO5v6.05 The following paragraphs are the combined computational sections of the published articles complied for this document [56-59].

For neutral molecules, the enthalpies of formation and densities were calculated using the Byrd and Rice method [60-62]. The molecular geometries were optimized using the B3LYP spin-restricted Kohn-Sham density functional theory (KS-DFT) [63-66] with the 6-31G** Pople Gaussian basis set [67-69], using the Gaussian09 program package [70]. Computational densities were obtained by dividing the mass of the molecule by the volume calculated from the volume contained within the B3LYP/6-31G** 0.001 electron/bohr^3 isosurface of the electron density, and subsequently modified by electrostatic parameters generated from charge distributions of said isosurface. For the prediction of the heat of formation, the B3LYP/6-311++G(2df,2p) energy was computed from the B3LYP/6-31G* optimized geometry to obtain the gas phase heat of formation. Heat of sublimation was calculated from the molecular surface area (determined from the volume contained within the 0.001 electron/bohr^3 isosurface of the electron density) and pertinent electrostatic parameters.

For energetic salts, the heat of formation method for computing ionic species [60] of Byrd and Rice was used in addition to the method for computing the densities [61-62] for all ionic compounds. The Gaussian09 program package [70] and the B3LYP spin-restricted Kohn−Sham density functional theory (KS-DFT) [63-66] with the 6-31G** Pople Gaussian basis sets [67-69] were used to predict gas phase geometries of each compound. Subsequently, the G3MP2-(B3LYP) [71] electronic energy was determined, a requirement to compute the ionic heat of formation. The Gutowski method [72] provided the lattice energy as determined from the molecular volume of each compound.

The detonation parameters, at the CJ point, were calculated with the EXPLO5v6.05 software package [73-74] using the computational heat of formation and the materials' density at room temperature measured by single-crystal X-ray diffraction. For solid carbon the software uses the Becker-Kistiakowsky-Wilson's equation of state (CFEOS) [75]. The equilibrium composition of detonation products was calculated utilizing the modified White, Johnson, and Dantzig's free energy minimization technique. BKWN parameters (α, β, κ, θ) were used in the following BKW equation, with X_i representing the mol fraction of the i^{th} gaseous product and k_i being the molar co-volume of said i^{th} gaseous product: [74, 76-78]

$$\frac{pV}{RT} = 1 + \ xe^{\beta x}\ x = \frac{(\kappa\ \Sigma\ \mathrm{X}_i k_i)}{[\ V\ (T + \ \theta\ )]^{a}}$$

$\alpha = 0.5$, $\beta = 0.38$, $\kappa = 9.41$, $\theta = 4250$

1.3.3 Thermal Stability and Mechanical Sensitivity Determinations

Determining the thermal stability and mechanical sensitivity of an energetic materials is key in categorizing them in terms of safety and potential for future use. The widespread use of energetic materials in a diverse array of environments requires an inherently high thermal stability as the materials may need to be stored or used at elevated temperatures. The materials sensitivity limit toward mechanical stimuli is key to preventing accident during synthesis, transport, and use. Energetic materials which are thermally stable and insensitive are less hazardous and therefore more viable for use.

Thermal Stability

The thermal stability of energetic materials is commonly determined via thermogravimetric analysis (TGA) or differential scanning calorimetry (DSC). These techniques require 1 to 2 milligrams of dried material, which is obtained by prolonged storage in a sealed desiccator with Drierite™. The dried samples are measured into platinum pans and loaded into the instrument where the sample is then heated at a rate of 5 °C min^{-1} until reaching 500 °C. The resulting data curve displays changes in relative weight percent over the temperature gradient upon which both hydrate loss (if occurring) and material decomposition can be observed. The overall change in weight percent during the period of hydrate loss can be used to calculate the initial amount of hydrate units and the number lost. Material decomposition may occur either rapidly, as an instantaneous loss of mass, or gradually; as such, the onset of decomposition temperature is determined at the temperature at which 5 % weight loss occurs after the loss of hydration units.

Mechanical Sensitivity

Mechanical sensitivity is defined by the materials sensitivity to impact and friction. These tests are done in accordance with the NATO standardization standards respectively, STANAG 4489 [79] and 4487 [80], modified under instruction [81-82]. Impact sensitivity is performed using

a drop/fallhammer (Figure3) which drops a weight of known mass (*m*) from a specific height (*h*) allowing for the conversion to equivalent Joules using the gravitational potential energy equation $E=mgh$ where *g* is the gravitational constant. A portion of sample, approximately 3-5 μm^3, is placed between two steel cylinders in a steel ring (Figure4) upon which the weight is dropped. The material is then determined to have either a positive or negative response as indicated audibly by snap, bang, or crack or visually by the presence of smoke or a change in coloration.

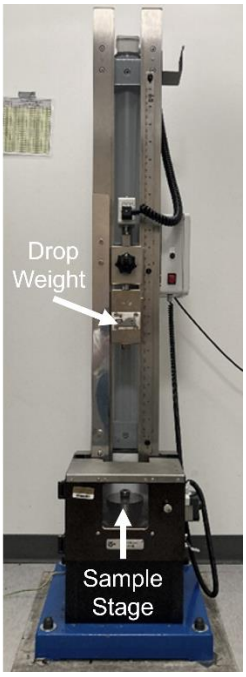

Figure 3. Drophammer for impact testing.

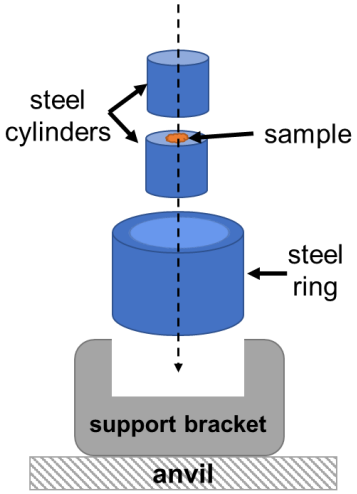

Figure 4. Drophammer sample holder diagram.

Tests for friction sensitivity are done on a friction test apparatus (Figure5) by moving a porcelain peg across a porcelain plate with the sample in between the two surfaces (Fig 6). A known amount of force (Newtons) is consistently applied to the peg as it moves across the plate perpendicular to the gradient. The amount of force applied is varied by the placement of calibrated weights at one of six specified locations along a metal rod. A chart supplied by the instrument manufacturer converts weight and position to applied force (N).

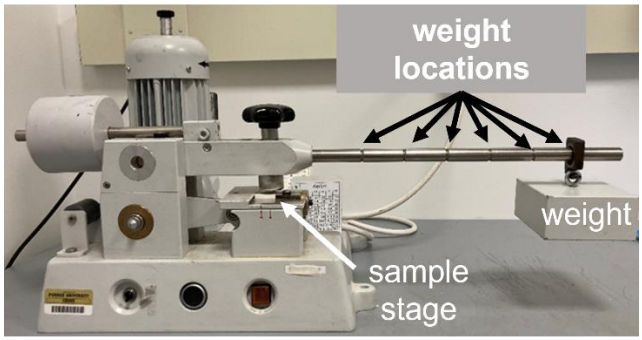

Figure 5. Friction tester.

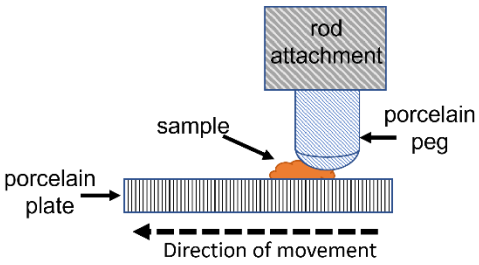

Figure 6. Sample and peg placement diagram.

Each method of sensitivity determination is performed on a 1-of-6 basis (BAM method), with tests being repeated at higher sensitivity values until only 1 out of 6 tests performed at a given value are positive. It is common for materials to possess sensitivities within in a range as defined by the sensitivity values at which 2-of-6 and 0-of-6 yield positive results. Once the values of sensitivity have been determined, sensitivity categorization of the materials is done by applying the UN recommendations of the transport of dangerous goods:

> "Impact: Insensitive > 40 J, Less Sensitive ≥ 35 J, Sensitive ≥ 4 J, Very Sensitive ≤ 3 J; Friction: Insensitive > 360 N, Less Sensitive = 360 N, Sensitive < 360 N and > 80 N, Very Sensitive ≤ 80 N, Extremely Sensitive ≤ 10 N." [83]

1.4 Chapter Previews

1.4.1 Energetic 1,2,4-Triazine

High-nitrogen heterocycles, possessing both inherently high heats of formation and ring strain, have a greater store of potential energy. The simple synthesis of the 1,2,4-triazine, presented in this document, is valuable to the development of industrially feasible energetic material. The 1,2,4-triazine backbone can be further modified for improved performance, stability, and sensitivity by alteration of attached functional groups and the strategic addition of ions in the formation of an energetic salt.

Chapter 2: Synthesis and Characterization of the Energetic 3-Azido-5-amino-6-nitro-1,2,4-triazine [56]

This chapter addresses the synthesis and energetic characterization of 3-Azido-5-amino-6-nitro-1,2,4-triazine (AANT) and a competing monohydrate hydrolysis product (**1**●H_2O) from diazotetrazole and the potassium salt of nitroacetonitrile. While AANT was previously synthesized via reaction with unstable nitroacetonitrile, converted to its sodium salt in situ, this work characterized it as an energetic material for the first time. The *N*-oxide of AANT was also synthesized by oxidation of AANT with hypofluorous acid. This material proved highly unstable, returning to the parent compound under acidic conditions and decomposing in the presence of water and drying agents. The simple synthesis of a heterocyclic system is valuable to the development of industrially feasible energetic materials.

Chapter 3: DANT & DANTX [57]

The first functional group modification to the synthesized AANT was the reduction of the azide via a modified Staudinger reaction with triphenylphosphine yielding 3,5-diamino-6-nitro-1,2,4-triazine (DANT). This reaction was easily tracked by mass spectrometry through the formation of the iminophosphorane to triphenylphosphine oxide and DANT. Oxidation of DANT to DANTX, was achieved using portions of potassium peroxymonosulfate, as its $2KHSO_5 \cdot KHSO_4 \cdot K_2SO_4$, triple salt (Oxone®). DANTX crystallized as two distinct polymorphs with different packing structures and densities. The different bonding structures were examined using Hirshfeld surfaces and the subsequently generated fingerprint plots.

Chapter 3: TANT+ & Energetic Salts[59]

The improved stability DANT displayed made it promising as a parent compound for energetic salt synthesis. Formation of an *N*-amine through amination with *O*-tosylhydroxylamine (THA) converted the neutral DANT to the charged cation 2,3,5-triamino-6-nitro-1,2,4-triazin-2-ium (TANT). By mixing the TANT toslyate salt with diammonium 5,5´-bis(tetrazole-1-oxide) in hot water the first energetic salt, di(2,3,5-triamino-6-nitro-1,2,4-triazin-2-ium) 5,5´-bis(tetrazole-1-oxide) (BTO), of this series was obtained as a dihydrate. For further salt synthesis, the initial tosylate anion was readily converted to a chloride anion via ion exchange resin. Metathesis

reactions with the TANT chloride salt was used to synthesize nitrate, perchlorate, and 5-nitrotetrazolate salts producing silver chloride as a byproduct. A second synthesis route for the BTO salt was obtained through the reaction of the TANT nitrate salt with the disodium salt of BTO. This second synthesis was needed due to the large amount of decomposition contamination present in the first as a result of heating the solution. All the TANT salts, excluding the tosylate, decomposed when in solution and air for a prolonged period, a process which was accelerated by heat; as such, rapid removal of the solvent in vacuum was necessary.

1.4.2 Improved nitro formation

Once an appropriate backbone has been developed, focus shifts to adjusting performance and sensitivity through the presence of choice explosophores. The most basic modification is the addition of a nitro group which can serve as a source of energy through the addition of oxygen and in stability through increased bonding. Bearing in mind the downsides of traditional nitration methods, such as large amounts of acidic waste and complex competing pathways, oxidation via metal-superoxides presents a predictable simple solution.

Chapter 4: Titanium Superoxide for the Oxidation of Amines: Synthesis of bis(3-nitro-1H-1,2,4-triazol-5-yl)methane and its Metal Salts [58]

In this chapter, the material bis(3-nitro-1H-1,2,4-triazol-5-yl)methane (BNTM) was synthesized from bis(3-amino-1H-1,2,4-triazol-5-yl)methane (BATM) with two different reaction methods. The first method used the traditional nitration route of a modified Sandmeyer reaction while the second oxidized the amines with superoxide generated on a hydrated titanium matrix. The modified Sandmeyer method was previously used to synthesize the compound [84-85] and the material was fully characterized as an energetic by me providing the information necessary for a complete comparison of methods. Both methods produced the target compound in same yield as confirmed by NMR and single-crystal X-ray crystallography. Attempts were made to convert the material into an energetic salt, however the material remained in its neutral state with the cyclic nitrogen remaining protonated. Being of good stability and sensitivity for a pyrotechnic, metal salts were made and burn images of the resulting-colored flames collected.

1.5 References

[1] Akhavan, J. *The Chemistry of Explosives*. The Royal Society of Chemistry. **2011**. ISBN 978-1-84973-330-4.

[2] Agrawal, J.P. *Status of Explosives, In High Energy Materials*, J.P. Agrawal (Ed.). **2010**. https://doi.org/10.1002/9783527628803.ch2.

[3] Klapötke, T. M. *Chemistry of High-Energy Materials*, Berlin, Boston: De Gruyter, 2017. https://doi.org/10.1515/9783110536515.

[4] Agrawal, J.P. *Salient Features of Explosives, In High Energy Materials*, J.P. Agrawal (Ed.). **2010**. https://doi.org/10.1002/9783527628803.ch1.

[5] Agrawal, J.P. and Hodgson, R.D. *Front Matter, In Organic Chemistry of Explosives* (eds J.P. Agrawal and R.D. Hodgson). **2006**. https://doi.org/10.1002/9780470059364.fmatter.

[6] S. Todd, in *Energetic Materials Fundamentals and Applications Course of Instruction*, Perth, Australia, **2020**.

[7] Q. N. Tariq, S. Manzoor, M.-u.-N. Tariq, W.-L. Cao, J.-G. Zhang, Recent advances in the synthesis and energetic properties of potassium-based potential green primary explosives *Defence Technology* **2021**.https://doi.org/10.1016/j.dt.2021.11.003

[8] D. Piercey, *Advanced Energetic Materials: Strategies and Compounds, Doctoral Thesis*, Ludwig-Maximilians-University of Munich, Munich, Germany, **2012**.

[9] D. Fischer, T. M. Klapötke, J. Stierstorfer, Potassium 1,1′-Dinitramino-5,5′-bistetrazolate: A Primary Explosive with Fast Detonation and High Initiation Power *Angewandte Chemie International Edition* **2014**, *53*, 8172-8175.https://doi.org/10.1002/anie.201404790

[10] J. W. Fronabarger, M. D. Williams, W. B. Sanborn, J. G. Bragg, D. A. Parrish, M. Bichay, DBX-1 – A Lead Free Replacement for Lead Azide *Propellants, Explosives, Pyrotechnics* **2011**, *36*, 541-550.https://doi.org/10.1002/prep.201100056

[11] D. G. Piercey, D. E. Chavez, B. L. Scott, G. H. Imler, D. A. Parrish, An Energetic Triazolo-1,2,4-Triazine and its N-Oxide *Angewandte Chemie International Edition* **2016**, *55*, 15315-15318.10.1002/anie.201608723

[12] D. Kumar, G. H. Imler, D. A. Parrish, J. M. Shreeve, A Highly Stable and Insensitive Fused Triazolo–Triazine Explosive (TTX) *Chemistry – A European Journal* **2017**, *23*, 1743-1747.doi:10.1002/chem.201604919

[13] M. A. Kettner, T. M. Klapötke, in *Chemical Rocket Propulsion: A Comprehensive Survey of Energetic Materials* (Eds.: L. T. De Luca, T. Shimada, V. P. Sinditskii, M. Calabro), Springer International Publishing, Cham, **2017**, pp. 63-88.

[14] M. C. Schulze, B. L. Scott, D. E. Chavez, A high density pyrazolo-triazine explosive (PTX) *Journal of Materials Chemistry A* **2015**, *3*, 17963-17965.10.1039/C5TA05291B

[15] T. W. Myers, C. J. Snyder, D. E. Chavez, R. J. Scharff, J. M. Veauthier, Synthesis and Electrochemical Behavior of Electron-Rich s-Tetrazine and Triazolo-tetrazine Nitrate Esters *Chemistry – A European Journal* **2016**, *22*, 10590-10596.10.1002/chem.201601422

[16] Virginia W. Manner, M. J. Cawkwell, E. M. Kober, T. W. Myers, G. W. Brown, H. Tian, C. J. Snyder, R. Perriot, D. N. Preston, Examining the chemical and structural properties that influence the sensitivity of energetic nitrate esters *Chemical Science* **2018**, *9*, 3649-3663.10.1039/C8SC00903A

[17] H. Gao, Q. Zhang, J. M. Shreeve, Fused heterocycle-based energetic materials (2012–2019) *Journal of Materials Chemistry A* **2020**, *8*, 4193-4216.10.1039/C9TA12704F

[18] T. M. Klapotke, D. G. Piercey, J. r. Stierstorfer, Amination of energetic anions: high-performing energetic materials *Dalton Transactions* **2012**, *41*, 9451-9459.10.1039/C2DT30684K

[19] M. Göbel, K. Karaghiosoff, T. M. Klapötke, D. G. Piercey, J. Stierstorfer, Nitrotetrazolate-2N-oxides and the Strategy of N-Oxide Introduction *Journal of the American Chemical Society* **2010**, *132*, 17216-17226.10.1021/ja106892a

[20] A. A. Dippold, D. Izsák, T. M. Klapötke, C. Pflüger, Combining the Advantages of Tetrazoles and 1,2,3-Triazoles: 4,5-Bis(tetrazol-5-yl)-1,2,3-triazole, 4,5-Bis(1-hydroxytetrazol-5-yl)-1,2,3-triazole, and their Energetic Derivatives *Chemistry – A European Journal* **2016**, *22*, 1768-1778.doi:10.1002/chem.201504624

[21] Y. Huang, H. Gao, B. Twamley, J. M. Shreeve, Nitroamino Triazoles: Nitrogen-Rich Precursors of Stable Energetic Salts *European Journal of Inorganic Chemistry* **2008**, *2008*, 2560-2568.doi:10.1002/ejic.200800160

[22] T. M. Klapötke, P. C. Schmid, S. Schnell, J. Stierstorfer, 3,6,7-Triamino-[1,2,4]triazolo[4,3-b][1,2,4]triazole: A Non-toxic, High-Performance Energetic Building Block with Excellent Stability *Chemistry – A European Journal* **2015**, *21*, 9219-9228.doi:10.1002/chem.201500982

[23] A. S. Kumar, V. D. Ghule, S. Subrahmanyam, A. K. Sahoo, Synthesis of Thermally Stable Energetic 1,2,3-Triazole Derivatives *Chemistry – A European Journal* **2013**, *19*, 509-518.doi:10.1002/chem.201203192

[24] Q. Ma, G. Fan, L. Liao, H. Lu, Y. Chen, J. Huang, Thermally Stable Energetic Salts Composed of Heterocyclic Anions and Cations Based on 3,6,7-Triamino-7 H-s-triazolo[5,1-c]-s-triazole: Synthesis and Intermolecular Interaction Study *ChemPlusChem* **2017**, *82*, 474-482.doi:10.1002/cplu.201700058

[25] Y. Tang, S. Dharavath, G. H. Imler, D. A. Parrish, J. M. Shreeve, Nitramino- and Dinitromethyl-Substituted 1,2,4-Triazole Derivatives as High-Performance Energetic Materials *Chemistry – A European Journal* **2017**, *23*, 9185-9191.doi:10.1002/chem.201701407

[26] M. Dachs, A. A. Dippold, J. Gaar, M. Holler, T. M. Klapötke, A Comparative Study on Insensitive Energetic Derivatives of 5-(1,2,4-Triazol-C-yl)-tetrazoles and their 1-Hydroxy-tetrazole Analogues *Zeitschrift fur Anorganische und Allgemeine Chemie* **2013**, *639*, 2171-2180.doi:10.1002/zaac.201300304

[27] D. Fischer, T. M. Klapötke, D. G. Piercey, J. Stierstorfer, Copper Salts of Halo Tetrazoles: Laser-Ignitable Primary Explosives *Journal of Energetic Materials* **2012**, *30*, 40-54.10.1080/07370652.2010.539998

[28] N. Fischer, D. Izsák, T. M. Klapötke, J. Stierstorfer, The Chemistry of 5-(Tetrazol-1-yl)-2H-tetrazole: An Extensive Study of Structural and Energetic Properties *Chemistry – A European Journal* **2013**, *19*, 8948-8957.doi:10.1002/chem.201300691

[29] T. M. Klapötke, M. Q. Kurz, R. Scharf, P. C. Schmid, J. Stierstorfer, M. Sućeska, 5-(1H-Tetrazolyl)-2-Hydroxy-Tetrazole: A Selective 2N-Monoxidation of Bis(1H-Tetrazole) *ChemPlusChem* **2015**, *80*, 97-106.doi:10.1002/cplu.201402124

[30] T. M. Klapötke, J. Stierstorfer, Nitration Products of 5-Amino-1H-tetrazole and Methyl-5-amino-1H-tetrazoles – Structures and Properties of Promising Energetic Materials *Helvetica Chimica Acta* **2007**, *90*, 2132-2150.doi:10.1002/hlca.200790220

[31] T. M. Klapötke, J. C. p. Stierstorfer, in *Green Energetic Materials*, **2014**, pp. 133-178.

[32] H. Wei, J. Zhang, J. M. Shreeve, Synthesis, Characterization, and Energetic Properties of 6-Amino-tetrazolo[1,5-b]-1,2,4,5-tetrazine-7-N-oxide: A Nitrogen-Rich Material with High Density *Chemistry – An Asian Journal* **2015**, *10*, 1130-1132.10.1002/asia.201500086

[33] Q. Wang, Y. Shao, M. Lu, Amino-tetrazole functionalized fused triazolo-triazine and tetrazolo-triazine energetic materials *Chemical Communications* **2019**, *55*, 6062-6065.10.1039/C9CC01777A

[34] K. O. Christe, D. A. Dixon, M. Vasiliu, R. I. Wagner, R. Haiges, J. A. Boatz, t. l. H. L. Ammon, Are DTTO and iso-DTTO Worthwhile Targets for Synthesis? *Propellants, Explosives, Pyrotechnics* **2015**, *40*, 463-468.doi:10.1002/prep.201400259

[35] T. M. Klapötke, D. G. Piercey, J. Stierstorfer, M. Weyrauther, The Synthesis and Energetic Properties of 5,7-Dinitrobenzo-1,2,3,4-tetrazine-1,3-dioxide (DNBTDO) *Propellants, Explosives, Pyrotechnics* **2012**, *37*, 527-535.doi:10.1002/prep.201100151

[36] D. G. Piercey, D. E. Chavez, S. Heimsch, C. Kirst, T. M. Klapötke, J. Stierstorfer, An Energetic N-Oxide and N-Amino Heterocycle and its Transformation to 1,2,3,4-Tetrazine-1-oxide *Propellants, Explosives, Pyrotechnics* **2015**, *40*, 491-497.doi:10.1002/prep.201400224

[37] X. Song, J. Li, H. Hou, B. Wang, Extensive theoretical studies of a new energetic material: Tetrazino-tetrazine-tetraoxide (TTTO) *Journal of Computational Chemistry* **2009**, *30*, 1816-1820.doi:10.1002/jcc.21182

[38] G. Wang, T. Lu, G. Fan, C. Li, H. Yin, F.-X. Chen, The Chemistry and Properties of Energetic Materials Bearing [1,2,4]Triazolo[4,3-b][1,2,4,5]tetrazine Fused Rings *Chemistry – An Asian Journal* **2018**, *13*, 3718-3722.10.1002/asia.201801145

[39] H. Wei, H. Gao, J. M. Shreeve, N-Oxide 1,2,4,5-Tetrazine-Based High-Performance Energetic Materials *Chemistry – A European Journal* **2014**, *20*, 16943-16952.10.1002/chem.201405122

[40] C. C. Ye, Q. An, W. A. Goddard Iii, T. Cheng, W.-G. Liu, S. V. Zybin, X.-H. Ju, Initial decomposition reaction of di-tetrazine-tetroxide (DTTO) from quantum molecular dynamics: implications for a promising energetic material *Journal of Materials Chemistry A* **2015**, *3*, 1972-1978.10.1039/C4TA05676K

[41] G. D. Zhang, Z. Wang, J.-G. Zhang, An Unusual Layered Crystal Packing Gives Rise to a Superior Thermal Stability of Energetic Salt of 3,6-Bishydrazino-1,2,4,5-tetrazine *Zeitschrift fur Anorganische und Allgemeine Chemie* **2018**, *644*, 512-517.10.1002/zaac.201800086

[42] D. E. Chavez, J. C. Bottaro, M. Petrie, D. A. Parrish, Synthesis and Thermal Behavior of a Fused, Tricyclic 1,2,3,4-Tetrazine Ring System *Angewandte Chemie International Edition* **2015**, *54*, 12973-12975.10.1002/anie.201506744

[43] Y. Tang, C. He, G. H. Imler, D. A. Parrish, J. M. Shreeve, A C–C bonded 5,6-fused bicyclic energetic molecule: exploring an advanced energetic compound with improved performance *Chemical Communications* **2018**, *54*, 10566-10569.10.1039/C8CC05987J

[44] S. E. Creegan, D. G. Piercey, Nitroacetonitrile as a versatile precursor in energetic materials synthesis *RSC Advances* **2020**, *10*, 39478-39484.10.1039/D0RA07579E

[45] Y. Tang, D. Kumar, J. M. Shreeve, Balancing Excellent Performance and High Thermal Stability in a Dinitropyrazole Fused 1,2,3,4-Tetrazine *Journal of the American Chemical Society* **2017**, *139*, 13684-13687.10.1021/jacs.7b08789

[46] P. Yin, J. M. Shreeve, From N-Nitro to N-Nitroamino: Preparation of High-Performance Energetic Materials by Introducing Nitrogen-Containing Ions *Angewandte Chemie International Edition* **2015**, *54*, 14513-14517.https://doi.org/10.1002/anie.201507456

[47] A. A. Dippold, T. M. Klapötke, N. Winter, Insensitive Nitrogen-Rich Energetic Compounds Based on the 5,5′-Dinitro-3,3′-bi-1,2,4-triazol-2-ide Anion *European Journal of Inorganic Chemistry* **2012**, *2012*, 3474-3484.10.1002/ejic.201200221

[48] L. Türker, S. Variş, A REVIEW OF POLYCYCLIC AROMATIC ENERGETIC MATERIALS *Polycyclic Aromatic Compounds* **2009**, *29*, 228-266.10.1080/10406630903135971

[49] S. G. Zlotin, G. N. Varnaeva, O. A. Luk'yanov, α-Nitronitriles *Russian Chemical Reviews* **1989**, *58*, 470-478.10.1070/rc1989v058n05abeh003454

[50] C. J. Thomas, *Vol. 87, Chem. Eng. New*, **2009**, p. 4.

[51] E. K. Voinkov, E. N. Ulomskiy, V. L. Rusinov, O. N. Chupakhin, E. B. Gorbunov, R. A. Drokin, V. V. Fedotov, Potassium salt of nitroacetonitrile in the synthesis of nitrogen heterocycles *Chemistry of Heterocyclic Compounds* **2015**, *51*, 1057-1060.10.1007/s10593-016-1819-5

[52] E. K. Voinkov, E. N. Ulomskiy, V. L. Rusinov, K. V. Savateev, V. V. Fedotov, E. B. Gorbunov, M. L. Isenov, O. S. Eltsov, New stable form of nitroacetonitrile *Mendeleev Communications* **2016**, *26*, 172-173.https://doi.org/10.1016/j.mencom.2016.03.031

[53] Y. Tang, C. He, G. H. Imler, D. A. Parrish, J. M. Shreeve, Aminonitro Groups Surrounding a Fused Pyrazolotriazine Ring: A Superior Thermally Stable and Insensitive Energetic Material *ACS Applied Energy Materials* **2019**, *2*, 2263-2267.10.1021/acsaem.9b00049

[54] I. L. Dalinger, I. A. Vatsadse, T. K. Shkineva, G. P. Popova, B. I. Ugrak, S. A. Shevelev, Nitropyrazoles *Russian Chemical Bulletin* **2010**, *59*, 1631-1638.10.1007/s11172-010-0287-9

[55] C. J. Snyder, T. W. Myers, G. H. Imler, D. E. Chavez, D. A. Parrish, J. M. Veauthier, R. J. Scharff, Tetrazolyl Triazolotriazine: A New Insensitive High Explosive *Propellants, Explosives, Pyrotechnics* **2017**, *42*, 238-242.10.1002/prep.201600294

[56] S. E. Creegan, M. Zeller, E. F. C. Byrd, D. G. Piercey, Synthesis and Characterization of the Energetic 3-Azido-5-amino-6-nitro-1,2,4-triazine *Propellants, Explosives, Pyrotechnics* **2021**, *46*, 214-221.https://doi.org/10.1002/prep.202000136

[57] S. E. Creegan, M. Zeller, E. F. C. Byrd, D. G. Piercey, Energetic 1,2,4-Triazines: 3,5-Diamino-6-nitro-1,2,4-triazine and Its Oxide *Crystal Growth & Design* **2021**, *21*, 3922-3927.10.1021/acs.cgd.1c00241

[58] S. E. Creegan, M. Zeller, E. F. C. Byrd, D. G. Piercey, Titanium Superoxide for the Oxidation of Amines: Synthesis of bis(3-nitro-1H-1,2,4-triazol-5-yl)methane and its Metal Salts *Zeitschrift fur Anorganische und Allgemeine Chemie*, *n/a*, e202200007.https://doi.org/10.1002/zaac.202200007

[59] S. E. Creegan, M. Zeller, E. F. C. Byrd, D. G. Piercey, Energetic Triazinium Salts from N-amination of 3,5-diamino-6-nitro-1,2,4-triazine *Energetic Materials Frontiers* **2022**, *In Submission*

[60] E. F. C. Byrd, B. M. Rice, A Comparison of Methods To Predict Solid Phase Heats of Formation of Molecular Energetic Salts *The Journal of Physical Chemistry A* **2009**, *113*, 345-352.10.1021/jp807822e

[61] B. M. Rice, E. F. C. Byrd, Evaluation of electrostatic descriptors for predicting crystalline density *Journal of Computational Chemistry* **2013**, *34*, 2146-2151.doi:10.1002/jcc.23369

[62] B. M. Rice, J. J. Hare, E. F. C. Byrd, Accurate Predictions of Crystal Densities Using Quantum Mechanical Molecular Volumes *The Journal of Physical Chemistry A* **2007**, *111*, 10874-10879.10.1021/jp073117j

[63] A. D. Becke, Density-functional thermochemistry. III. The role of exact exchange *The Journal of Chemical Physics* **1993**, *98*, 5648-5652.10.1063/1.464913

[64] C. Lee, W. Yang, R. G. Parr, Development of the Colle-Salvetti correlation-energy formula into a functional of the electron density *Physical Review B* **1988**, *37*, 785-789.10.1103/PhysRevB.37.785

[65] S. H. Vosko, L. Wilk, M. Nusair, Accurate spin-dependent electron liquid correlation energies for local spin density calculations: a critical analysis *Canadian Journal of Physics* **1980**, *58*, 1200-1211.10.1139/p80-159

[66] P. J. Stephens, F. J. Devlin, C. F. Chabalowski, M. J. Frisch, Ab Initio Calculation of Vibrational Absorption and Circular Dichroism Spectra Using Density Functional Force Fields *The Journal of Physical Chemistry* **1994**, *98*, 11623-11627.10.1021/j100096a001

[67] R. Krishnan, J. S. Binkley, R. Seeger, J. A. Pople, Self-consistent molecular orbital methods. XX. A basis set for correlated wave functions *The Journal of Chemical Physics* **1980**, *72*, 650-654.10.1063/1.438955

[68] M. J. Frisch, J. A. Pople, J. S. Binkley, Self-consistent molecular orbital methods 25. Supplementary functions for Gaussian basis sets *The Journal of Chemical Physics* **1984**, *80*, 3265-3269.10.1063/1.447079

[69] P. V. R. Schleyer, T. Clark, A. J. Kos, G. W. Spitznagel, C. Rohde, D. Arad, K. N. Houk, N. G. Rondan, Structures and stabilities of α-hetero-substituted organolithium and organosodium compounds. Energetic unimportance of d-orbital effects *Journal of the American Chemical Society* **1984**, *106*, 6467-6475.10.1021/ja00334a001

[70] H. B. M. J. Frisch. G. W. Trucks, G. E. S. Schlegel, M. A. Robb, J. R. Cheesseman, G. Scalmani, V. Barone,, G. A. P. B. Mennucci, *Wallingford CT*, **n.d.**

[71] A. G. Baboul, L. A. Curtiss, P. C. Redfern, K. Raghavachari, Gaussian-3 theory using density functional geometries and zero-point energies *The Journal of Chemical Physics* **1999**, *110*, 7650-7657.10.1063/1.478676

[72] K. E. Gutowski, R. D. Rogers, D. A. Dixon, Accurate Thermochemical Properties for Energetic Materials Applications. II. Heats of Formation of Imidazolium-, 1,2,4-Triazolium-, and Tetrazolium-Based Energetic Salts from Isodesmic and Lattice Energy Calculations *The Journal of Physical Chemistry B* **2007**, *111*, 4788-4800.10.1021/jp066420d

[73] M. Sućeska, Zagreb. Croat., **2018**.

[74] M. Sućeska, *Vol. 465-466, Mater. Sci. Forum,* **2009**, p. 325.

[75] M. Sućeska, Zagreb, Coatia, **2017**.

[76] M. Sućeska, Calculation of the Detonation Properties of C-H-N-O explosives *Propellants, Explosives, Pyrotechnics* **1991**, *16*, 197-202.doi:10.1002/prep.19910160409

[77] M. Sućeska, Evaluation of Detonation Energy from EXPLO5 Computer Code Results *Propellants, Explosives, Pyrotechnics* **1999**, *24*, 280-285.doi:10.1002/(SICI)1521-4087(199910)24:5<280::AID-PREP280>3.0.CO;2-W

[78] M. L. Hobbs, M. R. Baer, Boston, MA,, **July 12-16, 1993**, p. 409.

[79] NATO Standardization Agreement (STANAG) on Explosives, Impact Sensitivity Test, no. 4489, 1, Brussels, September 17, **1999**.

[80] NATO Standardization Agreement (STANAG) on Explosives, Friction Sensitivity Tests, no. 4487, 1, Brussels, August 22, **2002.**

[81] WIWEB-Standardarbeitsanweisung 4-5.1.02, Ermittlung der Explosions- gefährlichkeit, hier: der Schlagempfindlichkeit mit demFallhammer, Erding, November 8, **2002**.

[82] WIWEB-Standardarbeitsanweisung 4-5.1.03, Ermittlung der Explosions gerfährlichkeit oder der Reibeempfindlichkeir mit dem Reibeapparat, Erding, November 8, **2002**.

[83] U. Nations, *Recommendations on the Transport of Dangerous Goods: Manual of Tests and Criteria*, UN, **2003**.

[84] L. I. Bagal, M. S. Pevzner, A. N. Frolov, N. I. Sheludyakova, Heterocyclic nitro compounds *Chemistry of Heterocyclic Compounds* **1970**, *6*, 240-244.10.1007/BF00475005

[85] B. Yan, H. Li, H. Ma, Y. Ma, X. Ma, F. Zhao, Crystal Structure, Thermal Behavior and Detonation Characterization of Bis(3-nitro-1H-1,2,4-triazol-5-yl)methane *Propellants, Explosives, Pyrotechnics* **2020**, *45*, 1714-1719.https://doi.org/10.1002/prep.202000004

2. SYNTHESIS AND CHARACTERIZATION OF THE ENERGETIC 3-AZIDO-5-AMINO-6-NITRO-1,2,4-TRIAZINE

Authors: Shannon E. Creegan, Matthias Zeller, Edward F. C. Byrd, and Davin G. Piercey
Funding: Financial support of this work was provided by the Office of Naval Research under grant N00014-19-1-2089. Our lab is also supported by Purdue University and The Army Research Office (ARO). The National Science Foundation is acknowledged through the Major Research Instrumentation Program under Grant No. CHE 1625543 for the single crystal X-ray diffractometer.

2.1 Abstract

The reaction of diazotetrazole with nitroacetonitrile led to the isolation of the simple 1,2,4-triazine-based energetic 3-azido-5-amino-6-nitro-1,2,4-triazine. It and related compounds were chemically characterized by NMR, IR, and single crystal X-Ray crystallography. Their energetic sensitivities (impact, friction) were experimentally determined and energetic performances calculated. Their ability to form *N*-oxides was also studied.

2.2 Introduction

The research of new energetics is fuelled by the demand for high performing, insensitive, green, and inexpensive materials. High nitrogen heterocycles have become a staple of energetic materials design as they possess high heats of formation, as a result of the desire to decompose into nitrogen gas and can be tailored with additional explosophoric substituents. Many energetic materials suffer from long or expensive synthesis routes with low yields, difficult workup, or costly or dangerous reagents. For example, octanitrocubane (ONC) [1-2] and tetrazino-tetrazine1,3,6,8-tetraoxide (TTTO) [3-5], are both high-performing energetic materials but have long, expensive syntheses with low yields. As economics and industrial scalability of any new energetic material will ultimately determine whether it gets adopted, the development of energetic materials with inexpensive and simple synthesis routes starting with commercially available precursors is important to pursue.

Many heterocyclic systems such as triazoles [6-12], tetrazoles [6, 11, 13-17], and tetrazines [4, 18-26] have been extensively investigated as a backbone of new energetic materials. While these heterocycles have been well explored as the basis of energetic materials, 1,2,4-triazines have

been much less investigated but hold potential for high performing insensitive energetic materials with cost-effective synthesis routes. Recent examples of this are 7-amino-2,3,6-trinitropyrazolo[5,1-c][1,2,4]triazine (PTX) [27-28] and 4-amino-3,7-dinitrotriazolo-[5,1-c][1,2,4] triazine (DPX-26) [29-30] which have simple synthesis routes and show good detonation properties comparable or higher than 1,3,5-trinitro-hexahydro-1,3,5-triazine (RDX). PTX and DPX-26 exhibit enhanced thermal stability over RDX and lower mechanical sensitivity when compared to HMX and RDX.

It has been demonstrated that annulated heterocyclic systems have properties useful for energetic materials, often including higher thermal stabilities, low sensitivities, and higher densities when compared to the related non-annulated materials [31-32]. Additionally, their synthesis from a diazonium compound and nitroacetonitrile followed by cyclization is simple and scalable. While neutral nitroacetonitrile has been known to cause explosions [33], the potassium salt of nitroacetonitrile is easily prepared via an indirect route and does not pose a lab hazard [34].

In this work, we synthesized 3-azido-5-amino-6-nitro-1,2,4-triazine (AANT) from diazotetrazole and the potassium salt of nitroacetonitrile (Scheme 1). While this compound was known previously [35] it has never been characterized as an energetic material. We report its full energetic characterization as well as that of an energetic byproduct (**1**) formed during synthesis via nitrile hydrolysis. We also synthesized, for the first time, an isomer of the energetic *N*-oxide of AANT. AANT represents the simplest known energetic material based on the 1,2,4-triazine backbone, and the only non-annulated 1,2,4-triazine energetic material, and can serve as a useful precursor for further energetic derivatives.

2.3 Results and Discussion

2.3.1 Synthesis

Diazotetrazole was prepared from the addition of equimolar sodium nitrite to an acidic aqueous solution of 5-aminotetrazole monohydrate at -2 °C. This was performed in dilute solution as to prevent the very sensitive diazotetrazole from precipitating as it can spontaneously detonate upon crystallization [13]. A solution of the potassium salt of nitroacetonitrile [10] in water was added dropwise to the reaction mixture and the solution allowed to warm to room temperature for 1.5 to 3 hours. This resulted in the initial precipitation of (**1**●H_2O) in 4.6% yield. After isolation

by filtration and continued stirring of the filtrate for 3 days AANT precipitated as a microcrystalline yellow precipitate in 19.2% yield (Scheme 3). Alternately, AANT was isolated by the reduction of solution volume and filtration or extracted from solution with ether or ethyl acetate. Crystals of (**1**•H_2O) suitable for X-ray structural analysis were obtained by slow evaporation of a nitromethane solution and of AANT by slow evaporation of an ethanol solution.

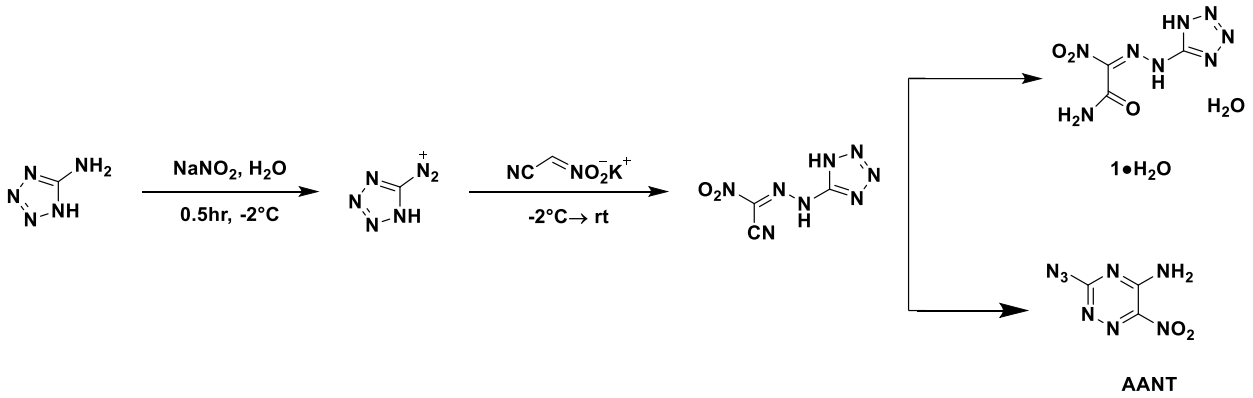

Scheme 3. Synthesis of compounds (**1**•H_2O) and AANT.

Several attempts were made to synthesize and characterize an oxide (**2a-c**) from AANT (Scheme 4). Initial synthesis routes explored the use of Oxone ($2KHSO_5$•$KHSO_4$•K_2SO_4) or hydrogen peroxide under various conditions; however, no product was detected by mass spectroscopy. Further attempts made use of hypofluorous acid acetonitrile complex (HOF•MeCN).

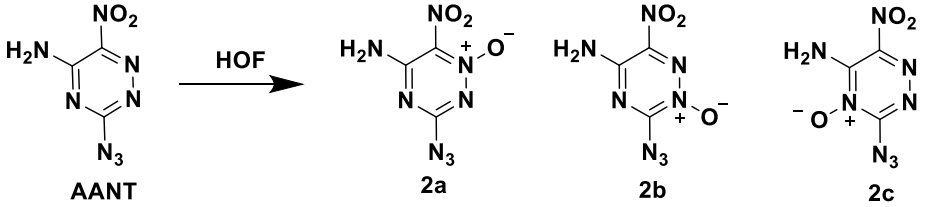

Scheme 4. Synthesis of oxide isomers (**2a-c**) by HOF oxidation of AANT.

An oxide (**2a-c**) was successfully obtained by HOF oxidation as confirmed by mass spectroscopy. However (**2a-c**) proved to be very unstable reverting to AANT under acidic conditions and decomposing in the presence of water, molecular sieves, salt, or sodium sulfate based on LRMS analysis. Attempts to isolate and crystalize also resulted in decomposition; as a result, it was uncertain which potential isomer of the oxide (**2a-3c**) was formed.

2.3.2 Spectroscopy

NMR Spectroscopy

The ^{13}C NMR signals for (**1**●H_2O) occurred at 158 (C3), 156 (C2), and 155 ppm (C1). In AANT the three carbon signals appeared at 163 (C1), 151 (C3), and 146 ppm (C2). In the proton NMR spectrum, the amine in AANT appeared at 9.2 and 8.5 ppm.

Mass Spectrometry

The [M-H] anion was observed by electrospray ionization (ESI) low-resolution mass spectrometry in negative mode at 199 m/z for (**1**●H_2O) and 181 m/z for AANT a high-resolution experiment. [M-16] signals were observed in both samples. (**2a-c**) was observed in negative mode ESI by low-resolution mass spectrometer at 197 m/z and confirmed by a high-resolution.

FTIR Spectroscopy

(**1**●H_2O) and AANT were analysed by infrared spectroscopy. Bands characteristic of N-H stretching were found at 3582 and 3447 $cm^{-}1$ for (**1**●H_2O) and 3432 and 3320 cm^{-1} for AANT. Asymmetric N-O stretches for (**1**●H_2O) and AANT were found at 1515 and 1510 cm^{-1} respectively. Symmetric N-O stretches for (**1**●H_2O) an AANT were located at 1307 and 1315 cm^{-1} respectively. Additionally, (**1**●H_2O) has a band characteristic for an amide carbonyl at 1669 cm^{-1} and AANT has a characteristic azide N=N=N stretching band at 2169 cm^{-1}. The values recorded for AANT were comparable to values previously reported for the compound [35].

2.3.3 Crystal Structures

(**1**●H_2O) and AANT were characterized using single crystal X-ray diffraction. Their crystal and structural data are listed in Appendix A.3.2 and their structures are shown in Figures 7 and 8. A single crystal of AANT was coated with a trace of Fomblin oil and were transferred to the goniometer head of a Bruker Quest diffractometer with a fixed chi angle, a Mo K_α wavelength (λ = 0.71073 Å) sealed tube fine focus X-ray tube, single crystal curved graphite incident beam monochromator, a Photon100 CMOS area detector.

A single crystal of (1•H_2O) analyzed the same way on a Bruker Quest diffractometer with kappa geometry, a Cu K_α wavelength (λ = 1.54178 Å) I-μ-S microsource X-ray tube, laterally graded multilayer (Goebel) mirror single crystal for monochromatization, a Photon2 CMOS area detector. Both instruments were equipped with an Oxford Cryosystems low temperature device and examination and data collection were performed at 150 K. Data were collected, reflections were indexed and processed, and the files scaled and corrected for absorption using APEX3 [36] and SADABS [37].

The space groups were assigned and the structures were solved by direct methods using XPREP within the SHELXTL suite of programs [38-39] and refined by full matrix least squares against F^2 with all reflections using Shelxl2018 [40-41] using the graphical interface Shelxle [42]. For (**1**•H_2O) H atoms attached to nitrogen atoms were positioned geometrically and constrained to ride on their parent atoms with N-H bond distances of 0.88 Å. Water H atoms were refined and U_{iso}(H) values were set to a multiple of U_{eq}(O/N) with 1.5 for OH, and 1.2 for N-H and NH_2 units, respectively. In the structure of AANT all H atoms and U_{iso}(H) values were freely refined. Additional data collection and refinement deatil are listed in Appendix B: Table 1.

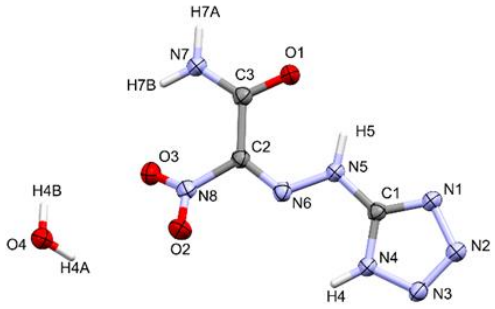

Figure 7. Molecular unit of (**1**•H_2O). Ellipsoids are drawn at the 50 % probability level.

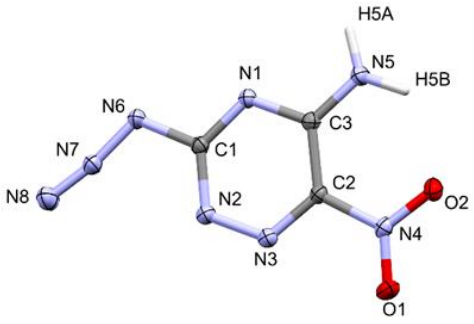

Figure 8. Molecular unit of AANT. Ellipsoids are drawn at the 50 % probability level.

(**1**•H_2O) crystallizes in the triclinic space group $P\bar{1}$ with the inclusion of a single hydration water per molecule (**1**) with two formula units within the unit cell and a density of 1.808 g cm^{-3} at 150 K. AANT crystallizes in the orthorhombic space group $P2_12_12_1$ with four formula units in the unit cell and a density of 1.824 g cm^{-3} at 150 K. The unit cells of each were subsequently remeasured to obtain room temperature densities 1.703 g cm^{-3} for (**1**•H_2O) and 1.781 g cm^{-3} for AANT, for use in the calculation of energetic properties.

2.3.4 Thermal Stability and Energetic Properties

The thermal stabilities of (**1**●H_2O) and AANT were measured using differential scanning calorimetry (DSC) performed in sealed aluminium pans at a heating rate of 5 °C min^{-1}. The DSC trace shows AANT melting at 160 °C and decomposing at 162 °C. Comparatively, (**1**●H_2O) showed loss of water at 118 °C and decomposition at 148 °C. When directly heated from below with a torch under a metal plate both compounds decomposed without explosion.

For initial safety testing, impact and friction sensitivities were determined for (**1**●H_2O) and AANT. Impact sensitivity was carried out according to STANAG 4489 [43] and modified according to instruction [44] on an OZM drophammer by the BAM method [45]. Friction sensitivity was carried out in accordance with STANAG 4487 [46] and modified according to instruction [47] using a BAM friction tester. During testing it was noted both compounds experience discoloration from yellow to burnt orange upon decomposition. (**1**●H_2O) possesses an impact sensitivity of 10 J and a friction sensitivity of 96 N, where AANT was recorded at 7 J and 120 N, comparable to RDX. As a result, both are classified as sensitive to friction and impact [48].

The enthalpies of formation and densities were calculated using the Byrd and Rice method [49-51]. The heats of formations were calculated for all possible oxide isomers, as we were unable to confirm the position at which the oxide was introduced. Theoretical densities were additionally predicted. The heats of formation for all oxide isomers were within 6% of the value for AANT. The calculated enthalpies of formation and densities are given in Table 2.

The detonation parameters for (**1**●H_2O), AANT, and (**2a-c**) were calculated using the EXPLO5v6.05 software package [52-53]. For (**1**●H_2O) and AANT the experimental crystal densities were used in the calculation of detonation performances. For oxides (3a-c) as they were unable to be isolated pure without decomposition, calculated densities were used in the calculation of detonation performances. The calculated results for all compounds are summarized in Table 2. (**1**●H_2O) has the lowest detonation velocity of 7409 m s^{-1} while AANT has a PETN-like detonation velocity of 8310 m s^{-1}. The detonation pressures for both compounds are less than PETN at 19.76 GPa for (**1**●H_2O) and 28.88 GPa for AANT. The calculated heat of formation for (**1**●H_2O) and was between that of PETN and RDX, while the calculated heat of formation for AANT exceeded that of RDX.

The three potential oxide isomers (**2a-c**) possess detonation parameters between those of PETN and RDX. Of the three isomers, (**2b**) has the largest detonation pressure (31.78 GPa) and

detonation velocity (8738 m s^{-1}) followed by (**2c**) and then (**2a**) with detonation pressures of 31.09 and 30.72 GPa and detonation velocities of 8680 and 8635 m s^{-1}, respectively.

Table 2. Energetic Properties and detonation parameters of (**1**●H_2O), AANT and (**2a-c**).

	(**1**●H_2O)	AANT	(**2a**)	(**2b**)	(**2c**)	PETN	RDX
Formula	$C_3H_4N_8O_3$	$C_3H_2N_8O_2$	$C_3H_2N_8O_3$	$C_3H_2N_8O_3$	$C_3H_2N_8O_3$	$C_5H_8N_4O_{12}$	$C_3H_6N_6O_6$
FW [g mol^{-1}]	200.1	182.1	198.1	198.1	198.1	316.13	222.12
IS [J] [a]	10	7	–	–	–	3	7.5
FS [N] [b]	96	120	–	–	–	60	120
N [%][c]	55.99	61.53	56.56	56.56	56.56	17.7	37.84
Ω [%][d]	-39.97	-43.93	-32.30	-32.30	-32.30	-10.12	-21.61
T_{dec} [°C][e]	148	162	–	–	–	165	205
ρ [g·cm^{-3}][f]	1.703	1.781	–	–	–	1.778[m]	1.80[m]
ρ [g·cm^{-3}]^{calc}	1.752	1.752	1.807	1.828	1.801	-	-
$\Delta_f H_m^o$[kJ mol^{-1}] [g]	-16.0	494.3	468.6	478.6	508.1	-561.0	86.3
EXPLO5v6.05							
$-\Delta_{Ex}U°$ [kJ kg^{-1}][h]	-2947	-4624	-5090	-5149	-5273	-6012	-5740
T_{det} [K][i]	2457	3519	3817	3831	3926	3958	3745
P_{CJ} [GPa][j]	19.76	28.88	30.72	31.78	31.09	30.84	33.63
$V_{Det.}$ [m s^{-1}][k]	7409	8310	8635	8738	8680	8429	8801
V_o [cm^3 g^{-1}][l]	788	747	751	748	754	743	784

[a] impact sensitivity (BAM drophammer (1 of 6)); [b] friction sensitivity (BAM friction tester (1 of 6)); [c] nitrogen content; [d] oxygen balance (Ω = (xO–2yC–1/2zH)M/1600); [e] decomposition temperature from DSC (β = 5 °C); [f] room temperature density by X-ray diffraction; [g] calculated heat of formation; [h] energy of explosion; [i] detonation temperature; [j] detonation pressure; [k] detonation velocity; [l] volume of detonation gases (assuming only gaseous products); [m] density referenced from [54]

2.4 Conclusion

3-azido-5-amino-6-nitro-1,2,4-triazine AANT and related material (**1**●H_2O) were synthesized from 5-aminotetrazole by the formation of diazotetrazole and reaction with the potassium salt of nitroacetonitrile. These compounds were characterized for the first time as energetic materials. An oxide (**2a-c**) was synthesized by HOF oxidation and found to be unstable.

2.5 References

[1] M.-X. Zhang, P. E. Eaton, R. Gilardi, Hepta- and Octanitrocubanes *Angewandte Chemie International Edition* **2000**, *39*, 401-404.doi:10.1002/(SICI)1521-3773(20000117)39:2<401::AID-ANIE401>3.0.CO;2-P

[2] P. E. Eaton, M.-X. Zhang, R. Gilardi, N. Gelber, S. Iyer, R. Surapaneni, Octanitrocubane: A New Nitrocarbon *Propellants, Explosives, Pyrotechnics* **2002**, *27*, 1-6.doi:10.1002/1521-4087(200203)27:1<1::AID-PREP1>3.0.CO;2-6

[3] M. S. Klenov, A. A. Guskov, O. V. Anikin, A. M. Churakov, Y. A. Strelenko, I. V. Fedyanin, K. A. Lyssenko, V. A. Tartakovsky, Synthesis of Tetrazino-tetrazine 1,3,6,8-Tetraoxide (TTTO) *Angewandte Chemie International Edition* **2016**, *55*, 11472-11475.doi:10.1002/anie.201605611

[4] X. Song, J. Li, H. Hou, B. Wang, Extensive theoretical studies of a new energetic material: Tetrazino-tetrazine-tetraoxide (TTTO) *Journal of Computational Chemistry* **2009**, *30*, 1816-1820.doi:10.1002/jcc.21182

[5] M. S. Klenov, O. V. Anikin, A. M. Churakov, Y. A. Strelenko, I. V. Fedyanin, I. V. Ananyev, V. A. Tartakovsky, Toward the Synthesis of Tetrazino--tetrazine 1,3,6,8-Tetraoxide (TTTO): An Approach to Non-annulated 1,2,3,4-Tetrazine 1,3-Dioxides *European Journal of Organic Chemistry* **2015**, *2015*, 6170-6179.doi:10.1002/ejoc.201500923

[6] M. Dachs, A. A. Dippold, J. Gaar, M. Holler, T. M. Klapötke, A Comparative Study on Insensitive Energetic Derivatives of 5-(1,2,4-Triazol-C-yl)-tetrazoles and their 1-Hydroxy-tetrazole Analogues *Zeitschrift fur Anorganische und Allgemeine Chemie* **2013**, *639*, 2171-2180.doi:10.1002/zaac.201300304

[7] Y. Huang, H. Gao, B. Twamley, J. M. Shreeve, Nitroamino Triazoles: Nitrogen-Rich Precursors of Stable Energetic Salts *European Journal of Inorganic Chemistry* **2008**, *2008*, 2560-2568.doi:10.1002/ejic.200800160

[8] A. S. Kumar, V. D. Ghule, S. Subrahmanyam, A. K. Sahoo, Synthesis of Thermally Stable Energetic 1,2,3-Triazole Derivatives *Chemistry – A European Journal* **2013**, *19*, 509-518.doi:10.1002/chem.201203192

[9] Q. Ma, G. Fan, L. Liao, H. Lu, Y. Chen, J. Huang, Thermally Stable Energetic Salts Composed of Heterocyclic Anions and Cations Based on 3,6,7-Triamino-7 H-s-triazolo[5,1-c]-s-triazole: Synthesis and Intermolecular Interaction Study *ChemPlusChem* **2017**, *82*, 474-482.doi:10.1002/cplu.201700058

[10] Y. Tang, S. Dharavath, G. H. Imler, D. A. Parrish, J. M. Shreeve, Nitramino- and Dinitromethyl-Substituted 1,2,4-Triazole Derivatives as High-Performance Energetic Materials *Chemistry – A European Journal* **2017**, *23*, 9185-9191.doi:10.1002/chem.201701407

[11] A. A. Dippold, D. Izsák, T. M. Klapötke, C. Pflüger, Combining the Advantages of Tetrazoles and 1,2,3-Triazoles: 4,5-Bis(tetrazol-5-yl)-1,2,3-triazole, 4,5-Bis(1-hydroxytetrazol-5-yl)-1,2,3-triazole, and their Energetic Derivatives *Chemistry – A European Journal* **2016**, *22*, 1768-1778.doi:10.1002/chem.201504624

[12] A. A. Dippold, T. M. Klapötke, Nitrogen-Rich Bis-1,2,4-triazoles—A Comparative Study of Structural and Energetic Properties *Chemistry – A European Journal* **2012**, *18*, 16742-16753.doi:10.1002/chem.201202483

[13] D. Fischer, T. M. Klapötke, D. G. Piercey, J. Stierstorfer, Copper Salts of Halo Tetrazoles: Laser-Ignitable Primary Explosives *Journal of Energetic Materials* **2012**, *30*, 40-54.10.1080/07370652.2010.539998

[14] N. Fischer, D. Izsák, T. M. Klapötke, J. Stierstorfer, The Chemistry of 5-(Tetrazol-1-yl)-2H-tetrazole: An Extensive Study of Structural and Energetic Properties *Chemistry – A European Journal* **2013**, *19*, 8948-8957.doi:10.1002/chem.201300691

[15] T. M. Klapötke, M. Q. Kurz, R. Scharf, P. C. Schmid, J. Stierstorfer, M. Sućeska, 5-(1H-Tetrazolyl)-2-Hydroxy-Tetrazole: A Selective 2N-Monoxidation of Bis(1H-Tetrazole) *ChemPlusChem* **2015**, *80*, 97-106.doi:10.1002/cplu.201402124

[16] T. M. Klapötke, J. Stierstorfer, Nitration Products of 5-Amino-1H-tetrazole and Methyl-5-amino-1H-tetrazoles – Structures and Properties of Promising Energetic Materials *Helvetica Chimica Acta* **2007**, *90*, 2132-2150.doi:10.1002/hlca.200790220

[17] T. M. Klapötke, J. C. Stierstorfer, Energetic Tetrazole N-oxides **2014**, 133-178.doi:10.1002/9781118676448.ch06

[18] K. O. Christe, D. A. Dixon, M. Vasiliu, R. I. Wagner, R. Haiges, J. A. Boatz, t. l. H. L. Ammon, Are DTTO and iso-DTTO Worthwhile Targets for Synthesis? *Propellants, Explosives, Pyrotechnics* **2015**, *40*, 463-468.doi:10.1002/prep.201400259

[19] T. M. Klapötke, D. G. Piercey, J. Stierstorfer, M. Weyrauther, The Synthesis and Energetic Properties of 5,7-Dinitrobenzo-1,2,3,4-tetrazine-1,3-dioxide (DNBTDO) *Propellants, Explosives, Pyrotechnics* **2012**, *37*, 527-535.10.1002/prep.201100151

[20] J. L. Mendoza-Cortes, Q. An, W. A. Goddard Iii, C. Ye, S. Zybin, Prediction of the crystal packing of di-tetrazine-tetroxide (DTTO) energetic material *Journal of Computational Chemistry* **2016**, *37*, 163-167.10.1002/jcc.23893

[21] D. G. Piercey, D. E. Chavez, S. Heimsch, C. Kirst, T. M. Klapötke, J. Stierstorfer, An Energetic N-Oxide and N-Amino Heterocycle and its Transformation to 1,2,3,4-Tetrazine-1-oxide *Propellants, Explosives, Pyrotechnics* **2015**, *40*, 491-497.doi:10.1002/prep.201400224

[22] G. Wang, T. Lu, G. Fan, C. Li, H. Yin, F.-X. Chen, The Chemistry and Properties of Energetic Materials Bearing [1,2,4]Triazolo[4,3-b][1,2,4,5]tetrazine Fused Rings *Chemistry – An Asian Journal* **2018**, *13*, 3718-3722.10.1002/asia.201801145

[23] H. Wei, H. Gao, J. M. Shreeve, N-Oxide 1,2,4,5-Tetrazine-Based High-Performance Energetic Materials *Chemistry – A European Journal* **2014**, *20*, 16943-16952.10.1002/chem.201405122

[24] H. Wei, J. Zhang, J. M. Shreeve, Synthesis, Characterization, and Energetic Properties of 6-Amino-tetrazolo[1,5-b]-1,2,4,5-tetrazine-7-N-oxide: A Nitrogen-Rich Material with High Density *Chemistry – An Asian Journal* **2015**, *10*, 1130-1132.10.1002/asia.201500086

[25] C. C. Ye, Q. An, W. A. Goddard Iii, T. Cheng, W.-G. Liu, S. V. Zybin, X.-H. Ju, Initial decomposition reaction of di-tetrazine-tetroxide (DTTO) from quantum molecular dynamics: implications for a promising energetic material *Journal of Materials Chemistry A* **2015**, *3*, 1972-1978.10.1039/C4TA05676K

[26] G. D. Zhang, Z. Wang, J.-G. Zhang, An Unusual Layered Crystal Packing Gives Rise to a Superior Thermal Stability of Energetic Salt of 3,6-Bishydrazino-1,2,4,5-tetrazine *Zeitschrift fur Anorganische und Allgemeine Chemie* **2018**, *644*, 512-517.10.1002/zaac.201800086

[27] M. C. Schulze, B. L. Scott, D. E. Chavez, A high density pyrazolo-triazine explosive (PTX) *Journal of Materials Chemistry A* **2015**, *3*, 17963-17965.10.1039/C5TA05291B

[28] I. L. Dalinger, I. A. Vatsadse, T. K. Shkineva, G. P. Popova, B. I. Ugrak, S. A. Shevelev, Nitropyrazoles *Russian Chemical Bulletin* **2010**, *59*, 1631-1638.10.1007/s11172-010-0287-9

[29] D. G. Piercey, D. E. Chavez, B. L. Scott, G. H. Imler, D. A. Parrish, An Energetic Triazolo-1,2,4-Triazine and its N-Oxide *Angewandte Chemie International Edition* **2016**, *55*, 15315-15318.doi:10.1002/anie.201608723

[30] D. Kumar, G. H. Imler, D. A. Parrish, J. M. Shreeve, A Highly Stable and Insensitive Fused Triazolo–Triazine Explosive (TTX) *Chemistry – A European Journal* **2017**, *23*, 1743-1747.doi:10.1002/chem.201604919

[31] H. Gao, Q. Zhang, J. M. Shreeve, Fused heterocycle-based energetic materials (2012–2019) *Journal of Materials Chemistry A* **2020**, *8*, 4193-4216.10.1039/C9TA12704F

[32] Y. Tang, C. He, G. H. Imler, D. A. Parrish, J. M. Shreeve, A C–C bonded 5,6-fused bicyclic energetic molecule: exploring an advanced energetic compound with improved performance *Chemical Communications* **2018**, *54*, 10566-10569.10.1039/C8CC05987J

[33] C. J. Thomas, *Vol. 87*, Chem. Eng. New, **2009**, p. 4.

[34] E. K. Voinkov, E. N. Ulomskiy, V. L. Rusinov, K. V. Savateev, V. V. Fedotov, E. B. Gorbunov, M. L. Isenov, O. S. Eltsov, New stable form of nitroacetonitrile *Mendeleev Communications* **2016**, *26*, 172-173.https://doi.org/10.1016/j.mencom.2016.03.031

[35] V. L. Rusinov, T. V. Dragunova, V. A. Zyryanov, G. G. Aleksandrov, N. A. Klyuev, O. N. Chupakhin, Synthesis and transformations of 3-azido-5-amino-1,2,4-triazines *Chemistry of Heterocyclic Compounds* **1984**, *20*, 455-459.10.1007/BF00513869

[36] Bruker, Madison (WI), USA, **2019**.

[37] L. Krause, R. Herbst-Irmer, G. M. Sheldrick, D. Stalke, Comparison of silver and molybdenum microfocus X-ray sources for single-crystal structure determination *Journal of Applied Crystallography* **2015**, *48*, 3-10.doi:10.1107/S1600576714022985

[38] Bruker Advanced X-ray Solutions, Bruker AXS Inc., Madison, Wisconsin: USA **2000-2003**.

[39] G. Sheldrick, A short history of SHELX *Acta Crystallographica Section A* **2008**, *64*, 112-122.doi:10.1107/S0108767307043930

[40] G. Sheldrick, Crystal structure refinement with SHELXL *Acta Crystallographica Section C* **2015**, *71*, 3-8.doi:10.1107/S2053229614024218

[41] G. M. Sheldrick, *University of Göttingen, Germany* **2018**

[42] C. B. Hübschle, G. M. Sheldrick, B. Dittrich, ShelXle: a Qt graphical user interface for SHELXL *Journal of Applied Crystallography* **2011**, *44*, 1281-1284.10.1107/s0021889811043202

[43] *NATO Standardization Agreement (STANAG) on Explosives*, Impact Sensitivity Test, no. 4489, 1, Brussels, **September 17, 1999.**

[44] *WIWEB-Standardarbeitsanweisung 4-5.1.02*, Ermittlung der Explosions- gefährlichkeit, hier: der Schlagempfindlichkeit mit demFallhammer, Erding, **November 8, 2002**.

[45] BAM, https://www.bam.de/.

[46] *NATO Standardization Agreement (STANAG) on Explosives*, Friction Sensitivity Tests, no. 4487, 1, Brussels, **August 22, 2002**.

[47] *WIWEB-Standardarbeitsanweisung 4-5.1.03*, Ermittlung der Explosions gerfährlichkeit oder der Reibeempfindlichkeir mit dem Reibeapparat, Erding, **November 8, 2002**.

[48] ″Impact: Insensitive > 40 J, Less Sensitive ≥ 35 J, Sensitive ≥ 4 J, Very Sensitive ≤ 3 J; Friction: Insensitive > 360 N, Less Sensitive = 360 N, Sensitive < 360 N and > 80 N, Very Sensitive ≤ 80 N, Extremely Sensitive ≤ 10 N.″ *Recommendations on the Transport of Dangerous Goods: Manual of Tests and Criteria*, UN, **2003.**

[49] E. F. C. Byrd, B. M. Rice, A Comparison of Methods To Predict Solid Phase Heats of Formation of Molecular Energetic Salts *The Journal of Physical Chemistry A* **2009**, *113*, 345-352.10.1021/jp807822e

[50] B. M. Rice, E. F. C. Byrd, Evaluation of electrostatic descriptors for predicting crystalline density *Journal of Computational Chemistry* **2013**, *34*, 2146-2151.doi:10.1002/jcc.23369

[51] B. M. Rice, J. J. Hare, E. F. C. Byrd, Accurate Predictions of Crystal Densities Using Quantum Mechanical Molecular Volumes *The Journal of Physical Chemistry A* **2007**, *111*, 10874-10879.10.1021/jp073117j

[52] M. Sućeska, Zagreb. Croat., **2018**.

[53] M. Sućeska, *Vol. 465-466, Mater. Sci. Forum*, **2009**, p. 325.

[54] M. A. Kettner, T. M. Klapötke, in *Chemical Rocket Propulsion: A Comprehensive Survey of Energetic Materials* (Eds.: L. T. De Luca, T. Shimada, V. P. Sinditskii, M. Calabro), Springer International Publishing, Cham, **2017**, pp. 63-88.

3. ENERGETIC 1,2,4-TRIAZINES: 3,5-DIAMINO-6-NITRO-1,2,4-TRIAZINE AND ITS OXIDE

Authors: Shannon E. Creegan, Matthias Zeller, Edward F. C. Byrd, and Davin G. Piercey
Funding: Financial support of this work was provided by the Office of Naval Research under grant N00014-19-1-2089. Our lab is also supported by Purdue University and The Army Research Office (ARO). The National Science Foundation is acknowledged through the Major Research Instrumentation Program under Grant No. CHE 1625543 for the single crystal X-ray diffractometer.

3.1 Abstract

3,5-diamino-6-nitro-1,2,4-triazine (DANT) was identified as potentially insensitive energetic material with high symmetry and planar geometry yielding improved π-π stacking. The straight-forward generation of this energetic 1,2,4-triazine was accomplished by azide to amine reduction of 5-amino-3-azido-6-nitro-1,2,4-triazine (AANT) with triphenylphosphine via modified Staudinger reaction. Oxidation of DANT using potassium peroxymonosulfate triple salt produces the triazine *N*-oxide 3,5-diamino-6-nitro-1,2,4-triazine-2-oxide (DANTX). DANT and DANTX were characterized using mass spectroscopy, multinuclear NMR spectroscopy, infrared spectroscopy, and elemental analysis. The molecular structure and density of DANT (1.778 g cm^{-3}) was determined by single-crystal X-ray diffraction possessing a graphite-like packed structure. Crystallization of DANTX yielded low-density (1.747 g cm^{-3}) and high-density (1.852 g cm^{-3}) polymorphs. Both DANT and DANTX were characterized as energetic materials in terms of sensitivity towards impact, friction, and thermal stimuli as well as calculated detonation parameters are reported.

3.2 Introduction

Fueled by the demand for insensitive high explosives (IHEs), research into high-energy-density materials (HEDMs) is progressing rapidly. Many established energetic materials, such as 1,3,5-trinitro-1,3,5-triazinane (RDX), are cost effective, high-performing, and developed with the intent of achieving an ideal fuel-to-oxidizer ratio. This method of development produces materials with high detonation pressure and velocity, but they tend to be sensitive to stimuli. Newly developed IHEs need to meet increasingly higher safety standards. This need is being met by the

development of compounds using high-nitrogen heterocyclic systems which can achieve higher performances based on ring-strain, improved packing density, and high heat of formation. These materials often have a lower environmental impact and simpler syntheses than conventional materials, as demonstrated by the energetic high-nitrogen heterocyclic systems copper(I) 5-nitro-tetrazolate (DBX-1) [1-2], 4,7-diamine-3,8-dinitropyrazolo[5,1-c]-1,2,4-triazine (DADNPT) [3], dihydroxylammonium 5,50-bistetrazole-1,10-diolate(TKX-50) [4], 5,5'-bis(2,4,6-trinitrophenyl)-2,2'-bi(1,3,4-oxadiazole) (TKX-55) [5], triazolo-1,2,4-triazine (DPX-26) [6], nitrotetrazolate-2*N*-oxides [7], 3,6-diamino-s-tetrazine-1,4-dioxide (LAX-112) [8-9], and 4,4',5,5'-tetraamino-3,3'-azo-bis-1,2,4-triazole (TAABT) [10].

In the largely experimental field of new energetic compound synthesis, the development of new materials is often a trial-and-error screening process. New materials start with intuitive thought, based on the nature of backbone structures, functional groups, and knowledge of existing trends between sensitive and physical characteristics. Enter the Materials Genome Initiative (MGI) [11], created to accelerate advances in material innovation at lower cost by providing a supportive infrastructure. Following the success of materials genome approach in other materials fields, Zhang et al. [11] applied the materials genome approach to their research developing 1,3-dioxide-2,4,6-triamino-5-nitropyrimidine (ICM-102). Zhang et al. [11] identified three "genetic" features of IHEs: 1) low CO_2-based oxygen balance in the range of -80 to -40%; 2) high symmetry planar aromatic or hetero- aromatic structures; and 3) graphite-like crystal packing.

In the search for new insensitive energetic materials, we considered energetic 1,2,4-triazines due to the capability of its straight-forward generation, especially when considering the ease of their synthesis when substituted with vicinal nitro groups [12-13]. 1,2,4-triazines have been less studied as base energetic materials than other heterocyclic systems but still hold potential for high performance and good stability. The compound targeted for synthesis, 3,5-diamino-6-nitro-1,2,4-triazine (DANT), was previously identified by materials genome screening [11] as a potentially insensitive material with high symmetry and planar geometry. Following the successful synthesis of DANT the oxide 3,5-diamino-6-nitro-1,2,4-triazine-2-oxide (DANTX) was synthesized. This synthesis was targeted due to the potential of the *N*-oxide to potentially increase density, hydrogen bonding, and oxygen balance, and as such, both the performance and sensitivity of the prepared material.

3.3 Results and Discussion

3.3.1 Synthesis

The synthesis for DANT (Scheme 5) from 5-amino-3-azido-6-nitro-1,2,4-triazine (AANT) [13] was based on a modified Staudinger reaction by reduction with triphenylphosphine [14]. A screening process, of AANT's reduction, in ethanol, methanol, 1-propanol, and n-butanol all led to simple complete reductions, subsequently further reactions used ethanol as the solvent. After AANT had completely reacted with triphenylphosphine, determined by LRMS, water was added driving the formation of triphenylphosphine oxide and DANT (Figure9) from the iminophosphorane. After stirring overnight, solvent was removed in vacuo and the yellow solid extracted with near boiling ether to remove triphenylphosphine oxide providing a 68% yield of DANT. The reaction moved to completion with 1-equivalent of triphenylphosphine and was unaffected by solvent type leading to the use of 1-equivalent triphenylphosphine in ethanol for larger scale preparation.

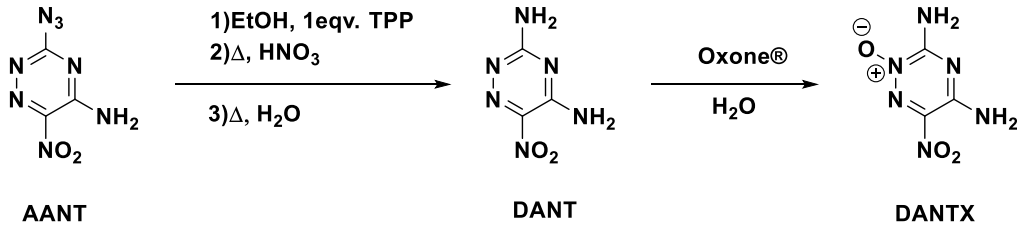

Scheme 5. Synthesis of DANT from AANT and the subsequent oxidation of DANT to DANTX

DANTX (Figure 10) was prepared by oxidizing DANT in water with small portions of potassium peroxymonosulfate, as its $2KHSO_5 \cdot KHSO_4 \cdot K_2SO_4$, triple salt (Oxone®) at 40 °C until the reaction was complete as determined by LRMS (Scheme 5). The reaction solution was then extracted with hexanes, filtered, and washed with cold water yielding a bright red solid. Other attempts for oxidizing DANT were made with HOF•MeCN [15-16] and higher equivalents of Oxone®, in the hopes of forming a double oxide, which resulted in over oxidation and loss of product.

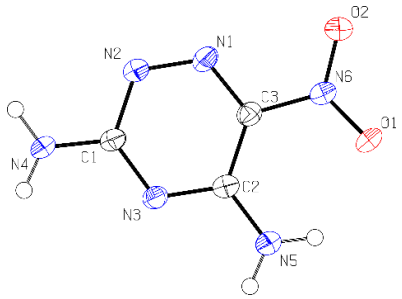

Figure 9. Molecular unit of DANT. Ellipsoids are drawn at the 50 % probability level.

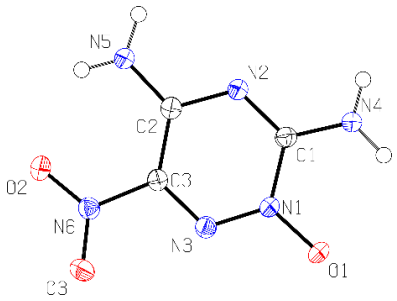

Figure 10. Molecular unit of DANTX. Ellipsoids are drawn at the 50 % probability level.

3.3.2 Chemical Analysis

Reaction progress was monitored by electrospray ionization (ESI) low-resolution mass spectrometry. The reaction of AANT with triphenylphosphine yields a [M+H] peak at 417 m/z and the formation of triphenylphosphine oxide was observed by the presence of [M+H] and [2M+H] peaks at 279 m/z and 557 m/z, respectively. DANT was observed as the [M-H] anion in negative mode at 155 m/z and as the [M+H] cation in positive mode at 157 m/z. DANTX was observed as an [M-H] anion at 171 m/z and [M+H] cation at 173 m/z. A trace peak for the double oxide was seen at 187 m/z [M-H].

With infrared spectroscopy bands characteristic of N-H primary amine stretching were seen at 3419 and 3392 cm^{-1} for DANT while the DANTX had bands at 3455, 3419, 3386 and 3362 cm^{-1}. Symmetric N-O stretches were found at 1306 and 1277 cm^{-1} for DANT and DANTX, respectively. Asymmetric N-O stretching was seen at 1546 cm^{-1} for DANT and 1463 cm^{-1} for DANTX.

By nuclear magnetic resonance spectroscopy, DANT was seen to possess four singlet peaks corresponding to the amine protons at 8.26, 7.98, 7.84, and 7.63 ppm with pairings being 8.26 and 7.84 ppm for one amine and 7.98 and 7.63 ppm for the second. A similar ^{1}H was observed for DANTX with amine pairings between 9.11 and 8.68 ppm and 8.49 and 8.22 ppm. The ^{13}C spectrum of DANT shows the C-amine carbons at 162 and 151 ppm with the C-nitro carbon at 143 ppm. All DANTX carbons are shifted upfield in comparison, with the C-amine carbons at 152 and 146 ppm and the C-nitro carbon at 127 ppm.

3.3.3 Crystallography

Single crystal X-ray diffraction data for DANT were collected on a Bruker Quest diffractometer with a fixed chi angle, a Mo Kα wavelength (λ = 0.71073 Å) sealed tube fine focus X-ray tube, single crystal curved graphite incident beam monochromator, and a Photon II area detector. Data for the DANTX samples were collected on a Bruker Quest diffractometer with kappa geometry, a Cu Kα wavelength (λ = 1.54178 Å) I-μ-S microsource X-ray tube, laterally graded multilayer (Goebel) mirror for monochromatization, and a Photon III C14 area detector. Both instruments were equipped with an Oxford Cryosystems low temperature device and examination and data collection were performed at 150 K. Data were collected, reflections were indexed and processed, and the files scaled and corrected for absorption using APEX3 [17] and SADABS[18]. The space groups were assigned using XPREP within the SHELXTL suite of programs[19-20] and solved by direct methods using ShelXS [20] and refined by full matrix least squares against F^2 with all reflections using Shelxl2018 [21-22] using the graphical interface Shelxle[23]. H atoms attached to carbon atoms were positioned geometrically and constrained to ride on their parent atoms. C-H bond distances were constrained to 0.98 Å for aliphatic CH_3 moieties and were allowed to rotate but not to tip to best fit the experimental electron density. The solvate molecule in the DANTX acetonitrile solvate is located on a two-fold axis and the methyl H-atoms are thus 1:1 disordered. N-H bond distances were either constrained to 0.88 Å and NH_2 groups were constrained to be planar (sp^2 hybridized) (for DANT, DANTX-DMSO solvate) or amine H atom positions were freely refined (DANTX low- and high-density polymorphs, DANTX-ACN solvate). U_{iso}(H) values were set to a multiple of U_{eq}(C) with 1.5 for CH_3 and 1.2 or 1.5 for NH_2 units, respectively. Additional data collection and refinement details are given in Appendix B: Table 2.

Crystallization of DANT from hot water yields thin yellow-gold flakes suitable for single crystal X-ray measurement (Figure 9). DANT self-assembles into a graphite-like structure (Figure 11a) with slightly undulated layers, similar to those found in other energetics and thought to be the source of reduced hotspot formation, increasing insensitivity and density.[11, 24] Through hydrogen bonding each molecule interacts with surrounding molecules, while inter-layer interactions are limited to Van der Waals contacts (Figure 11b-c). The crystal forms in the $P2_1/c$ monoclinic space group with four formula units per unit cell and measured densities of 1.816 g cm^{-3} at 150 K and 1.778 g cm^{-3} at room temperature.

Solvate-free single-crystal structures of DANTX (Figure 10) were obtained from nitromethane and a mixture of tetrahydrofuran (THF) and water. A low-density polymorph crystallized from nitromethane with measured densities of 1.780 g cm^{-3} at 150 K and 1.747 g cm^{-3} at room temperature. The low-density polymorph formed in the $P\bar{1}$ triclinic space group with four formula units per unit cell and a graphite-like structure (Figure 11d) with undulated layers similar as in the structure of DANT with intermolecular hydrogen bonds within layers (Figure 11e). Charge assisted close contacts between the oxygen of the *N*-oxide and the π-density of the triazine in neighboring layers are observed (Figure 11f).

Crystallization from THF and water led to a high-density polymorph with densities of 1.882 g cm^{-3} at 150 K and 1.852 g cm^{-3} at room temperature. The crystals used for analysis were obtained in small amounts during the crystallization process and further attempts to grow the high-density polymorphic structure did not yield additional material. The high-density polymorph formed in the $P2_1/c$ monoclinic space group with four formula units per unit cell. The structure (Figure 9g-i) shows π-stacking of molecules, but these stacked domains consist of ribbons only two molecules wide. Ribbons are tilted against each other by 70.34° (Appendix B: Figure 2-1), resulting in a mixed packing structure and preventing an indefinite layered graphite-like structure. Ribbons are formed through strong H-bonding between the *N*-oxide and the amine groups with the *N*-oxides at the center of the ribbon, while nitro groups are located at the edge of the ribbons. Weaker amine to nitro hydrogen bonds connect edges of neighboring ribbons with each other. Similar to the low-density polymorph, charge assisted close contacts between the oxygen of the *N*-oxide and the π-density of the triazine in neighboring layers are observed, but these are less pronounced for the high-density polymorph. Crystallization from dimethyl sulfoxide and acetonitrile yielded solvated structures (Appendix B: Figure 2-2,3).

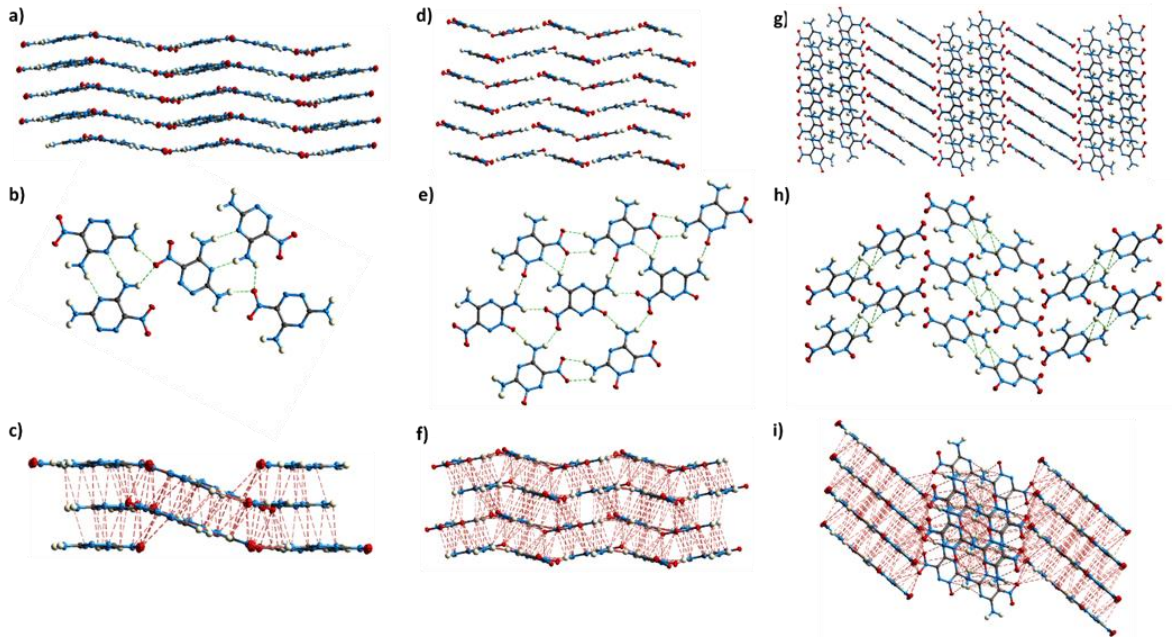

Figure 11. Packing Diagram (2D) a) DANT, d) low-density DANTX, g) high-density DANTX. Hydrogen bonding (expressed by green lines) between molecules of b) DANT, e) low-density DANTX, h) high-density DANTX. Close contact interactions between layers (red lines) wit

3.3.4 Thermal Stabilities

Thermal stabilities were measured by TGA in platinum pans with a heating rate of 5 °C per minute. The onset temperature of decomposition was determined as the temperature at which 5% of initial mass was lost. Both DANT and DANTX were less thermally stable than TATB but more thermally stable than DPX-26 [6] and DPX-27 [6], respectively. The TGA trace of DANT showed an onset temperature of 225 °C, while the DANTX polymorphs' onset temperatures were less than 200 °C. The TGA curves for the DANTX polymorphs show a sudden rapid loss of mass at 200 and 210 °C for high-density and low-density DANTX respectively.

3.3.5 Mechanical Sensitivity

It was determined DANT possesses an impact sensitivity greater than 40 J and a friction sensitivity between 160 and 192 N, categorizing it as insensitive to impact and sensitive to friction.[25] The impact sensitivity was less than DPX-26 and comparable to TATB and ICM-102. DANTX friction and impact sensitivities were performed on the low-density polymorph. The friction sensitivity of DANTX was determined to be 144 N and impact testing yielded a sensitivity

greater than 40 J with no observable sign of detonation or decomposition. Low-density DANTX was classified as insensitive to impact and sensitive friction [25] same as DANT. It was speculated that high-density DANTX would be more sensitive to stimuli due to the mixed stacking structure [26].

3.3.6 Energetic Properties

The solid-state heats of formation for DANT and DANTX were calculated using Gaussian09[27] to be 134.1 and 102.1 kJ mol^{-1}, respectively. The detonation parameters at the CJ point and oxygen balance were calculated using EXPLO5v6.05. The calculated oxygen balances were -61.5% for DANT and -46.5% for DANTX. These values are within the materials genome desired range, -80 to -40%, for the development of insensitive HEDMs and are comparable to the values listed for TATB and ICM-102.[11] DANT had a calculated detonation pressure of 22.91 GPa and detonation velocity of 7896 m s^{-1}. For DANTX, the high-density polymorph has a detonation pressure of 27.8 GPa and detonation velocity of 8407 m s^{-1}. The low-density polymorph has, as expected due to the lower density, lower performance than high-density DANTX with a detonation pressure of 24.2 GPa and detonation velocity of 7938 m s^{-1}. The calculated properties are summarized in Table 3.

Table 3. Energetic Properties of DANT and DATX polymorphs

	DANT	DANTX		DPX-26[6]	DPX-27[6]	ICM-102[11]	TATB[11]	RDX
Formula	$C_3H_4N_6O_2$	$C_3H_4N_6O_3$		$C_4H_2N_8O_4$	$C_4H_2N_8O_5$	$C_4H_6N_6O_4$	$C_6H_6N_6O_6$	$C_3H_6N_6O_6$
FW [g mol^{-1}]	156.10	172.10		226.11	242.12	202.13	258.15	222.12
IS [J] [a]	>40	>40[m]		29	10.3	>60	>60	7.5
FS [N] [b]	160-192	144[m]		>360	258	>360	>360	120
N [%][c]	52.7	47.97		46.30	46.3.0	-	-	37.84
Ω [%][d]	-61.49	-46.48		-	-	-55.45	-55.81	-21.61
T_{dec} [°C][e]	225	190[m]/196[n]		232	138	284	360	205
$\Delta_f H_m^o$ [kJ mol^{-1}] [f]	134.1	102.1		387	378	-8.1	-139.5	86.3
ρ [g·cm^{-3}]^{calc}	1.742	1.814		-	1.904	-	-	-
		Low-Density	High-Density					
ρ [g·cm^{-3}][g]	1.778	1.747	1.852	1.86	-	1.95[o]	1.94[o]	1.80[p]
EXPLO5v6.05								
$-\Delta_{Ex}U°$ [kJ kg^{-1}][h]	-3445	-4046	-4065	-	-	-	-	-5740
T_{det} [K][i]	2584	2973	2915	-	-	-	-	3745
P_{CJ} [GPa][j]	22.91	24.20	27.82	32	35.4	34.3	32.4	33.63
$V_{Det.}$ [m s^{-1}][k]	7896	7938	8407	8700	8970	9169	8114	8801
V_o [cm^3 g^{-1}][l]	774	772	761	-	-	-	-	784

[a] impact sensitivity (BAM drophammer (1 of 6)); [b] friction sensitivity (BAM friction tester (1 of 6)); [c] nitrogen content; [d] oxygen balance (Ω = (xO–2yC–1/2zH)M/1600); [e] onset decomposition temperature from DSC or TGA (β = 5 °C); [f] calculated solid-state heat of formation; [g] room temperature density by X-ray diffraction; [h] energy of explosion; [i] detonation temperature; [j] detonation pressure; [k] detonation velocity; [l] volume of detonation gases (assuming only gaseous products); [m] value determined for low-density DANTX polymorph; [n] value determined for high-density DANTX; [o] density measured by gas pycnometry; [p] density referenced from [28]

3.3.7 Hirshfeld Surfaces and Fingerprint Analysis

To further understand the behavior of DANT and the DANTX polymorphs, two-dimensional fingerprint plots and Hirshfeld electrostatic surfaces were generated using Crystal Explorer [29] to analyze the close contact interactions and hydrogen bonds. The colored regions of the Hirshfeld

surface represent regions of contact shorter than (red), equal to (white) and longer than (blue), the Van der Waal separation. From the images (Figure 10a-f), it can be seen, that all the compounds share a plate shape with the intermolecular interactions occurring on the edges. Additionally, the locations of same-type regions are similar for all structures with the greatest intensity of close contacts being found in high-density DANTX. From the fingerprint plots (Fig 12a-c), the O-H and N-H interactions accounted for 52.8% of total interaction for both DANT and low-density DANTX and 51% for high-energy DANTX suggesting that hydrogen bonding is an important characteristic for all three compounds. Though the majority of the low-density DANTX hydrogen interactions are O-H while DANT and high-density DANTX have approximately equal percentages of N-H and O-H interaction. The percentage of C-N and O-C interactions increase through the three structures with 7.8% for DANT, 8.2% for low-density DANTX, and 10.6% for high-density DANTX. From knowledge of these interactions, it was concluded that the increased density seen in the DANTX polymorph was due to the presence of stronger π-π interactions.

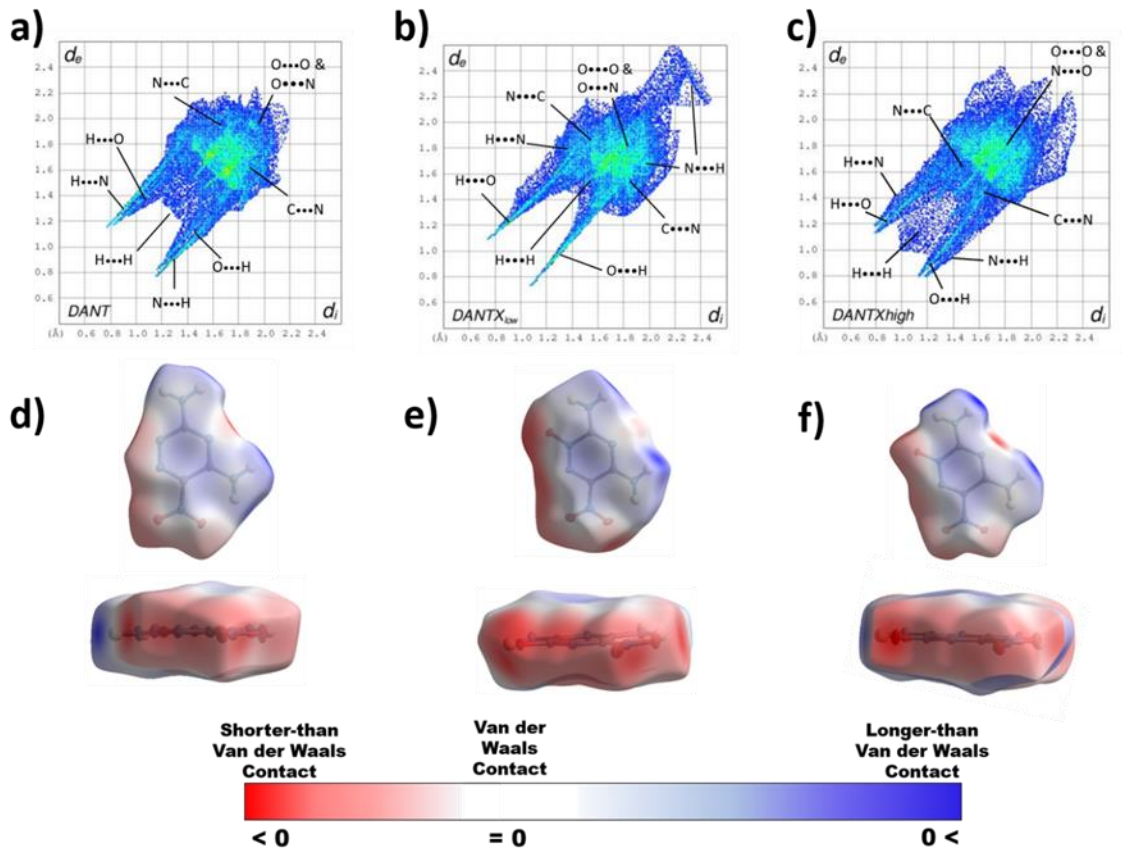

Figure 12. Two-dimensional fingerprint plots in crystal stacking a) DANT, b) low-density DANTX, and c) high-density DANTX. Hirshfeld surfaces of molecules d) DANT, e) low-density DANTX, and f) high-density DANTX.

3.4 Conclusion

In this work, two new energetic materials that were identified via the materials genome approach were prepared and characterized. DANT proved to be a low-sensitivity energetic material with a graphite-like packing structure which self-assembled through hydrogen bonding. The oxide of this, DANTX, was more sensitive and higher performing. The polymorphs of DANTX adopted different extended structures, while the low-density polymorph assumed a graphitic-like extended structure, the high-density higher performing polymorph assumed a mixed packing structure. Of the three molecular structures studied, DANT and low-density DANTX correspond well to the materials genome predictions with low oxygen balances, planar structures, and a high percentage of hydrogen bonding and π-interactions.

3.5 References

[1] D. D. Ford, S. Lenahan, M. Jörgensen, P. Dubé, M. Delude, P. E. Concannon, S. R. Anderson, K. D. Oyler, G. Cheng, N. Mehta, J. S. Salan, Development of a Lean Process to the Lead-Free Primary Explosive DBX-1 *Organic Process Research & Development* **2015**, *19*, 673-680.10.1021/acs.oprd.5b00107

[2] T. M. Klapötke, D. G. Piercey, N. Mehta, K. D. Oyler, M. Jorgensen, S. Lenahan, J. S. Salan, J. W. Fronabarger, M. D. Williams, Preparation of High Purity Sodium 5-Nitrotetrazolate (NaNT): An Essential Precursor to the Environmentally Acceptable Primary Explosive, DBX-1 *Zeitschrift fur Anorganische und Allgemeine Chemie* **2013**, *639*, 681-688.https://doi.org/10.1002/zaac.201300010

[3] Y. Tang, C. He, G. H. Imler, D. A. Parrish, J. M. Shreeve, Aminonitro Groups Surrounding a Fused Pyrazolotriazine Ring: A Superior Thermally Stable and Insensitive Energetic Material *ACS Applied Energy Materials* **2019**, *2*, 2263-2267.10.1021/acsaem.9b00049

[4] N. Fischer, D. Fischer, T. M. Klapötke, D. G. Piercey, J. Stierstorfer, Pushing the limits of energetic materials – the synthesis and characterization of dihydroxylammonium 5,5′-bistetrazole-1,1′-diolate *Journal of Materials Chemistry* **2012**, *22*, 20418-20422.10.1039/C2JM33646D

[5] T. M. Klapötke, T. G. Witkowski, 5,5′-Bis(2,4,6-trinitrophenyl)-2,2′-bi(1,3,4-oxadiazole) (TKX-55): Thermally Stable Explosive with Outstanding Properties *ChemPlusChem* **2016**, *81*, 357-360.https://doi.org/10.1002/cplu.201600078

[6] D. G. Piercey, D. E. Chavez, B. L. Scott, G. H. Imler, D. A. Parrish, An Energetic Triazolo-1,2,4-Triazine and its N-Oxide *Angewandte Chemie International Edition* **2016**, *55*, 15315-15318.doi:10.1002/anie.201608723

[7] M. Göbel, K. Karaghiosoff, T. M. Klapötke, D. G. Piercey, J. Stierstorfer, Nitrotetrazolate-2N-oxides and the Strategy of N-Oxide Introduction *Journal of the American Chemical Society* **2010**, *132*, 17216-17226.10.1021/ja106892a

[8] D. E. Chavez, M. A. Hiskey, 1,2,4,5-tetrazine based energetic materials *Journal of Energetic Materials* **1999**, *17*, 357-377.10.1080/07370659908201796

[9] M. A. Hiskey, D. E. Chavez, D. L. Naud, Los Alamos National Lab., NM (US), **2001**.

[10] J. R. Yount, M. Zeller, E. F. C. Byrd, D. G. Piercey, 4,4′,5,5′-Tetraamino-3,3′-azo-bis-1,2,4-triazole and the electrosynthesis of high-performing insensitive energetic materials *Journal of Materials Chemistry A* **2020**, *8*, 19337-19347.10.1039/D0TA05360K

[11] Y. Wang, Y. Liu, S. Song, Z. Yang, X. Qi, K. Wang, Y. Liu, Q. Zhang, Y. Tian, Accelerating the discovery of insensitive high-energy-density materials by a materials genome approach *Nature Communications* **2018**, *9*, 2444.10.1038/s41467-018-04897-z

[12] S. E. Creegan, D. G. Piercey, Nitroacetonitrile as a versatile precursor in energetic materials synthesis *RSC Advances* **2020**, *10*, 39478-39484.10.1039/D0RA07579E

[13] S. E. Creegan, M. Zeller, E. F. C. Byrd, D. G. Piercey, Synthesis and Characterization of the Energetic 3-Azido-5-amino-6-nitro-1,2,4-triazine *Propellants, Explosives, Pyrotechnics* **2021**, *46*, 214-221.10.1002/prep.202000136

[14] B. Pal, P. Jaisankar, V. S. Giri, Versatile Reagent for Reduction of Azides to Amines *Synthetic Communications* **2004**, *34*, 1317-1323.10.1081/SCC-120030322

[15] S. Rozen, S. Dayan, At Last, 1,10-Phenanthroline-N,N′-dioxide, A New Type of Helicene, has been Synthesized using HOF·CH3CN *Angewandte Chemie International Edition* **1999**, *38*, 3471-3473.doi:10.1002/(SICI)1521-3773(19991203)38:23<3471::AID-ANIE3471>3.0.CO;2-O

[16] S. Rozen, M. Brand, Epoxidation of Olefins with Elemental Fluorine in Water/Acetonitrile Mixtures *Angewandte Chemie International Edition in English* **1986**, *25*, 554-555.doi:10.1002/anie.198605541

[17] Bruker, Madison (WI), USA, **2019**.

[18] L. Krause, R. Herbst-Irmer, G. M. Sheldrick, D. Stalke, Comparison of silver and molybdenum microfocus X-ray sources for single-crystal structure determination *Journal of Applied Crystallography* **2015**, *48*, 3-10.doi:10.1107/S1600576714022985

[19] Bruker Advanced X-ray Solutions, Bruker AXS Inc., Madison, Wisconsin: USA **2000-2003**.

[20] G. Sheldrick, A short history of SHELX *Acta Crystallographica Section A* **2008**, *64*, 112-122.doi:10.1107/S0108767307043930

[21] G. Sheldrick, Crystal structure refinement with SHELXL *Acta Crystallographica Section C* **2015**, *71*, 3-8.doi:10.1107/S2053229614024218

[22] G. M. Sheldrick, *University of Göttingen, Germany* **2018**

[23] C. B. Hübschle, G. M. Sheldrick, B. Dittrich, ShelXle: a Qt graphical user interface for SHELXL *Journal of Applied Crystallography* **2011**, *44*, 1281-1284.10.1107/s0021889811043202

[24] M. C. Schulze, B. L. Scott, D. E. Chavez, A high density pyrazolo-triazine explosive (PTX) *Journal of Materials Chemistry A* **2015**, *3*, 17963-17965.10.1039/C5TA05291B

[25] ″Impact: Insensitive > 40 J, Sensitive ≥ 4 J, Very Sensitive ≤ 3 J; Friction: Insensitive > 360 N, Less Sensitive = 360 N, Sensitive < 360 N and > 80 N, Very Sensitive ≤ 80 N, Extremely Sensitive ≤ 10 N.″ *Recommendations on the Transport of Dangerous Goods: Manual of Tests and Criteria, UN,* ***2003.***

[26] Y. Ma, A. Zhang, C. Zhang, D. Jiang, Y. Zhu, C. Zhang, Crystal Packing of Low-Sensitivity and High-Energy Explosives *Crystal Growth & Design* **2014**, *14*, 4703-4713.10.1021/cg501048v

[27] H. B. M. J. Frisch. G. W. Trucks, G. E. S. Schlegel, M. A. Robb, J. R. Cheesseman, G. Scalmani, V. Barone,, G. A. P. B. Mennucci, *Wallingford CT*, **n.d.**

[28] M. A. Kettner, T. M. Klapötke, in *Chemical Rocket Propulsion: A Comprehensive Survey of Energetic Materials* (Eds.: L. T. De Luca, T. Shimada, V. P. Sinditskii, M. Calabro), Springer International Publishing, Cham, **2017**, pp. 63-88.

[29] J. J. M. M. J. Turner, S. K. Wolff, D. J. Grimwood, P. R. Spackman, D. Jayatilaka and M. A. Spackman, University of Western Australia, **2017**.

4. ENERGETIC TRIAZINIUM SALTS FROM N-AMINATION OF 3,5-DIAMINO-6-NITRO-1,2,4-TRIAZINE

Authors: Shannon E. Creegan, Janine K. Lee, Matthias Zeller, Edward F. C. Byrd, and Davin G. Piercey
Funding: Financial support of this work was provided by the Office of Naval Research under grant N00014-19-1-2089. Our lab is also supported by Purdue University and The Army Research Office (ARO). The National Science Foundation is acknowledged through the Major Research Instrumentation Program under Grant No. CHE 1625543 for the single crystal X-ray diffractometer.

4.1 Abstract

The *N*-amination of 3,5-diamino-6-nitro-1,2,4-triazine via treatment with O-tosylhydroxylamine (THA) resulted in the formation of the 2,3,5-triamino-6-nitro-1,2,4-triazinium cation as the tosylate salt. The tosylate anion was easily exchanged using ion exchange resin to the chloride salt from which several energetic triazinium salts were synthesized via metathesis reaction. These energetic compounds were chemically and structurally characterized utilizing NMR, IR, and single-crystal X-ray crystallography. The thermal stabilities were determined by thermal gravimetric analysis (TGA) and energetic sensitivities (impact, friction) were experimentally determined with an BAM Drophammer and BAM friction tester. The energetic performances were calculated with Explo5v6.05 using Gaussian09 generated heats of formation. The energetic triazinium salts were found to be sensitive high performing energetic materials that have low decomposition temperatures.

4.2 Introduction

Increasingly higher safety standards and environmental restrictions are driving the demand for high performing, insensitive, green, and inexpensive high energy density materials (HEDMs). Research into new energetics begins with fundamental knowledge on the nature of backbone structures, functional groups, and knowledge of existing trends between sensitivity and structural characteristics. The three primary ways of imparting energy to a molecule are: increasing ring or cage strain, increasing heat of formation, and balancing the fuel and oxidizer ratio. High nitrogen heterocycles have become a staple of energetic material design, due to their inherently high heats

of formation and ability to decompose into nitrogen gas. Additionally, these materials are often high performing and insensitive while having cost-effective synthesis routes.

The use of triazole [1-7], tetrazole [1, 6, 8-12], triazine [13-19], and tetrazine [20-29] heterocycles as backbones for new energetics has been well explored. The ongoing quest for new materials delves into modification of these systems through the addition of various functional groups and formation of numerous salts. While the introduction of nitro groups and oxides readily serves to improve oxygen balance and increase intermolecular bonding, the addition of *N*-amines can increase heat of formation and energetic performance. The synthesis of an *N*-amine can be accomplished by amination with reagents such as hydroxylamine (HOSA) and *O*-tosylhydroxylamine (THA) as seen in the synthesis of 2,2'-Diamino-5,5'-dinitro-4,4'-bis(1,2,3-triazole) [30], 2,2'-Diamino-5,5'-dinitro-3,3'-bis(1,2,4-triazole) [31], 2-amino-4-nitro-1,2,3-triazole [32], and 1-Amino-3,5-dinitro-1,2,4-triazole [33]. In cases for which the addition of *N*-amine results in an energetic cation further modification of properties can be done by pairing the resultant cation with the multitude of existing energetic anions.

In this work, the new energetic 2,3,5-triamino-6-nitro-1,2,4-triazinium cation **(1)** was synthesized by the amination of 3,5-diamino-6-nitro-1,2,4-triazine (DANT) using *O*-tosylhydroxylamine (THA) (Scheme 1). The initial tosylate salt was converted to the chloride by use of the chloride loaded ion exchange resin Amberlite™ IRA910-Cl500. Subsequent energetic salts containing the nitrate, perchlorate, 5-nitrotetrazolate, and 5,5'-bistetrazole-1,1'-diolate anions were synthesized by metathesis and fully characterized as energetic materials.

4.3 Results and Discussion

4.3.1 Synthesis

The precursor material DANT, was aminated using 1.5 equivalents of freshly prepared *O*-tosylhydroxylamine (THA) (Scheme 6). The THA was synthesized by stirring ethyl *O*-*p*-tolylsulphonylacetohydroximate in perchloric acid for 2 hours before pouring over ice-water and extracting with dichloromethane. A mixture of DANT, water, and acetonitrile was then added to the THA containing dichloromethane extract and stirred for 18 hours at room temperature. Evaporation of the volatile organics was permitted over the stirring period and the remaining water removed by evaporation under air. It was noted that the solubility of the animated product, **(1)**, in

water was greater than DANT, thus reaction progress could be estimated by the extent of dissolution. The resulting solid was purified by recrystallization from ethanol, yielding **(1)** as yellow-brown crystalline flakes.

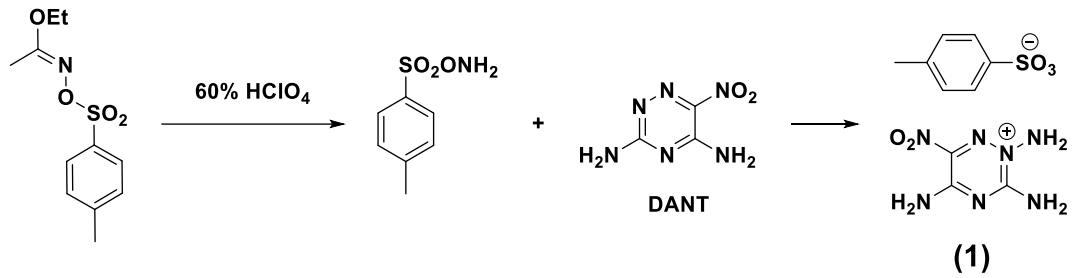

Scheme 6. Synthesis of (**1**) via *N*-amination of DANT

From the tosylate salt **(1)**, synthesis of **(3•**2H2O**)** (Scheme 7) and **(6)** was attempted via metathesis reactions by dissolving diammonium 5,5'-bistetrazole-1,1'-diolate and sodium nitrotetrazole, respectively, in water with the necessary equivalents of **(1)**. This method was successful in the synthesis of **(3•**2H2O**)**; however, the application of heat, needed to dissolve materials in solution, caused a large amount of decomposition in the cation and tosylate anion as seen by NMR. Additionally, the solution containing **(1)** and 5-nitrotetrazole salt resulted in the formation of unaffected independent crystal structures of both materials.

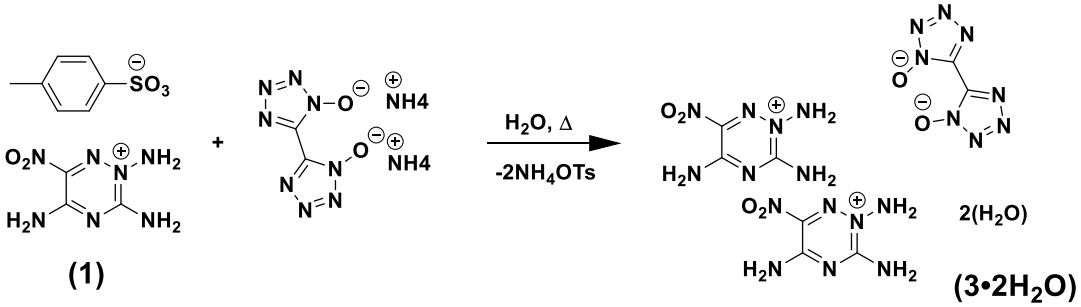

Scheme 7. Synthesis of (**3•**H2O) from (**1**) via method A

From the inability of **(1)** and the 5-nitrotetrazolate salt to undergo metathesis and the large amount of observed decomposition it was concluded that a more readily exchangeable anion was necessary for the synthesis of additional energetic triazinium salts. Initial attempts made to form the bromide salt using hydrobromic acid were futile, resulting in less than 1 % yield. In contrast,

the chloride salt was readily synthesized using chloride loaded ion exchange resin (Scheme 8). Amberlite™ IRA910-Cl500 was rinsed with deionized water before being added to a solution of **(1)** in water. The resin was removed by filtration after the mixture was stirred for 30 minutes and let set for 30 minutes. This process was repeated until tosylate was no longer detected by LRMS. Solvent was removed by high vacuum at room temperature in under 72 hours to avoid excessive decomposition as determined by NMR and coloration with yellow being pure. It was during the process of synthesizing the chloride salt the conditions for decomposition of **TANT+** were explicitly defined. It came to be understood that **TANT+** decomposed when in solution and the process was accelerated by the presence of heat and air, as well as non-neutral conditions (pH ≠ 7). The solution could be stored for several days in the freezer when under argon and the dried material was determined to be shelf stable by weekly analysis with NMR. Decomposition had a marked effect on material coloration changing bright yellow to a gray-purple.

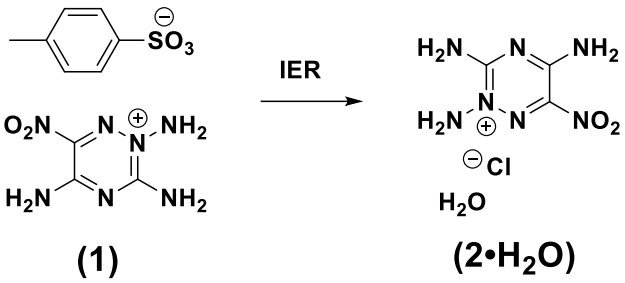

Scheme 8. Synthesis of (**2**•H_2O) from (**1**) using chloride loaded ion exchange resin

Synthesis of **(4**•H_2O**)** (Scheme 9) and **(5)** (Scheme 10) as well as a second attempts to synthesize **(6)** (Scheme 11) and **(3**•$2H_2O$**)** were performed using the respective silver salts of each compound. Though the extreme insolubility of disilver 5,5'-bistetrazole-1,1'-diolate rendered this method ineffective as an alternate synthesis for the **(3**•$2H_2O$**)**. In a dark environment, each silver salt was added to **(2**•H_2O**)** dissolved in minimal water resulting in immediate precipitation of silver chloride as a gray solid. After 30 minutes the mixture was filtered with a 0.45 μm syringe filter resulting in a clear yellow liquid. The solvent was removed by evaporation under high vacuum, as done with **(2**•H_2O**)**, resulting in a powder ranging from gray to purple in coloring.

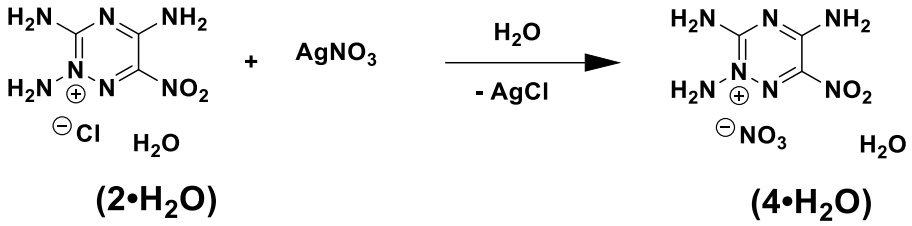

Scheme 9. Synthesis of (**4**•H_2O) from (**2**•H_2O).

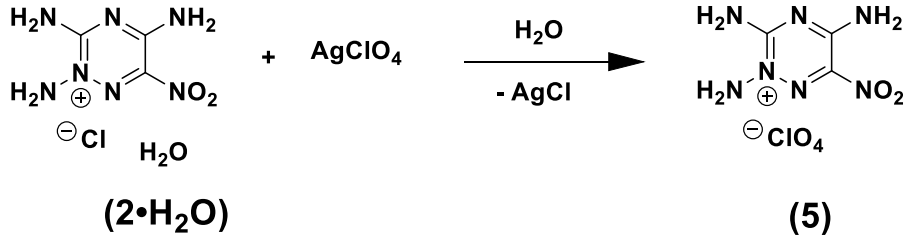

Scheme 10. Synthesis of (**5**) from (**2**•H_2O).

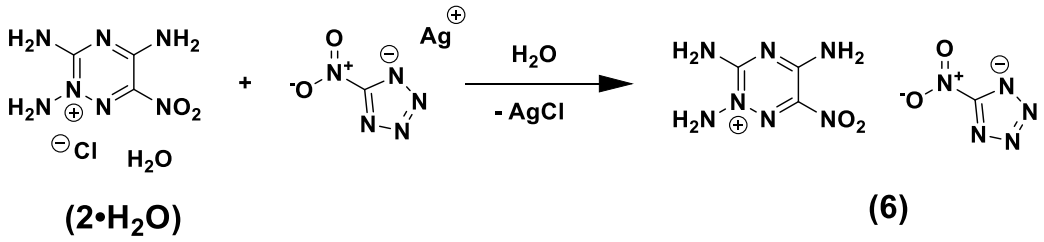

Scheme 11. Synthesis of (**6**) from (**2**•H_2O).

Still seeking an alternate route for the synthesis of **(3**•2H_2O**)**, the solubilities of various salt combinations were considered leading to the use of the disodium 5,5'-bistetrazole-1,1'-diolate and **(4**•H_2O**)** (Scheme 12). Which resulted in the formation of highly soluble sodium nitrate and insoluble **(3**•2H_2O**)**. Collection of the olive-green solid, by filtration, was done in two parts; the first filtration was performed with the initial volume of solvent and the second after the solvent volume had been reduced by half. The **(3**•2H_2O**)** synthesized by this method showed minimal signs of decomposition, especially when compared to the dark brown crystals collected from the first synthesis method.

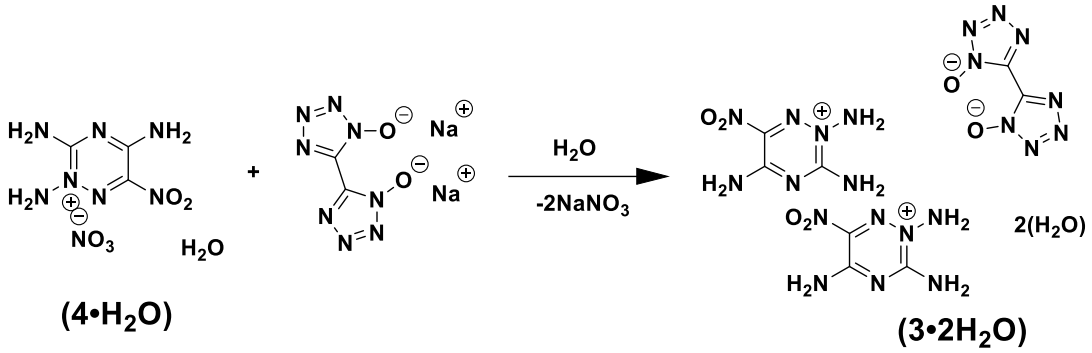

Scheme 12. Synthesis of (**3**•2H2O) from (**4**•H2O) via method B

4.3.2 Chemical Characterization

Each triazinium salt was chemically characterized using IR and NMR spectroscopy while reaction progress was monitored with LRMS. Observed decomposition rendered elemental analysis (EA) and ^{1}H NMR senseless for all but the precursor salts, **(1)** and **(2**•H2O**)**. EA of the precursor salts allowed for the determination of hydrates, independent of crystal structure, and verified material purity.

TANT+ was present in the positive (ESI+) spectra at 172 m/z, while the anionic components appeared in negative (ESI-) spectra. Though the chloride, nitrate, and perchlorate anions possessed molecular weights too small to be observed by our system, the remaining anions were easily identified with tosylate seen at 171 m/z and 5-nitrotetrazolate at 114 m/z. The 5,5'-bistetrazole-1,1'-diolate anion appeared at 169 m/z (ESI-) which corresponds to $[M^{2-}+H]$, indicating the dianion picked up a hydrogen.

NMR spectroscopy was performed with deuterium oxide and the generated spectra were compared to those of DANT and DANTX anion for analysis. The addition of an *N*-amine resulted in a noticeable upfield shift of signal for both the carbon and proton spectra when compared to DANT. The overall carbon shift is less than the one generated by the presence of *N*-oxide with peaks for the *C*- amine carbons presenting at 154 and 150 ppm and the *C*-nitro carbon at 135 ppm. The proton peaks of the pre-existing amino groups were similar to those observed for DANTX at 9.2, 8.8, 8.7, and 8.43 ppm while the new amino group resulted in a single peak at 6.5 ppm. Trace amounts of the tosylate doublet peaks were observed in the chloride salt; however, no other peaks were observed, and the material was determined to be pure monohydrate by EA. As decomposition progressed in **(2**•H2O**)**, along with the change in color, a peak at 70 ppm began to appear. The

appearance of this peak remained a consistent mark of decomposition progression for all remaining salts. The 5,5'-bistetrazole-1,1'-diolate and 5-nitrotetrazolate anions added carbon peaks matching those in literature [34-36].

The predominant aspect of the collective IR spectra is the peaks associated with the primary amines on the TANT cation. These peaks are affected by the relationship between the cation and anion resulting in wavenumber shift and peak broadness. The amine peaks where generally located at between 3300 and 3350 cm^{-1} and 3421 to 3471 cm^{-1}, while just below the spectra displayed broad shouldering peaks at approximately 3100 cm^{-1}. Each of the salts displayed an intense peak in the range of 1620 to 1650 cm^{-1} corresponding to the N-H bend of primary amines. The IR spectra were also useful in determining purity as the 2000 region developed peaks only when decomposition was present.

4.3.3 Single Crystal X-ray Crystallography

The salts discussed in this paper were characterized by single-crystal X-ray diffraction; the associated crystal and structural data are listed in Table 1. The bond lengths observed for **TANT+** are very similar to those seen in DANTX [19] suggesting the addition of the *N*-amine has a similar effect to the *N*-oxide on the ring structure. Internally the bond length within the ring have increased relative to DANT, continuing the trend established with DANTX. The ring's N-N bond lengths progressed from 1.315 Å in DANT, to 1.3026 Å in DANTX, and 1.3155 Å in **TANT+**. While the presence the *N*-oxide increases the associated C-N ring bond more than *N*-amine, 1.398 compared to 1.389 Å, the presence of the *N*-amine results in longer C-C and C-NO_2 bonds.

The crystal structures, suitable for analysis, of **(1)** and **(3•**$2H_2O$**)** formed during synthesis by slow evaporation from ethanol and water respectively. **(1)** formed in the monoclinic crystal system in $P2_1/c$ space group with 4 formula units per cell. It formatted in the system and group as DANT with similar packing structure. **(3•**$2H_2O$**)**, was comparable to low-density DANTX, forming brown dihydrate crystals in the triclinic $P\bar{1}$ space group with a single formula unit per cell. The addition of the 5,5'-bistetrazole-1,1'-diolate anion and hydrate units flattened the undulated packing structure in comparison to both **(1)** and DANTX.

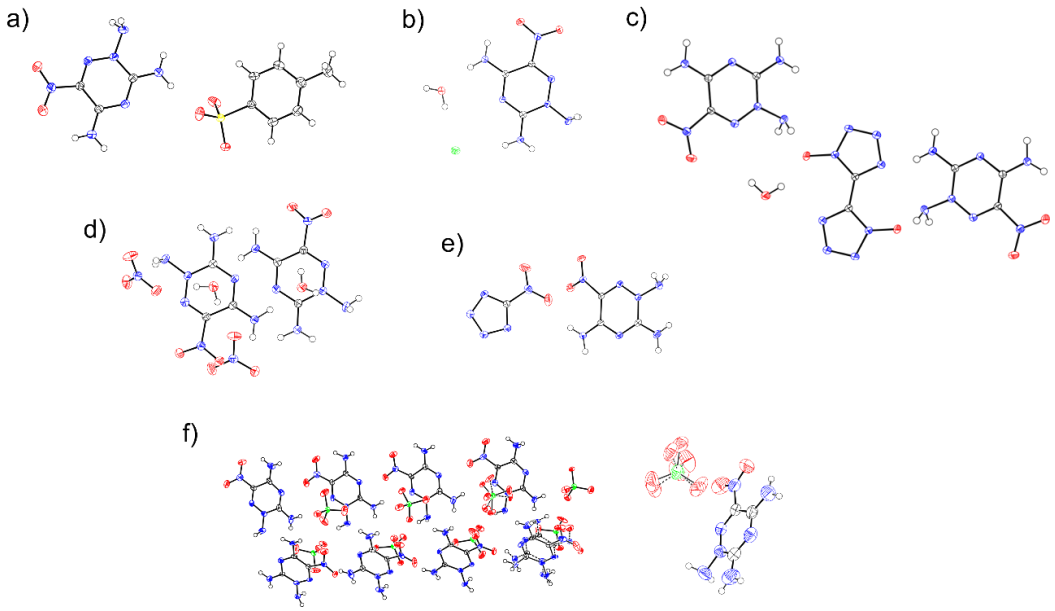

Figure 13. Crystal structure ORTEP Plots with displacement ellipsoids drawn at the 50% probability level of a) (**1**), b) (**2**•H_2O), c) (**3**•$2H_2O$), d), (**4**•H_2O), e) (**6**), and f) (**5**) at both 150 K (left) and room temperature (right).

The crystal structures from the remaining salts were obtained by slow evaporation of the reaction solution at room temperature. **(2**•H_2O**)** crystalized as a monohydrate with 4 units per cell in the monoclinic $P2_1/n$ with a packing structure comparable to that of DANT. Compounds **(4**•H_2O**)** and **(6)** crystalized with 4 units per cell in the monoclinic system in the $P2_1$ and $P2_1/c$ space groups respectively. **(4**•H_2O**)** displayed a packing structure similar to that seen in high-density DANTX with alternating ribbons offset by ~40°**.** Both **(6)** and **(5)** possessed far more disordered structures than previously seen**. (5)** underwent rearrangement upon cooling with slight modulations of anions and cations along a quadrupled axis. The salt began in the orthorhombic $Pna2_1$ space group with 4 formula units per cell transitioning to monoclinic *Pc* with 16 units per cell. At room temperature the molecules rapidly switched between multiple shallow minima giving an average or disordered position for the atoms. When cooled, the molecules were trapped in local minima and a long-range order was established with stronger individual interactions for each molecule. While the rotations of the perchlorate ions and fixing of hydrogen bonds clearly played a role, the 150 K structure also has shorter O…N and O…O contacts than the room temperature structure.

4.3.4 Thermal Stability, Mechanical Sensitivity, and Energetic Properties

The thermal stabilities were measured using thermal gravimetric analysis (TGA) with platinum sample pans and a heating rate of 5 °C per minute. The onset temperature of decomposition was determined as the temperature at which the sample had lost 5 % of its initial weight after, if any, hydrate loss. Of the salts, **(1)** had the highest onset temperature at 205 °C, comparable to the temperature reported for DANTX [19]. All subsequent salts possessed onset temperatures below 200 °C: **(2•**H_2O**)** began to decompose at 177 °C, **(5)** at 180 °C, **(6)** at 158 °C, **(4•**H_2O**)** at 150 °C, and **(3•**$2H_2O$**)** at 130 °C. The TGA graphs for **(2•**H_2O**)** and **(4•**H_2O**)** showed approximately 7 % weight loss due to hydrate loss which corresponds to the loss of a single hydration molecule. Overall, the onset of decomposition temperatures were lower than expected based on the decomposition temperatures observed for DANTX and other energetic salts containing these anions; such as, diammonium 5,5'-bistetrazole-1,1'-diolate which decomposes at 290 °C [36].

Impact and friction sensitivities were determined, respectively, in accordance with STANAG 4489 [37] and 4487 [38] and modified according to instruction [39-40] on an BAM drop hammer and BAM friction tester [41]. The precursor salt **(2•**H_2O**)** was more sensitive than DANT and DANTX to friction with a range sensitivity between 80 and 108 N while possessing an impact sensitivity between that of DANT and DANTX at 20 J. All the energetic salts were more sensitive than both DANT and DANTX to friction and impact, with the most sensitive being **(3•**$2H_2O$**)** demonstrating sensitivities < 1 J and < 5 N, respectively, for impact and friction. Of the remaining salts, **(5)** was the least sensitive to impact at 5 J, as both **(6)** and **(4•**H_2O**)** had impact sensitivities < 1 J. An interesting event, only observed for **(4•**H_2O**)**, was the delayed decomposition experienced by **(4•**H_2O**)** after impact (Figure 14). After impact at 1 J the material displayed minimal signs of decomposition which rapidly progressed to fully decomposed. The friction sensitivities for these salts were determined as ranges with the sensitivity of **(5)** and **(6)** being between 40 and 48 N and the sensitivity of **(4•**H_2O**)** between 48 and 54 N. According to the UN recommendations on the transport of dangerous goods [42]: **(5)** is sensitive to impact while **(3•**$2H_2O$**)**, **(4•**H_2O**)**, and **(6)** are very sensitive and **(3•**$2H_2O$**)** is extremely sensitive to friction while **(4•**H_2O**)**, **(6)**, and **(5)** are classified as very sensitive.

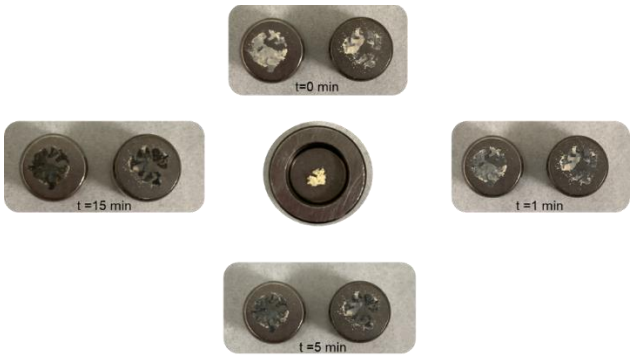

Figure 14. Observed delayed decomposition after impact on (**4**•H_2O)

The calculated values for heat of formation and energetic properties of the energetic salts are compiled in Table 4. For the hydrated structures, the anhydrous heat of formation and associated calculated density were used to compile the theoretical performance of the non-hydrated structures **(3)** and **(4)**. The anhydrous calculated densities are larger than those of the hydrated structures which is reflected in the calculated energetic performance. With the highest density, **(5)** produced the greatest expected detonation velocity, 8774 m s^{-1} and pressure, 34.88 GPa. Less than the perchlorate salt, **(3**•2H_2O**)** had detonation parameters comparable to DANTX with a velocity of 8494 m s^{-1} and pressure of 27.4 GPa. The remaining salts, **(6)** and **(4**•H_2O**),** possessed parameters similar to each other with detonation velocities of 8247 and 8184 m s^{-1} and pressures of 26.04 and 26.08 GPa, respectively.

4.4 Conclusion

In this work, six 2,3,5-triamino-6-nitro-1,2,4-triazinium salts were synthesized and characterized both chemically and structurally. The presence of an *N*-amine was observed to cause an increase in bond length for all ring bonds in **TANT+** over the previously published DANT and DANTX [19]. For the four energetic salts, full energetic characterization was performed determining thermal stability, mechanical sensitivity, and expected detonation parameters. The energetic salts did display improved detonation parameters compared to the precursor compound DANT. However, these salts proved to be less thermally stable and more sensitive to mechanical stimuli than both DANT and DANTX.

Table 4. Energetic properties and detonation parameters of triazinium salts

	(1)	**(2)**•H_2O	**(3)**•2(H_2O)	**(3)**[p]	**(4)**•H_2O	**(4)**$_{[p]}$	**(5)**	**(6)**	DANT	DANTX
Formula	$C_{10}H_{13}N_7O_5S$	$C_3H_8N_7O_3Cl$	$C_8H_{16}N_{22}O_8$	$C_8H_{12}N_{22}O_6$	$C_3H_8N_8O_6$	$C_3H_8N_8O_6$	$C_3H_6N_7O_6Cl$	$C_4H_6N_{12}O_4$	$C_3H_4N_6O_2$	$C_3H_4N_6O_3$
FW [g mol^{-1}]	343.3	225.6	548.4	512.4	252.2	252.2	271.6	286.2	156.1	172.1
IS [J] [a] [o]	-	20	< 1	-	< 1	-	5	< 1	>40	8
FS [N] [b] [o]	-	80 - 108	< 5	-	48 - 54	-	40 – 48	40 - 48	160-192	360
N [%] [c]	28.56	43.46	56.2	60.15	44.44	47.86	36.1	58.73	52.7	47.97
Ω [%] [d]	-	-	-46.68	-49.96	-23.38	-27.33	-14.727	-39.13	-61.49	-46.48
T_{dec} [°C] [e]	205	177	130	-	150	-	180	158	225	190[m]/196[n]
ρ [$g.cm^{-3}$] [f]	1.538	-	1.744	-	1.718	-	1.823	1.734	1.778	1.747[m]/1.852[n]
ρ [$g.cm^{-3}$] calc	1.6	1.73	1.77[q]	1.78	1.75[q]	1.81	1.9	1.77	1.74	1.81
$\Delta_f H_m°$ [kJ mol^{-1}] [g]	5.4	168.5	797.5	1287.47	-236.3	8.08	415.3	445.8	134.1	102.1
Explo5v6.05										
$-\Delta_{Ex}U°$ [kJ kg^{-1}][h]	-	-	-4567.9	-4895.5	-4113.3	-4435.58	-6119.8	-4370.1	-3445	-4046[m]/-4065[n]
$T_{det.}$ [K] [i]	-	-	3129.5	3367.9	2917.8	3119.2	4350.4	3205.1	2584	2973[m]/2915[n]
P_{CJ} [GPa] [j]	-	-	27.4	29	26.08	29.8	34.88	26.04	22.91	24.20[m]/27.82[n]
$V_{Det.}$ [m s^{-1}] [k]	-	-	8494	8666	8184	8564	8774	8247	7896	7938[m]/8407[n]
V_o [cm^3 g^{-1}][l]	-	-	837	804.2	846.8	806.5	782.5	807.1	774	772[m]/761[n]

[a] impact sensitivity (BAM drophammer (1 of 6)); [b] friction sensitivity (BAM friction tester (1 of 6)); [c] nitrogen content; [d] oxygen balance (Ω = (xO–2yC–1/2zH)M/1600); [e] decomposition temperature from DSC (β = 5 °C); [f] room temperature density by X-ray diffraction; [g] calculated heat of formation; [h] energy of explosion; [i] detonation temperature; [j] detonation pressure; [k] detonation velocity; [l] volume of detonation gases (assuming only gaseous products); [m] value determined for low-density DANTX polymorph; [n] value determined for high-density DANTX; [o] a 'go' was determined by the presence of smoke, light, sound, or the occurrence of decomposition; [p] theoretical values generated from Gaussian09 for anhydrous structures; [q] calculated from 150 K single crystal x-ray.

4.5 References

[1] M. Dachs, A. A. Dippold, J. Gaar, M. Holler, T. M. Klapötke, A Comparative Study on Insensitive Energetic Derivatives of 5-(1,2,4-Triazol-C-yl)-tetrazoles and their 1-Hydroxy-tetrazole Analogues *Zeitschrift fur Anorganische und Allgemeine Chemie* **2013**, *639*, 2171-2180.doi:10.1002/zaac.201300304

[2] Y. Huang, H. Gao, B. Twamley, J. M. Shreeve, Nitroamino Triazoles: Nitrogen-Rich Precursors of Stable Energetic Salts *European Journal of Inorganic Chemistry* **2008**, *2008*, 2560-2568.doi:10.1002/ejic.200800160

[3] A. S. Kumar, V. D. Ghule, S. Subrahmanyam, A. K. Sahoo, Synthesis of Thermally Stable Energetic 1,2,3-Triazole Derivatives *Chemistry – A European Journal* **2013**, *19*, 509-518.doi:10.1002/chem.201203192

[4] Q. Ma, G. Fan, L. Liao, H. Lu, Y. Chen, J. Huang, Thermally Stable Energetic Salts Composed of Heterocyclic Anions and Cations Based on 3,6,7-Triamino-7 H-s-triazolo[5,1-c]-s-triazole: Synthesis and Intermolecular Interaction Study *ChemPlusChem* **2017**, *82*, 474-482.doi:10.1002/cplu.201700058

[5] Y. Tang, S. Dharavath, G. H. Imler, D. A. Parrish, J. M. Shreeve, Nitramino- and Dinitromethyl-Substituted 1,2,4-Triazole Derivatives as High-Performance Energetic Materials *Chemistry – A European Journal* **2017**, *23*, 9185-9191.doi:10.1002/chem.201701407

[6] A. A. Dippold, D. Izsák, T. M. Klapötke, C. Pflüger, Combining the Advantages of Tetrazoles and 1,2,3-Triazoles: 4,5-Bis(tetrazol-5-yl)-1,2,3-triazole, 4,5-Bis(1-hydroxytetrazol-5-yl)-1,2,3-triazole, and their Energetic Derivatives *Chemistry – A European Journal* **2016**, *22*, 1768-1778.doi:10.1002/chem.201504624

[7] A. A. Dippold, T. M. Klapötke, Nitrogen-Rich Bis-1,2,4-triazoles—A Comparative Study of Structural and Energetic Properties *Chemistry – A European Journal* **2012**, *18*, 16742-16753.doi:10.1002/chem.201202483

[8] D. Fischer, T. M. Klapötke, D. G. Piercey, J. Stierstorfer, Copper Salts of Halo Tetrazoles: Laser-Ignitable Primary Explosives *Journal of Energetic Materials* **2012**, *30*, 40-54.10.1080/07370652.2010.539998

[9] N. Fischer, D. Izsák, T. M. Klapötke, J. Stierstorfer, The Chemistry of 5-(Tetrazol-1-yl)-2H-tetrazole: An Extensive Study of Structural and Energetic Properties *Chemistry – A European Journal* **2013**, *19*, 8948-8957.doi:10.1002/chem.201300691

[10] T. M. Klapötke, M. Q. Kurz, R. Scharf, P. C. Schmid, J. Stierstorfer, M. Sućeska, 5-(1H-Tetrazolyl)-2-Hydroxy-Tetrazole: A Selective 2N-Monoxidation of Bis(1H-Tetrazole) *ChemPlusChem* **2015**, *80*, 97-106.doi:10.1002/cplu.201402124

[11] T. M. Klapötke, J. Stierstorfer, Nitration Products of 5-Amino-1H-tetrazole and Methyl-5-amino-1H-tetrazoles – Structures and Properties of Promising Energetic Materials *Helvetica Chimica Acta* **2007**, *90*, 2132-2150.doi:10.1002/hlca.200790220

[12] T. M. Klapötke, J. C. Stierstorfer, Energetic Tetrazole N-oxides **2014**, 133-178.doi:10.1002/9781118676448.ch06

[13] M. C. Schulze, B. L. Scott, D. E. Chavez, A high density pyrazolo-triazine explosive (PTX) *Journal of Materials Chemistry A* **2015**, *3*, 17963-17965.10.1039/C5TA05291B

[14] I. L. Dalinger, I. A. Vatsadse, T. K. Shkineva, G. P. Popova, B. I. Ugrak, S. A. Shevelev, Nitropyrazoles *Russian Chemical Bulletin* **2010**, *59*, 1631-1638.10.1007/s11172-010-0287-9

[15] D. G. Piercey, D. E. Chavez, B. L. Scott, G. H. Imler, D. A. Parrish, An Energetic Triazolo-1,2,4-Triazine and its N-Oxide *Angewandte Chemie International Edition* **2016**, *55*, 15315-15318.doi:10.1002/anie.201608723

[16] D. Kumar, G. H. Imler, D. A. Parrish, J. M. Shreeve, A Highly Stable and Insensitive Fused Triazolo–Triazine Explosive (TTX) *Chemistry – A European Journal* **2017**, *23*, 1743-1747.doi:10.1002/chem.201604919

[17] S. E. Creegan, D. G. Piercey, Nitroacetonitrile as a versatile precursor in energetic materials synthesis *RSC Advances* **2020**, *10*, 39478-39484.10.1039/D0RA07579E

[18] S. E. Creegan, M. Zeller, E. F. C. Byrd, D. G. Piercey, Synthesis and Characterization of the Energetic 3-Azido-5-amino-6-nitro-1,2,4-triazine *Propellants, Explosives, Pyrotechnics* **2021**, *46*, 214-221.https://doi.org/10.1002/prep.202000136

[19] S. E. Creegan, M. Zeller, E. F. C. Byrd, D. G. Piercey, Energetic 1,2,4-Triazines: 3,5-Diamino-6-nitro-1,2,4-triazine and Its Oxide *Crystal Growth & Design* **2021**, *21*, 3922-3927.10.1021/acs.cgd.1c00241

[20] K. O. Christe, D. A. Dixon, M. Vasiliu, R. I. Wagner, R. Haiges, J. A. Boatz, t. l. H. L. Ammon, Are DTTO and iso-DTTO Worthwhile Targets for Synthesis? *Propellants, Explosives, Pyrotechnics* **2015**, *40*, 463-468.doi:10.1002/prep.201400259

[21] T. M. Klapötke, D. G. Piercey, J. Stierstorfer, M. Weyrauther, The Synthesis and Energetic Properties of 5,7-Dinitrobenzo-1,2,3,4-tetrazine-1,3-dioxide (DNBTDO) *Propellants, Explosives, Pyrotechnics* **2012**, *37*, 527-535.10.1002/prep.201100151

[22] J. L. Mendoza-Cortes, Q. An, W. A. Goddard Iii, C. Ye, S. Zybin, Prediction of the crystal packing of di-tetrazine-tetroxide (DTTO) energetic material *Journal of Computational Chemistry* **2016**, *37*, 163-167.10.1002/jcc.23893

[23] D. G. Piercey, D. E. Chavez, S. Heimsch, C. Kirst, T. M. Klapötke, J. Stierstorfer, An Energetic N-Oxide and N-Amino Heterocycle and its Transformation to 1,2,3,4-Tetrazine-1-oxide *Propellants, Explosives, Pyrotechnics* **2015**, *40*, 491-497.doi:10.1002/prep.201400224

[24] X. Song, J. Li, H. Hou, B. Wang, Extensive theoretical studies of a new energetic material: Tetrazino-tetrazine-tetraoxide (TTTO) *Journal of Computational Chemistry* **2009**, *30*, 1816-1820.doi:10.1002/jcc.21182

[25] G. Wang, T. Lu, G. Fan, C. Li, H. Yin, F.-X. Chen, The Chemistry and Properties of Energetic Materials Bearing [1,2,4]Triazolo[4,3-b][1,2,4,5]tetrazine Fused Rings *Chemistry – An Asian Journal* **2018**, *13*, 3718-3722.10.1002/asia.201801145

[26] H. Wei, H. Gao, J. M. Shreeve, N-Oxide 1,2,4,5-Tetrazine-Based High-Performance Energetic Materials *Chemistry – A European Journal* **2014**, *20*, 16943-16952.10.1002/chem.201405122

[27] H. Wei, J. Zhang, J. M. Shreeve, Synthesis, Characterization, and Energetic Properties of 6-Amino-tetrazolo[1,5-b]-1,2,4,5-tetrazine-7-N-oxide: A Nitrogen-Rich Material with High Density *Chemistry – An Asian Journal* **2015**, *10*, 1130-1132.10.1002/asia.201500086

[28] C. C. Ye, Q. An, W. A. Goddard Iii, T. Cheng, W.-G. Liu, S. V. Zybin, X.-H. Ju, Initial decomposition reaction of di-tetrazine-tetroxide (DTTO) from quantum molecular dynamics: implications for a promising energetic material *Journal of Materials Chemistry A* **2015**, *3*, 1972-1978.10.1039/C4TA05676K

[29] G. D. Zhang, Z. Wang, J.-G. Zhang, An Unusual Layered Crystal Packing Gives Rise to a Superior Thermal Stability of Energetic Salt of 3,6-Bishydrazino-1,2,4,5-tetrazine *Zeitschrift fur Anorganische und Allgemeine Chemie* **2018**, *644*, 512-517.10.1002/zaac.201800086

[30] C. He, J. M. Shreeve, Energetic Materials with Promising Properties: Synthesis and Characterization of 4,4′-Bis(5-nitro-1,2,3-2H-triazole) Derivatives *Angewandte Chemie International Edition* **2015**, *54*, 6260-6264.https://doi.org/10.1002/anie.201412303

[31] D. E. Chavez, J. C. Bottaro, M. Petrie, D. A. Parrish, Synthesis and Thermal Behavior of a Fused, Tricyclic 1,2,3,4-Tetrazine Ring System *Angewandte Chemie International Edition* **2015**, *54*, 12973-12975.10.1002/anie.201506744

[32] D. R. Wozniak, B. Salfer, M. Zeller, E. F. C. Byrd, D. G. Piercey, Sensitive Energetics from the N-Amination of 4-Nitro-1,2,3-Triazole *ChemistryOpen* **2020**, *9*, 806-811.https://doi.org/10.1002/open.202000053

[33] T. M. Klapotke, D. G. Piercey, J. r. Stierstorfer, Amination of energetic anions: high-performing energetic materials *Dalton Transactions* **2012**, *41*, 9451-9459.10.1039/C2DT30684K

[34] T. M. Klapötke, C. M. Sabaté, Safe 5-nitrotetrazolate anion transfer reagents *Dalton Transactions* **2009**, 1835-1841.10.1039/B818900P

[35] T. M. Klapötke, D. G. Piercey, N. Mehta, K. D. Oyler, M. Jorgensen, S. Lenahan, J. S. Salan, J. W. Fronabarger, M. D. Williams, Preparation of High Purity Sodium 5-Nitrotetrazolate (NaNT): An Essential Precursor to the Environmentally Acceptable Primary Explosive, DBX-1 *Zeitschrift fur Anorganische und Allgemeine Chemie* **2013**, *639*, 681-688.https://doi.org/10.1002/zaac.201300010

[36] N. Fischer, T. M. Klapötke, M. Reymann, J. Stierstorfer, Nitrogen-Rich Salts of 1H,1′H-5,5′-Bitetrazole-1,1′-diol: Energetic Materials with High Thermal Stability *European Journal of Inorganic Chemistry* **2013**, *2013*, 2167-2180.https://doi.org/10.1002/ejic.201201192

[37] NATO Standardization Agreement (STANAG) on Explosives, Impact Sensitivity Test, no. 4489, 1, Brussels, September 17, **1999**.

[38] NATO Standardization Agreement (STANAG) on Explosives, Friction Sensitivity Tests, no. 4487, 1, Brussels, August 22, **2002**.

[39] WIWEB-Standardarbeitsanweisung 4-5.1.02, Ermittlung der Explosions- gefährlichkeit, hier: der Schlagempfindlichkeit mit demFallhammer, Erding, November 8, **2002**.

[40] WIWEB-Standardarbeitsanweisung 4-5.1.03, Ermittlung der Explosions gerfährlichkeit oder der Reibeempfindlichkeir mit dem Reibeapparat, Erding, November 8, **2002**.

[41] BAM, https://www.bam.de/.

[42] ″Impact: Insensitive > 40 J, Sensitive ≥ 4 J, Very Sensitive ≤ 3 J; Friction: Insensitive > 360 N, Less Sensitive = 360 N, Sensitive < 360 N and > 80 N, Very Sensitive ≤ 80 N, Extremely Sensitive ≤ 10 N.″ *Recommendations on the Transport of Dangerous Goods: Manual of Tests and Criteria, UN, **2003.***

5. TITANIUM SUPEROXIDE FOR THE OXIDATION OF AMINES: SYNTHESIS OF BIS(3-NITRO-1H-1,2,4-TRIAZOL-5-YL)METHANE AND ITS METAL SALTS

Authors: Shannon E. Creegan, Matthias Zeller, Edward F. C. Byrd, Davin G. Piercey
Funding: Financial support of this work was provided by the Office of Naval Research under grant N00014-19-1-2089. Our lab is also supported by Purdue University and The Army Research Office (ARO). The National Science Foundation is acknowledged through the Major Research Instrumentation Program under Grant No. CHE 1625543 for the single crystal X-ray diffractometer.

5.1 Abstract

Bis(3-nitro-1H-1,2,4-triazol-5-yl)methane (BNTM) was synthesized in 79 % yield via the oxidation of 5,5´-diamino-3,3'-methylene-1H-1,2,4-triazole (DABTM) with titanium superoxide in a water and hydrogen peroxide solution. BNTM synthesized by this method was characterized via low-resolution mass spectrometry (LRMS), nuclear magnetic resonance spectroscopy (NMR), infrared spectroscopy (IR), elemental analysis, and single crystal X-ray crystallography for comparison with BNTM produced by traditional routes. The cesium, lithium, potassium, rubidium, sodium, and strontium salts of BNTM were characterized for their thermal stabilities and mechanical sensitives. Each of the salts possessed multiple hydrates, the loss of the associated water can clearly be seen by thermal gravimetric analysis (TGA). All the salts were less sensitive to impact than neutral BNTM and, except for the sodium and cesium salts, were less sensitive to friction. Single crystal X-ray crystallography was utilized to analyze the crystal structures obtained for the cesium, strontium, and sodium salts.

5.2 Introduction

Pyrotechnics are a subgroup of energetic materials which are designed to produce light, heat, gas, smoke, or sound [1]. Commonly used in road flares and fireworks the toxicity of traditional pyrotechnics has resulted in many being banned in recent years under stricter environmental regulations [2], and as such the need for materials with environmentally safer components has grown. Metal salts of high-nitrogen anions, such as lithium and strontium are one method of designing new pyrotechnic ingredients.

Research into new energetics is driven by the need for high performing materials that are environmentally friendly, inexpensive, and insensitive towards stimuli. The successful adoption of new materials is dependent, not only on performance, but also on economic feasibility and regulatory compliance. While being high performing, traditional energetic materials are often expensive to produce, sensitive towards stimuli, and are either hazardous substances themselves or generate them during their synthesis. High-nitrogen heterocyclic systems possessing increased heats of formation and ring-strain have become staple backbones for new energetics[3-9]. With the creation of an inherently energetic backbone, modification of performance and sensitivity through the presence of select explosophores is key.

The nitro group may act as both a source of energy through the addition of oxygen which can oxidize fuel moieties in a molecule and as a stabilizing group through inter- and intramolecular bonding. Traditional methods of nitro addition are nitration (mixed acid), the modified Sandmeyer, and amine oxidation reactions. Nitration reactions are widely used due to ease of reaction and the ability to separate products from spent acid [10]; a drawback of this traditional method is the large amount of acidic waste. The alternative Sandmeyer reaction proceeds though an unstable diazo intermediate [11] which creates very sensitive intermediate explosive materials when on a heterocyclic backbone [12]. Amine oxidation through the use of oxidants such as hydrogen peroxide, Oxone®, and potassium permanganate [13-15] are also known; however, oxidation reactions are often aggressive, hard to direct, and the process of oxidizing the amine is usually complicated due to competing pathways leading to a range of products [16] such as azo- and azoxy-compounds as well as nitroso compounds.

As oxidation reactions may allow for the avoidance of hazardous conditions, such as large amounts of acids and the creation of unstable diazo intermediates, research into the use of metal-stabilized superoxide in biological syntheses has expanded [17-21]. Metal-superoxides, such as potassium [12-13] and titanium superoxide [16, 19, 22], present the possibility for more predictable and controlled routes [22]. Potassium superoxide generates the superoxide anion in the presence of polar aprotic solvents [12] while titanium superoxide in hydrogen peroxide solution generates superoxide anions on the hydrated titanium matrix from the decomposition of hydrogen peroxide [16]. In the field of energetic materials, the use of superoxide for oxidation reactions is novel. To date potassium superoxide has been used in the synthesis of energetic materials such as 3-amino-5-nitro-1,2,4-triazole (ANTA),[13] 5-nitrotetrazole, [12] 2-nitrobenzimidazole [23] and

5-(5-nitro-2H-1,2,3-triazol-4-yl)-1H-tetrazole [24] while the use of titanium superoxide remains relatively unknown.

In this work, we synthesized bis(3-nitro-1H-1,2,4-triazol-5-yl)methane (BNTM) from 5,5´-diamino-3,3'-methylene-1H-1,2,4-triazole (DABTM) via oxidation of the amines using titanium superoxide and hydrogen peroxide. BNTM was previously synthesized in 1970 by Bagal *et al.* [25] as part of a study on nitro derivatives and characterized as an energetic in 2020 by Yan *et al.* [26] In both cases BNTM was synthesized using non-catalytic Sandmeyer reactions at elevated temperatures (≥ 40 °C). Additionally, we determined BNTM held potential as a pyrotechnic backbone and thus synthesized and characterized the sensitivity of six colored salts: cesium, lithium, potassium, rubidium, sodium, and strontium.

5.3 Results and Discussion

5.3.1 Synthesis

For comparison, we first developed an optimized nitration pathway reaction towards the synthesis of BNTM. The method we employed (Scheme 13. Method A) was based on a modification of the synthesis for silver 3,6-dinitro-[1,2,4]triazolo[4,3-b][1,2,4]triazolate [27]. A solution of DABTM in water and 20% sulfuric acid was added dropwise to a solution of sodium nitrite while maintaining a temperature between 60 and 70 °C. The combined mixture was then stirred for 2 hours at temperature before being subsequently cooled, acidified, and extracted with ethyl acetate. This method utilized a different temperature system than that of Bagal *et al*. (45 °C) or Yan *et al.* [26] who used two different temperatures for the addition (40 °C) and stir periods (100 °C).

Avoiding nitration or Sandmeyer conditions we then attempted synthesizing BNTM using various oxidizing agents and conditions (Scheme 13. Method B). Initial attempts to oxidize DABTM to BNTM were made using potassium superoxide in THF or DMSO. These attempts were unsuccessful resulting in no change to the precursor. However, the oxidation of DABTM to BNTM using titanium superoxide in water and hydrogen peroxide resulted in a yield of 78.5% of a pale-yellow solid, which was analytically identical to the material produced via traditional nitration methods.

The titanium superoxide utilized in the reaction with DABTM was prepared by dropwise addition of 50% hydrogen peroxide to a solution of titanium isopropoxide and anhydrous methanol in an argon atmosphere over 40 minutes [19]. The pale-yellow precipitate was collected by filtration and dried in a desiccator with Drierite® overnight. To a vigorously stirred solution of DABTM in water and 50% hydrogen peroxide, titanium superoxide was slowly added in four portions every 30 minutes, being mindful of foaming. After stirring overnight, the precursor had completely reacted to the di-nitro and single-nitro derivatives. After 72 hours all singly nitrated material had fully converted to di-nitrated BNTM. At this point the material was extracted from solution with ethyl acetate and evaporation of the extracts resulted in a bright-yellow solid. Purification of this solid was achieved by recrystallization from water yielding a pale-yellow solid. It was noted that the effectiveness of the reaction was strongly impacted by the purity and freshness of the titanium superoxide with the best results obtained when the superoxide was no older than 3-days and completely dry.

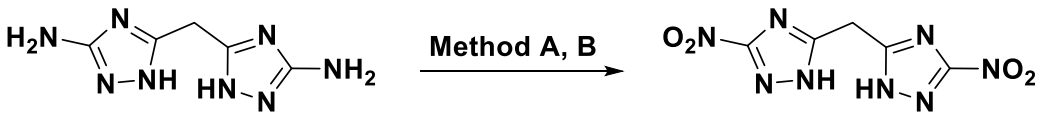

Scheme 13. Synthesis of BNTM via routes A) $NaNO_2$, 20% H_2SO_4 and B) Titanium superoxide, H_2O_2, H_2O.

Attempts were made to form the ammonium, hydrazinium, and hydroxylammonium salts by dissolving BNTM in water and adding the associated base (ammonia, hydrazine hydrate, and hydroxylamine) to the solution. However, each of the attempts resulted in the crystallization of BNTM out of solution. It was concluded BNTM was not sufficiently acidic to protonate these weak bases and that the materials' respective pK_a values were incompatible for the formation of proton transfer salts. Using much stronger bases, such as metal hydroxide, we were successful in deprotonating BNTM and were able to synthesize various BNTM metal salts: potassium, sodium, lithium, cesium, rubidium, and strontium. For the five alkali metal salts (Scheme 14) the respective hydroxide solution was added dropwise to a slurry of BNTM in water at 10 °C. After addition was complete BNTM was fully dissolved in the lithium and sodium batches; for the potassium, cesium, and rubidium batches, however, there was still undissolved BNTM after stirring for 30 minutes, so additional portions of hydroxide were added. Even after the addition of excess base the reaction

mixtures of the cesium and rubidium salts still contained undissolved BNTM. For purification of the metal salts, the solvent volume was doubled, and the solutions were heated to 60 °C before being filtered through a 0.45-micron syringe filter. For all salts the solvent, was removed by slow evaporation resulting in the formation of hydrated BNTM metal salts.

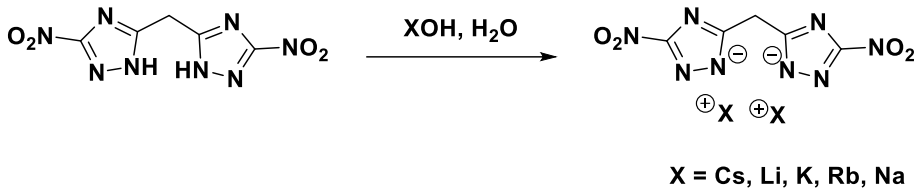

Scheme 14. General Synthesis for the Cesium, Lithium, Potassium, Rubidium, and Sodium salts of BNTM.

The strontium salt was synthesized by the addition of a solution of sodium hydroxide in water to a slurry of BNTM and strontium nitrate (Scheme 15). The solvent was removed by evaporation and the material recrystallized out of water yielding the hydrated strontium salt.

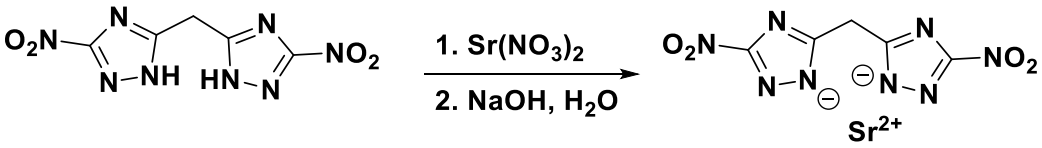

Scheme 15. Synthesis of the Strontium Salt of BNTM.

5.3.2 Spectroscopy

The progress of oxidation was monitored by electrospray ionization (ESI) low-resolution mass spectrometry. The formation of the single-nitro was observed in both positive [M+H] and negative [M-H] modes at 211 and 209 m/z, respectively. BNTM was observed in negative mode as two peaks at 239 m/z for [M-H] and at 479 m/z corresponding to [2M-H]. The infrared spectra of BNTM had bands characteristic of N-O stretches at 1537 and 1487 cm^{-1}. All metal salts possessed a distinct band in the 3600 – 3000 cm^{-1} range correlating to the presence of water in the materials.

By nuclear magnetic resonance (NMR), it was verified that both synthesis methods produce BNTM, with a single peak at 4.59 ppm in the proton spectrum corresponding to the methylene

hydrogen atoms. In the carbon spectra three peaks were observed at 162.9, 153.7, and 25 ppm corresponding to the nitro-bound triazole carbon, the methylene bound triazole carbon, and the methylene carbon respectively. The peaks positions are in agreement with the values reported by Yan *et al*.[26] No difference in the NMR spectra between BNTM and its salts was resolved, and salt purity was therefore verified by elemental analysis. Elemental analysis as well as thermal gravimetric analysis (TGA) indicated that each salt possessed between one and six water molecules of hydration. (All spectra can be found in SI)

5.3.3 Crystallography

Crystallization of BNTM from hot water gave pale-yellow needle-like crystals (Figure 15). BNTM crystals were also obtained from ethanol, methanol, and isopropanol. The crystallography data collected from BNTM synthesized via oxidation matches those reported by Yan *et al*.,[26] and BNTM crystallized in the orthorhombic *Fdd*2 space group with eight formula units per unit cell and possessed a room temperature density of 1.67 g cm^{-3}.

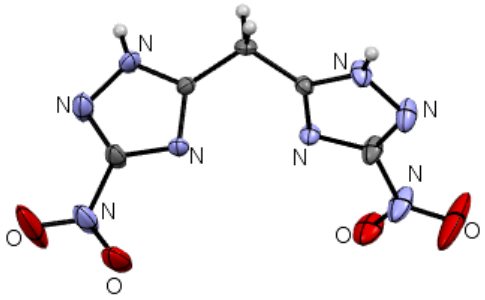

Figure 15. Molecular unit of BNTM. Ellipsoids are drawn at the 50% probability level.

The crystal structure for the strontium, sodium, and cesium salts were obtained via slow evaporation after redissolving in hot water. The strontium salt crystalized in the triclinic $P\bar{1}$ space group with two formula units in the unit cell and 7.17 water molecules of hydration per unit of (BNTM)Sr (Figure 16a). Five of these water molecules are covalently bonded to the strontium cation, forming isolated (BNTM)Sr$(OH_2)_5$ molecules. The strontium cation is coordinated solely to the two isolated triazolate nitrogen atoms, in a chelating fashion. The other two heterocycle nitrogen atoms are not metal bound and are instead involved in O-H…N hydrogen bonds. These,

and additional O-H…O hydrogen bonds are connecting the (BNTM)Sr(OH_2)$_5$ molecules to each other in the solid state. One of the interstitial hydrate water molecules is tightly H-bound and well defined. The other is excessively disordered (see appendix B for a detailed description of structure and disorder refinement). The sodium salt crystallized in the monoclinic *C*2/*c* space group with four formula units per unit cell and three hydrate water molecules covalently bound to the sodium cation per unit of (BNTM)Na_2 (Figure 16b). The cesium salt also crystalized in the monoclinic *C*2/*c* space group with four formula units per unit cell (Figure 16c). It features two hydrate units covalently bound to the metal ion. Both the Cs and Na salts form infinite 3D lattices in which the cations are bound to triazolate nitrogen atoms. The sodium is seven-coordinate, to three nitro O-atoms, two triazolate N-atoms, and two water molecules. The two triazolate N-atoms coordinate in a chelating fashion with each one nitro-O atom. The third coordinated nitro group binds in a terminal way. The water molecules bridge between Na ions and are H-bonded to the third nonmetal coordinated triazole N-atoms. In the Cs salt two water molecules bridge between two Cs cations and are H-bound to triazolate N-atoms of neighboring units. Nitro O-atoms coordinate in a monodentate fashion, triazolate N atoms are either monodentate or bidentate bridging, with one being side-on coordinated to the Cs cation. The total coordination number of the cation is ten, from two water molecules, four nitro-O atoms, and four triazolate N-atoms.

The vastly different structures, isolated (BNTM)Sr(OH_2)$_5$ with ill-defined waters of solvation for the strontium salts and heavily interconnected 3D networks for the Na and Cs salts, have a large impact on the densities of the salts. At 150 K, the density for the strontium salt is only 1.85 g cm^{-3}, barely surpassing that of the Na salt at 1.80 g cm^{-3} despite the much lower atomic weight of sodium, The highest density is at 2.64 g cm^{-3} observed for the Cs salt being both densely packed and featuring a heavy metal ion.

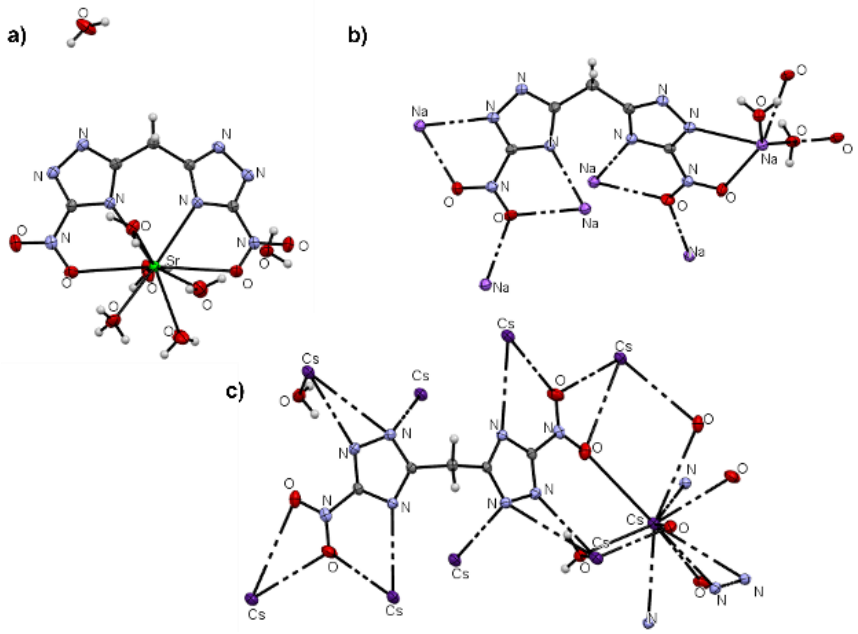

Figure 16. a) Hydrated strontium salt b) hydrated sodium salt c) hydrated cesium salt.

5.3.4 Thermal Stabilities and Energetic Properties

Thermal stabilities were measured by Thermal Gravimetric Analysis (TGA) in platinum pans with a heating rate of 5 °C per minute. The onset of decomposition temperature was determined as the temperature at which 5 % of the initial mass was lost, after loss of solvate water molecules. Based on this criterion, it was determined that the onset of decomposition occurred at approximately 250 °C for BNTM, similar to the value reported by Yan *et al*. [26] The lithium, sodium, strontium, and cesium salts displayed onset decomposition temperatures of 260, 247, 230, and 210 °C respectively. The potassium salt possessed an onset decomposition temperature of 210 °C and displayed a mass spike followed by an abrupt decomposition at 250 °C. The latter trend was similarly displayed in the rubidium salt at 248 °C. This trend could be explained by energetic decomposition or an intense release of gas. Which is also suspected to account for the descrienpency between expected and actual residual mass for the elemental analysis determined di-Rubidium salt. (Summarized in Table 5).

For all the salts, initial loss of hydrate waters was clearly observed in the TGA. There were two separate events of water loss in the lithium and strontium salts, while hydrate loss for cesium, potassium, and sodium occurred in one single step. This agrees with the presence of two types of water molecules in the crystal structure of the Sr salt (metal coordinated and interstitial), while

only metal coordinated water is present for the sodium and cesium structures. For the lithium and potassium salts, of which no single crystal structures could be obtained, one can assume the presence of both tightly and weakly bound water (for Li, elemental analysis and TGA suggest a trihydrate) and just tightly bound water (for K, elemental analysis and TGA suggest a monohydrate). For the rubidium salt, the loss of water is drawn out over a long temperature range (ending at 110 °C) with no distinct water loss events, indicating the presence of multiple types of water molecules with varying binding energies (Elemental analysis suggests a trihydrate).

The observed weight loss which occurred due to hydrate loss, was converted to number of hydrate units lost by the material. The cesium and rubidium salts underwent single step hydrate losses, with rubidium salt displaying a 4 % weight loss corresponding to the loss of a single hydrate (from 3 to 2 hydrates), while cesium salt showed a 7 % weight loss indicating loss of 2 hydrates (from 2 to 0 hydrates). For these salts, the original total number of hydrates matched the values generated by crystal analysis and elemental analysis. For the salts in which 2-step hydrate losses were observed the combined weight loss, for both steps, was used to calculate hydrate loss. The strontium salt exhibited 13 % weight loss corresponding to the loss of 3 hydrates (5 to 2), the lithium salt displayed a 22 % weight loss for 4 hydrates (4 to 0), the sodium salt showed 12 % weight loss for 2 hydrates (2 to 0), and the potassium salt presented 9 % weight loss for 2 hydrates (4 to 2). The nonequivalence in hydrate numbers between crystal structure, elemental analysis, and TGA was due to the duration of storage time in a desiccator with Drierite® before the respective analyses were performed.

Table 5. Onset of decomposition temperatures for BNTM and salts

	BNTM	Sr	Li	Na	Cs	K	Rb
$T_{dec.}$ [°C] [a]	250	230	260	247	210	210/250	248

[a] Onset decomposition temperature from TGA (β = 5 °C).

Friction sensitivity was performed according to STANAG 4487 [28] and modified according to instruction [29] using a BAM friction tester. Impact sensitivity was tested using an OZM drop hammer using the BAM method[30] according to STANAG 4489[31] and modified according to instruction [32]. Based on “UN recommendations on the transport of dangerous goods” [33], we determined BNTM to be sensitive to both friction, 120 N, and impact, 20 J.

Comparatively, the strontium, sodium, cesium, and rubidium salts were determined to be insensitive to impact, > 40 J, while the potassium and lithium salt were less sensitive at 40 J. The strontium, rubidium, lithium, and potassium salts were less sensitive than BNTM, with values of 360, 240, 216, and 120 – 160 N, respectively, earning the classifications of less sensitive and sensitive. The sodium and cesium salts were more sensitive to friction than BNTM and the other salts, though still classified as sensitive, with sensitivity values of 108 for cesium and between 108 and 120 N for sodium. (Summarized in Table 6).

Table 6. Mechanical Sensitivities for BNTM and salts

	BNTM	Sr	Na	K	Li	Cs	Rb
IS [J][a]	20	>40	>40	40	40	> 40	> 40
FS [N][b]	120	360	108-120	120 - 160	216	108	240

[a] Impact sensitivity (BAM drophammer (1 of 6)). [b] Friction sensitivity (BAM friction tester (1 of 6)).

Burn images for each salt were obtained for comparison. The lithium and strontium salts displayed their characteristic red flame (Figure 17a, b), the sodium salt was yellow (Figure 17c), and both the cesium and rubidium salts produce violet flames (Figure 17d, e). Due to a small percentage of sodium being present in the potassium hydroxide used to synthesize the potassium salt the potassium flame color was overwhelmed (Figure 17f).

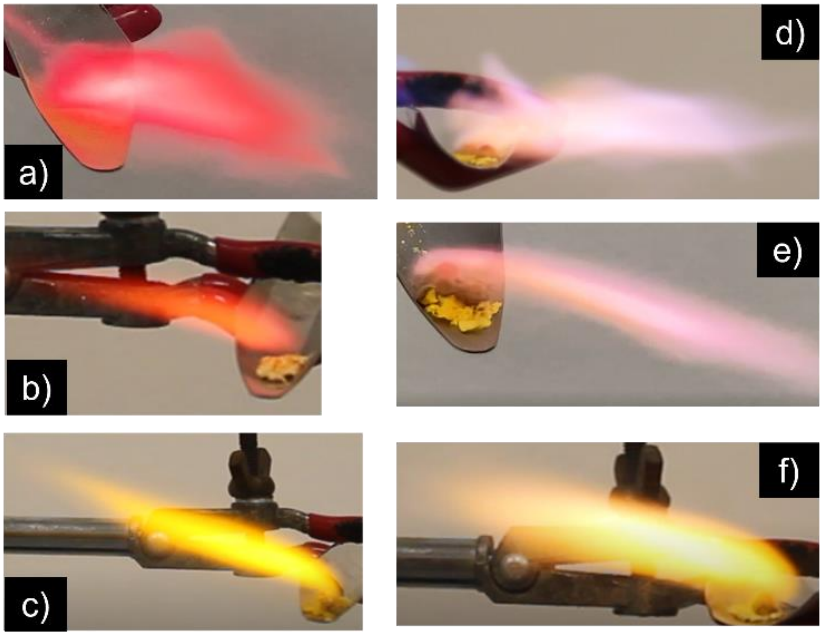

Figure 17. Burn images of BNTM salts: a) strontium, b) lithium, c) sodium, d) cesium, e) strontium, d) potassium with sodium contamination.

The solid-state heat of formation for BNTM was calculated using Gaussian09[34] to be 254.98 kJ mol^{-1}. The calculated oxygen balance of BNTM was reported to be -53.3 %. The detonation parameters at the CJ point and the oxygen balance were calculated using EXPLO5v6.05. This provided a detonation pressure of 20.6 GPa and a detonation velocity of 7361 m s^{-1}.

5.4 Conclusion

BNTM was successfully synthesized from DABTM via oxidation with titanium superoxide. This oxidation method resulted in 79 % of the total producible amount of BNTM, comparable to the 79 % produced by a modified Sandmeyer reaction while avoiding the use of acid and the unstable diazonium intermediate. Six salts of BNTM, cesium, lithium, potassium, rubidium, sodium, and strontium were synthesized and characterized. These salts occurred as hydrates with roughly the same thermal stability as free BNTM. The salts were less sensitive to stimuli than BNTM, except the sodium and cesium salts which were more sensitive to friction.

5.5 References

[1] G. Steinhauser, T. M. Klapötke, Using the Chemistry of Fireworks To Engage Students in Learning Basic Chemical Principles: A Lesson in Eco-Friendly Pyrotechnics *Journal of Chemical Education* **2010**, *87*, 150-156.10.1021/ed800057x

[2] J. J. Sabatini, A Review of Illuminating Pyrotechnics *Propellants, Explosives, Pyrotechnics* **2018**, *43*, 28-37.https://doi.org/10.1002/prep.201700189

[3] A. A. Dippold, T. M. Klapötke, Nitrogen-Rich Bis-1,2,4-triazoles—A Comparative Study of Structural and Energetic Properties *Chemistry – A European Journal* **2012**, *18*, 16742-16753.doi:10.1002/chem.201202483

[4] N. Fischer, D. Fischer, T. M. Klapötke, D. G. Piercey, J. Stierstorfer, Pushing the limits of energetic materials – the synthesis and characterization of dihydroxylammonium 5,5′-bistetrazole-1,1′-diolate *Journal of Materials Chemistry* **2012**, *22*, 20418-20422.10.1039/C2JM33646D

[5] N. Fischer, D. Izsák, T. M. Klapötke, J. Stierstorfer, The Chemistry of 5-(Tetrazol-1-yl)-2H-tetrazole: An Extensive Study of Structural and Energetic Properties *Chemistry – A European Journal* **2013**, *19*, 8948-8957.doi:10.1002/chem.201300691

[6] T. M. Klapötke, T. G. Witkowski, 5,5′-Bis(2,4,6-trinitrophenyl)-2,2′-bi(1,3,4-oxadiazole) (TKX-55): Thermally Stable Explosive with Outstanding Properties *ChemPlusChem* **2016**, *81*, 357-360.https://doi.org/10.1002/cplu.201600078

[7] Y. Tang, C. He, G. H. Imler, D. A. Parrish, J. M. Shreeve, Aminonitro Groups Surrounding a Fused Pyrazolotriazine Ring: A Superior Thermally Stable and Insensitive Energetic Material *ACS Applied Energy Materials* **2019**, *2*, 2263-2267.10.1021/acsaem.9b00049

[8] M. A. Hiskey, D. E. Chavez, D. L. Naud, Los Alamos National Lab., NM (US), **2001**.

[9] K. O. Christe, D. A. Dixon, M. Vasiliu, R. I. Wagner, R. Haiges, J. A. Boatz, t. l. H. L. Ammon, Are DTTO and iso-DTTO Worthwhile Targets for Synthesis? *Propellants, Explosives, Pyrotechnics* **2015**, *40*, 463-468.doi:10.1002/prep.201400259

[10] T. Urbanski, S. Laverton, W. Ornaf, *Chemistry and technology of explosives, Vol. 1*, pergamon press New York, NY, **1964**.

[11] G. David, Reactions of Amines **1967**, 62-123.https://doi.org/10.1016/B978-0-08-011913-7.50014-8

[12] D. M. Smith, T. D. Manship, D. G. Piercey, Synthesis of 5-Nitrotetrazolates by the Direct Oxidation of 5-Aminotetrazole in a Single-Pot Synthesis without Isolation of Explosive Intermediates *ChemPlusChem* **2020**, *85*, 2039-2043.https://doi.org/10.1002/cplu.202000487

[13] T. D. Manship, D. M. Smith, D. G. Piercey, An Improved Synthesis of the Insensitive Energetic Material 3-Amino-5-Nitro-1,2,4-triazole (ANTA) *Propellants, Explosives, Pyrotechnics* **2020**, *45*, 1621-1626.https://doi.org/10.1002/prep.202000097

[14] N. Kornblum, R. J. Clutter, W. J. Jones, The Synthesis of Tertiary Nitroparaffins1,2 *Journal of the American Chemical Society* **1956**, *78*, 4003-4004.10.1021/ja01597a036

[15] G. P. Sollott, E. E. Gilbert, A facile route to 1,3,5,7-tetraaminoadamantane. Synthesis of 1,3,5,7-tetranitroadamantane *The Journal of Organic Chemistry* **1980**, *45*, 5405-5408.10.1021/jo01314a051

[16] G. K. Dewkar, M. D. Nikalje, I. Sayyed Ali, A. S. Paraskar, H. S. Jagtap, A. Sudalai, An Exceptionally Stable Ti Superoxide Radical Ion: A Novel Heterogeneous Catalyst for the Direct Conversion of Aromatic Primary Amines to Nitro Compounds *Angewandte Chemie International Edition* **2001**, *40*, 405-408.https://doi.org/10.1002/1521-3773(20010119)40:2<405::AID-ANIE405>3.0.CO;2-6

[17] R. B. Kamble, K. D. Mane, B. D. Rupanawar, P. Korekar, A. Sudalai, G. Suryavanshi, Ti-superoxide catalyzed oxidative amidation of aldehydes with saccharin as nitrogen source: synthesis of primary amides *RSC Advances* **2020**, *10*, 724-728.10.1039/C9RA10413E

[18] T. M. Shaikh, P. U. Karabal, G. Suryavanshi, A. Sudalai, Titanium superoxide: a heterogeneous catalyst for anti-Markovnikov aminobromination of olefins *Tetrahedron Letters* **2009**, *50*, 2815-2817.https://doi.org/10.1016/j.tetlet.2009.03.169

[19] R. Santhosh Reddy, T. M. Shaikh, V. Rawat, P. U. Karabal, G. Dewkar, G. Suryavanshi, A. Sudalai, A Novel Synthesis and Characterization of Titanium Superoxide and its Application in Organic Oxidative Processes *Catalysis Surveys from Asia* **2010**, *14*, 21-32.10.1007/s10563-010-9085-5

[20] S. Dey, S. K. Gadakh, A. Sudalai, Titanium superoxide – a stable recyclable heterogeneous catalyst for oxidative esterification of aldehydes with alkylarenes or alcohols using TBHP as an oxidant *Organic & Biomolecular Chemistry* **2015**, *13*, 10631-10640.10.1039/C5OB01586C

[21] S. Heinrich, M. Plettig, E. Klemm, Role of the Ti(IV)-Superoxide Species in the Selective Oxidation of Alkanes with Hydrogen Peroxide in the Gas Phase on Titanium Silicalite-1: An In Situ EPR Investigation *Catalysis Letters* **2011**, *141*, 251-258.10.1007/s10562-010-0534-6

[22] G. K. Dewkar, T. M. Shaikh, S. Pardhy, S. S. Kulkarni, A. Sudalai, Titanium Superoxide Catalyzed Selective Oxidation of Phenols to p-Quinones with aq. H2O2 *ChemInform* **2005**, *36*.https://doi.org/10.1002/chin.200545095

[23] T. M. Klapötke, A. Preimesser, J. Stierstorfer, Energetic Derivatives of 2-Nitrimino-5,6-dinitro-benzimidazole *Propellants, Explosives, Pyrotechnics* **2015**, *40*, 60-66.https://doi.org/10.1002/prep.201400045

[24] D. Izsák, T. M. Klapötke, C. Pflüger, Energetic derivatives of 5-(5-amino-2H-1,2,3-triazol-4-yl)-1H-tetrazole *Dalton Transactions* **2015**, *44*, 17054-17063.10.1039/C5DT03044G

[25] L. I. Bagal, M. S. Pevzner, A. N. Frolov, N. I. Sheludyakova, Heterocyclic nitro compounds *Chemistry of Heterocyclic Compounds* **1970**, *6*, 240-244.10.1007/BF00475005

[26] B. Yan, H. Li, H. Ma, Y. Ma, X. Ma, F. Zhao, Crystal Structure, Thermal Behavior and Detonation Characterization of Bis(3-nitro-1H-1,2,4-triazol-5-yl)methane *Propellants, Explosives, Pyrotechnics* **2020**, *45*, 1714-1719.https://doi.org/10.1002/prep.202000004

[27] M. L. Gettings, M. Zeller, E. Byrd, D. G. Piercey, Synthesis and Characterization of Salts of the 3,6-Dinitro-[1,2,4]triazolo[4,3-b][1,2,4]triazolate Anion: Insensitive Energetic Materials Available From Economical Precursors *Zeitschrift fur Anorganische und Allgemeine Chemie* **2019**, *645*, 1197-1204.https://doi.org/10.1002/zaac.201900164

[28] NATO Standardization Agreement (STANAG) on Explosives, Friction Sensitivity Tests, no. 4487, 1, Brussels, August 22, **2002**.

[29] WIWEB-Standardarbeitsanweisung 4-5.1.03, Ermittlung der Explosions gerfährlichkeit oder der Reibeempfindlichkeir mit dem Reibeapparat, Erding, November 8, **2002**

[30] BAM, https://www.bam.de/.

[31] NATO Standardization Agreement (STANAG) on Explosives, Impact Sensitivity Test, no. 4489, 1, Brussels, September 17, **1999**.

[32] WIWEB-Standardarbeitsanweisung 4-5.1.02, Ermittlung der Explosions- gefährlichkeit, hier: der Schlagempfindlichkeit mit demFallhammer, Erding, November 8, **2002.**

[33] "Impact: Insensitive > 40 J, Sensitive ≥ 4 J, Very Sensitive ≤ 3 J; Friction: Insensitive > 360 N, Less Sensitive = 360 N, Sensitive < 360 N and > 80 N, Very Sensitive ≤ 80 N, Extremely Sensitive ≤ 10 N." *Recommendations on the Transport of Dangerous Goods: Manual of Tests and Criteria, UN, **2003.***

[34] M. J. Frisch, J. A. Pople, J. S. Binkley, Self-consistent molecular orbital methods 25. Supplementary functions for Gaussian basis sets *The Journal of Chemical Physics* **1984**, *80*, 3265-3269.10.1063/1.447079

6. SYNOPSIS

1,2,4-Triazine [1-3]

The reaction of diazotetrazole with the stable potassium salt of nitroacetonitrile is a straightforward synthesis for the single-step formation of energetic 3-azido-5-amino-6-nitro-1,2,4-triazine (AANT) which stood as an excellent base for various functional group modifications. The first change was performed by oxidation, using hypofluorous acid, forming an *N*-oxide of indeterminant position as all attempts to isolate the material resulted in decomposition. The *N*-oxide decomposed in the presence of water, salt, acid, base, or drying agents. The second structural change, saw the reduction of the AANT azide via a modified Staudinger reaction readily yielding 3,5-diamino-6-nitro-1,2,4-triazine (DANT) which was oxidized with potassium peroxymonosulfate triple salt (Oxone®) gaining an *N*-oxide converting to 3,5-diamino-6-nitro-1,2,4-triazine-2-oxide (DANTX). Alternatively, when DANT was aminated with *O*-tosylhydroxylamine (THA) it gained an *N*-amine, on the same ring nitrogen atom as the DANTX oxide, forming 2,3,5-triamino-6-nitro-1,2,4-triazin-2-ium (TANT+). Four energetic triazinium TANT+ salts were synthesized by metathesis reactions.

AANT possessed a low thermal stability decomposing at 162 °C and was determined to be sensitive to both friction and impact by the UN recommendations on the transport of dangerous goods [4]. It had reasonable performance with a detonation pressure of 28.9 GPa and detonation velocity of 8310 m s^{-1}. The addition of an oxide is expected to increase the materials sensitivity while improving performance. Based on calculated densities for the indeterminate positioned AANT oxide, the performance for all possible oxide positions were calculated to be between 30.7 and 31.1 GPa for detonation pressure with detonation velocity between 8635 and 8680 m s^{-1}. Reduction of the azide improved thermal stability, increasing the decomposition onset temperature to 225 °C. The amino group, also, decreased the triazine's sensitivity classifying it as insensitive to impact and sensitive to friction. Loss of the azide lowered the performance of the energetic 1,2,4-triazine, while oxidation improved it with the higher-density polymorph yielding results closest to those of the azide at 27. 8 GPa and 8407 m s^{-1}. The energetic salts synthesized, upon addition of a third amine through amination, were more sensitive to impact and friction than AANT, DANT, or DANTX. The 5,5'-bistetrazole-1,1'-diolate (BTO) salt experienced a drastic drop in

thermal stability in comparison to both DANT and the initial diammonium 5,5'-bistetrazole-1,1'-diolate salt; reduced to 130 °C from initial onset values greater than 220 °C. The expected performance values are closer in range to that of DANTX than AANT with the exclusion of the perchlorate salt which had detonation parameters of 34.9 GPa and 8774 m s^{-1}. All values are summarized in Table 7 below.

Table 7. Summarized Energetic Properties of the 1,2,4-traizine associated materials

	AANT	AANT oxide			DANT	DANTX		TANT Salts			
	AANT	a	b	c	DANT	low	high	BTO	NO_3	ClO_4	5-NT
IS [J]	7	-	-	-	>40	8	-	< 1	< 1	5	< 1
FS [N]	120	-	-	-	160-192	360	-	< 5	48 - 54	40 – 48	40 - 48
Ω [%]	-43.9	-32	-32	-32	-61.49	-46.5	-46.5	-46.68	-23.38	-14.73	-39.13
T_{dec} [°C]	162	-	-	-	225	190	196	130	150	180	158
$\Delta_f H_m^o$ [kJ mol^{-1}]	494.3	469	479	508	134.1	102.1	-	797.5	-236.3	415.3	445.8
ρ [$g{\cdot}cm^{-3}$][calc]	1.824	1.81	1.83	1.8	1.742	1.814	1.814	1.744	1.718	1.823	1.734
ρ [$g{\cdot}cm^{-3}$]	1.781	-	-	-	1.778	1.747	1.852	1.78	1.81	1.9	1.77
T_{det} [K]	3519	3817	3831	3926	2584	2973	2915	3130	2918	4350.4	3205.1
P_{CJ} [GPa]	28.9	30.7	31.8	31.1	22.9	24.2	27.8	27.4	26.08	34.88	26.04
V_{det} [m s^{-1}]	8310	8635	8738	8680	7896	7938	8407	8494	8184	8774	8247

[a] impact sensitivity (BAM drophammer (1 of 6)); [b] friction sensitivity (BAM friction tester (1 of 6)); [c] nitrogen content; [d] oxygen balance (Ω = (xO−2yC−1/2zH)M/1600); [e] decomposition temperature from DSC (β = 5 °C); [f] room temperature density by X-ray diffraction; [g] calculated heat of formation; [h] energy of explosion; [i] detonation temperature; [j] detonation pressure; [k] detonation velocity; [l] volume of detonation gases (assuming only gaseous products); [m] value determined for low-density DANTX polymorph; [n] value determined for high-density DANTX; [o] a ' go' was determined by the presence of smoke, light, sound, or the occurrence of decomposition.

Nitro formation via superoxide [5]

The conversion of the dual amines on 5,5´-diamino-3,3'-methylene-1H-1,2,4-triazole (DABTM) to nitro groups forming bis(3-nitro-1H-1,2,4-triazol-5-yl)methane (BNTM) was accomplished via a simple one-pot synthesis through oxidation with superoxide. The formation of the superoxide occurred on a titanium matrix as hydrogen peroxide decomposed forming water as a byproduct, a process which avoids both the generation of acidic waste and an unstable diazo intermediate. While found to possess a good thermal stability the dinitro was sensitive to impact and friction. The formation of metal salts rendered the material insensitive to impact and less sensitive to friction, excluding the sodium salt which became slightly more sensitive to friction. Crystal structures were obtained for the neutral parent compound, as well as hydrated structures of the cesium, sodium, and strontium salts. Through both elemental analysis and thermal gravimetric analysis, it was apparent all the metal salts coordinated multiple hydrate units. The sensitivities and onset of decomposition temperatures are summarized below (Table 8).

Table 8. Summarized properties of BNTM and its metal salts.

	BNTM	Sr	Na	Li	K	Cs	Rb
IS [J]	20	> 40	> 40	40	40	> 40	> 40
FS [N]	120	360	108 – 120	216	120 - 160	108	240
$T_{dec.}$ [°C]	250	230	260	247	210	210/250	248

6.1 References

[1] S. E. Creegan, M. Zeller, E. F. C. Byrd, D. G. Piercey, Synthesis and Characterization of the Energetic 3-Azido-5-amino-6-nitro-1,2,4-triazine *Propellants, Explosives, Pyrotechnics* **2021**, *46*, 214-221.10.1002/prep.202000136

[2] S. E. Creegan, M. Zeller, E. F. C. Byrd, D. G. Piercey, Energetic 1,2,4-Triazines: 3,5-Diamino-6-nitro-1,2,4-triazine and Its Oxide *Crystal Growth & Design* **2021**, *21*, 3922-3927.10.1021/acs.cgd.1c00241

[3] S. E. Creegan, M. Zeller, E. F. C. Byrd, D. G. Piercey, Energetic Triazinium Salts from N-amination of 3,5-diamino-6-nitro-1,2,4-triazine *Energetic Materials Frontiers* **2022**, *In Submission*

[4] U. Nations, *Recommendations on the Transport of Dangerous Goods: Manual of Tests and Criteria*, UN, **2003**.

[5] S. E. Creegan, M. Zeller, E. F. C. Byrd, D. G. Piercey, Titanium Superoxide for the Oxidation of Amines: Synthesis of bis(3-nitro-1H-1,2,4-triazol-5-yl)methane and its Metal Salts *Zeitschrift fur Anorganische und Allgemeine Chemie*, *n/a*, e202200007.https://doi.org/10.1002/zaac.202200007

APPENDIX A. EXPERIMENTAL DETAILS

AANT

Experimental Section

General Methods

All reagents and solvents were used as received unless stated otherwise. The potassium salt of nitroacetonitrile and the hypofluorous acid acetonitrile complex were prepared according to literature [1-3]. ^{1}H and ^{13}C NMR spectra were recorded with a Bruker AV-III-500-HD and Bruker Avance-III-800 (5mm QCI Z-gradient cryoprobe) NMR spectrometer. All chemical shifts are quoted in ppm relative to TMS (^{1}H, ^{13}C). Infrared spectra were recorded with a PerkinElmer Spectrum Two spectrometer with UATR (Universal Attenuated Total Reflectance) accessory. Transmittance values are described as “strong” (s), “medium” (m), “weak” (w), and “very weak” (vw). Melting and decomposition points were measured with a TA Instruments Q20 DSC using heating rates of 5 °Cmin^{-1}. Low resolution mass spectra were measured with an Agilent 1260 Infinity II Quaternary LC instrument. High resolution mass spectra were measured with a Thermo Fisher Scientific LTQ Orbitrap. Sensitivity data were determined using a BAM friction tester and BAM Drophammer (OZM research). Elemental analysis was performed using an Elementar vario EL cube elemental analyzer

Synthesis

Caution! The materials prepared in this work are energetic with potential sensitivity to various stimuli. While no issues were encountered in the handling of these compounds, proper protective measures (face shield, ear protection, body armor, Kevlar gloves, and earthened equipment) are recommended. Special care should be taken with the aqueous solution of diazotetrazole as, should it crystalize, loud and disturbing detonations are possible. The probability of spontaneous detonation is diminished at diazotetrazole concentrations less than 3%.

3-azido-5-amino-6-nitro-1,2,4-triazine (AANT): 2.00 g (0.02 mol) of 5-aminotetrazole monohydrate was dissolved in a solution of water (100 mL) and conc. hydrochloric acid (5 mL). The solution was then cooled to -2°C and stirred vigorously while a solution of sodium nitrite (1.4g; 0.02 mol) and water (20 mL) was added dropwise. In the event of freezing the reaction solution was thawed before proceeding with further addition of sodium nitrite. The reaction was stirred between -2°C and 5°C for 30 minutes before a solution of nitroacetonitrile potassium salt (2.58 g; 0.02mol) in water (5mL) was added. After stirring for 1.5 hours, warming gradually to room temperature, the precipitate was filtered yielding 180 mg (4.6%) of (**1**●H_2O). Stirring for an additional 3 days at room temperature and filtering yields 680 mg (19.2%) of AANT.

(**1**●H_2O): ^{13}C NMR (500MHz, DMSO-d6) δ=158, 156, 155 ppm. HRMS 199 m/z. IR: ṽ 3582 (w), 3447 (w), 3422 (w), 3344(w) 3042 (w), 2440 (vw), 1669 (s), 1604 (m), a5a5 (s) 1409 (w), 1307 (vs), 1268 (m), 1221 (m) 1100 (m), 1069 (m), 1036 (m), 1001 (m), 944 (w), 835 (s), 808 (s)745 (w) 731(w), 703 (w), 689 (m), 631 (m), 576 (s), 509 (m) cm^{-1}. EA ($C_3H_4N_8O_3$, 200.1) calcd: C, 18.01; N, 55.99; H, 2.01%; Found: C, 17.18; N, 54.06; H, 2.75%

AANT: ^1H NMR (500MHz, DMSO-d6) δ=9.2 (s, H, NH_2), 8.5 (s, H, NH_2) ppm. ^{13}C NMR (500MHz, DMSO-d6) δ=163, 151, 146 ppm. HRMS 181 m/z. IR: ṽ 3432 (w), 3320 (m), 2399 (vw), 2255 (w), 2161 (m), 2105 (w), 1737 (vw), 1628 (m), 1613 (m), 1559 (m), 1509 (m), 1491 (m), 1466 (m), 1356 (s), 1294 (s), 1257 (m), 1200 (s), 1157 (m), 1097 (m), 1081 (m), 1057 (m), 975 (m) 841(m), 789 (s), 744 (m), 705 (m), 670 (w), 603 (s), 542 (s), 514 (s)467(s) cm^{-1}. EA ($C_3H_4N_8O_2$, 182.1) calcd: C, 19.79; N, 61.53; H, 1.11%; Found: C, 19.40; N, 61.89; H, 1.05%

3-azido-5-amino-6-nitro-1,2,4-triazine oxide (**2a-c**): 100 mg (0.549 mmol) AANT was dissolved in 5 mL acetonitrile and the solution cooled in an ice bath (<5 °C). Stirring vigorously, 4 equivalents of HOF●MeCN (0.4 M) were added dropwise followed by the addition of 8 mL acetonitrile. The bright red solution was stirred for 0.5 hr before being neutralized with excess sodium bicarbonate. After 1 hr the sodium bicarbonate was removed by filtration and the solvent removed by evaporation resulting in a red solid. Mass spectroscopy: 197 m/z.

DANT AND DANTX

Experimental Section

General

All reagents and solvents were used as received unless otherwise stated. 3-Azido-5-amino-6-nitro-1,2,4-triazine was prepared according to literature [4]. ^{1}H and ^{13}C NMR spectra were recorded with a Bruker AV-III-500-HD and Bruker Avance-III-800 (5mm QCI Z-gradient cryoprobe) NMR spectrometer. All chemical shifts are quoted in ppm relative to TMS (^{1}H, ^{13}C). Infrared spectra were recorded with a PerkinElmer Spectrum Two spectrometer with UATR (Universal Attenuated Total Reflectance) accessory. Transmittance values are described as "strong" (s), "medium" (m), "weak" (w), and "very weak" (vw). Melting and decomposition points were measured with a TA Instruments Q50 TGA using heating rates of 5 °Cmin^{-1}. Low resolution mass spectra were measured with an Agilent 1260 Infinity II Quaternary LC instrument. Sensitivity data were determined using a BAM friction tester and BAM Drop-hammer (OZM research). Elemental analysis was performed using an Elementar vario EL cube elemental analyzer.

Synthesis

Caution! The materials prepared in this work are energetic with potential sensitivity to various stimuli. While no issues were encountered in the handling of these compounds, proper protective measures (face shield, ear protection, body armor, Kevlar gloves, and earthened equipment) are recommended.

3,5-diamino-6-nitro-1,2,4-triazine (DANT)

3-azido-5-amino-6-nitro-1,2,4-triazine (AANT) (2 g; 10.98 mmol) was dissolved in ethanol (175 mL) and heated to 60°C. Stirring vigorously triphenylphosphine (1 eqv.; 2.89 g; 11.02 mmol) was added in portions. Upon the formation of precipitates nitric acid was added in 1 mL portions until solids dissolved. After AANT fully reacted with triphenylphosphine (2 hr.) water (100 ml, 500 eqv.) was added to the reaction solution and stirred overnight at 60°C. The solvent was then removed via vacuum and the remaining solid extracted with hot ether (5x; 25 mL) to give DANT

a pale-yellow solid (1.171 g; 68% yield). Recrystallization from hot water gives shiny-yellow flakes. ^{1}H NMR (DMSO-d): δ 8.26 (s, 1H), 7.98 (s, 1H), 7.84 (s, 1H) 7.63 (s, 1H); ^{13}C NMR: δ 162.49, 151.12, 143.07; LRMS: 156m/z; IR: 3419 (w), 3392 (w), 3315 (w), 3315 (w), 3215(w), 3169 (w), 3053 (w), 2840 (w), 2688 (w), 2154 (w), 1947 (w), 1623 (m), 1546 (m), 1499 (m), 1464 (m), 1432 (m), 1350 (m), 1306 (m), 1266 (w), 1194 (m), 1163 (m), 1120 (m), 1020 (m), 971 (m), 852 (m), 788 (m), 768 (m), 736 (m), 689 (m), 668 (m), 559 (s), 472 (s); Elemental Analysis (%) for $C_3N_6H_4O_2$ (156.1029 gmol^{-1}): Calcd. C 23.08; H 2.58; N 53.85; O 20.50; Found C 22.56; H 2.55; N 52.66; TGA: T_{dec}. 240°C; Impact Sensitivity: >40 J; Friction Sensitivity: 160-192 N.

DANTX

DANT (200mg; 1.28mmol) and Oxone® (0.6 eqv.; 472.6 mg) were stirred in water (5 mL) at 40°C for 12 hr. Additional portions of Oxone® (3x; 0.2 eqv.; 157.5 mg) were added in 12hr intervals and the reaction stirred at 40°C until completed. The solution was then extracted with hexane (3x; 10 mL), filtered and washed with water giving a reddish-orange solid (60 mg; 27% yield). The solid crystallized out of nitromethane and a THF/water mixture. ^{1}H NMR (DMSO-d): δ 9.11 (s, 1H), 8.68 (s, 1H), 8.49 (s, 1H), 8.22 (s, 1H); ^{13}C NMR: δ 152.13, 146.42, 127.27; LRMS: 172m/z; IR: 3480 (w), 3455 (w), 3419 (w), 3386 (w), 3362 (w), 3297 (w), 3224 (w), 3176 (w), 2157 (vw), 1664 (m), 1645 (m), 1606 (m), 1566 (m), 1525 (w), 1463 (m), 1435 (m), 1348 (w), 1320 (w), 1277 (m), 1189 (m), 1127 (m), 1080 (m), 965 (m), 912 (m), 868 (m), 803 (m), 758 (m), 744 (m), 721 (m), 690 (m), 668 (m), 643 (m), 601 (m), 552 (s), 498 (s), 470 (s); Elemental Analysis (%) for $C_3N_6H_4O_3$ (172.1023gmol^{-1}): Calcd. C 20.94; H 2.34; N 48.83; O 27.89; Found: C 20.32; H 2.21; N 47.97; TGA: $T_{dec.}$ 200°C; Impact Sensitivity: >40 J; Friction Sensitivity: 144 N (Sensitivity reported for the low-density DANTX polymorph).

TANT+ AND ENERGETIC SALTS

Experimental Section

General

All reagents and solvents were used as received unless otherwise stated. 3-Azido-5-amino-6-nitro-1,2,4-triazine[4], 3,5-diamino-6-nitro-1,2,4-triazine (DANT) [5], ethyl *O*-p-tolylsulphonylacetohydroximate [6], silver nitrotetrazole [7] , and diammonium 5,5'-bistetrazole-1,1'-diolate [8] were prepared according to literature. ^{1}H and ^{13}C NMR spectra were recorded with a Bruker Avance-III-800 (5mm QCI Z-gradient cryoprobe) NMR spectrometer. All chemical shifts are quoted in ppm relative to TMS (^{1}H, ^{13}C). Infrared spectra were recorded with a PerkinElmer Spectrum Two spectrometer with UATR (Universal Attenuated Total Reflectance) accessory. Transmittance values are described as "strong" (s), "medium" (m), "weak" (w), and "very weak" (vw). Onset decomposition temperatures were measured with a TA Instruments Q50 TGA using heating rates of 5 °Cmin^{-1}. Low resolution mass spectra were measured with an Agilent 1260 Infinity II Quaternary LC instrument. Sensitivity data were determined using a BAM friction tester and BAM Drophammer (OZM research). Elemental analysis was performed using an Elementar vario EL cube elemental analyzer.

Caution! The materials prepared in this work are energetic materials with potential sensitivity to various stimuli. While no issues were encountered in the handling of these compounds, proper protective measures (face shield, ear protection, body armor, Kevlar gloves, and earthened equipment) are recommended to be used during synthesis manipulation.

Synthesis

2,3,5-triamino-6-nitro-1,2,4-triazinium (TANT+) tosylate salt (TANT•OTs) (1)

2.47 g (9.6 mmol; 1.5 eqv.) of ethyl O-p-tolylsulphonylacetohydroximate was suspended in 60% perchloric acid (18.5 mL) and stirred at room temperature for 2 hours. The suspension was then poured over an ice-and-water mixture (15 mL water: 100 g ice) and stirred until all ice had melted before being extracted with dichloromethane (3x; 50 mL). The combined organic solvent was then

dried by extraction with brine (3x; 20 mL). To the dried dichloromethane was added 1 g (6.4 mmol) of DANT and 200 mL of a 75:25 acetonitrile/water mixture. The reaction mixture was stirred overnight in an uncovered beaker allowing for evaporation of the volatile solvents. After the remaining solution was removed under air-flow, the yellow-brown solid was recrystallized from ethanol producing 1.24 g (59 % yield) of shiny yellow or yellow-brown flakes of 2,3,5-triamino-6-nitro-1,2,4-triazinium.

^{1}H NMR (D2O): δ 9.2 (s, 1H), 8.8 (s, 1H), 8.7 (s, 1H) 8.43(s, 1H), 7.6 (d, J = 7.78Hz, 2H), 7.28 (d, J = 7.80 Hz, 2H), 6.5 (s, 2H, -N-NH2), 2.3 (s, 3H); ^{13}C NMR: δ 154.5, 150.6, 142.4, 139.3, 135.6, 129.3, 125.2, 20.4; LRMS: 171 m/z (ESI-), 172 m/z (ESI+); IR: 3661 (w), 3464 (w), 3306 (w), 3130 (m), 2981 (m), 2924 (w), 2887 (w), 1681 (m), 1643 (m), 1616 (m), 1599 (m), 1518 (m), 1495 (m), 1395 (m), 1330 (m), 1272 (m), 1175 (s), 1121 (s), 1106 (s), 1033 (m), 1008 (m), 942 (m), 878 (m), 818 (m), 798 (m), 766 (m), 711 (m), 681 (m), 637 (m), 549 (s), 492 (m), 461 (m); Elemental Analysis (%) for C3N7H6O2•C7H7SO3 (343.3191 gmol-1): Calcd. C 34.98; H 3.82; N 28.56; O 23.30; Found C 34.81; H 3.94; N 28.69; TGA: T_{dec}: 205 °C.

2,3,5-triamino-6-nitro-1,2,4-triazinium chloride monohydrate (TANT•Cl•H_2O) (2•H_2O)

Amberlite™ IRA910-Cl500 (5 tablespoons) was rinsed with deionized water and added to a solution of **(1)** (500 mg; 1.46 mmol) in water (25 mL). The mixture was stirred for 30 minutes and then left for another 30 minutes before the ion exchange resin was removed via filtration. The proceeding steps were repeated as needed for complete conversion to the chloride salt, as determined by LRMS, and the solvent was removed by evaporation under high vacuum while maintaining a solution temperature less than 27 °C. Upon reaching dryness, 211 mg (72 % yield) of bright yellow solid which based on elemental analysis was 2,3,5-triamino-6-nitro-1,2,4-triazinium chloride monohydrate was collected. It was noted that the material decomposed when in solution, gaining a purple-gray coloring, this was circumvented by removing the solution in *vacuo* and storing under argon at 0 °C until all solvent was removed.

^{1}H NMR (D_2O): δ 9.2 (s, 1H), 8.8 (s, 1H), 8.7 (s, 1H) 8.43(s, 1H), 6.5 (s, 2H, -N-NH_2); ^{13}C NMR: δ 154.5, 150.6, 135.6; LRMS: 172 m/z (ESI+); IR: 3661 (w), 3599 (m), 3419 (m), 3374 (m), 3216 (m), 3064 (m), 2981 (m), 2642 (m), 2530 (m), 2355 (m), 1658 (s), 1625 (s), 1602 (s), 1523 (m),

1494 (m), 1393 (m), 1312 (s), 1273 (s), 1211 (m), 1172 (s), 1123 (m), 1087 (m), 1019 (m), 952 (m), 883 (m), 820 (m), 794 (m), 759 (m), 718 (m), 619 (s), 523 (m); Elemental Analysis (%) for $C_3N_7H_6O_2Cl•H_2O$ (225.5937 $gmol^{-1}$): Calcd. C 15.97; H 3.57; N 43.46; O 21.28; Found C 15.82; H 3.57; N 43.10; TGA: T_{dec}: 177 °C; Impact Sensitivity: 20 J; Friction Sensitivity: 80 - 108 N.

Di(2,3,5-triamino-6-nitro-1,2,4-triazin-2-ium) 5,5'-bistetrazole-1,1'-diolate dihydrate (TANT•BTO•2H₂O) (3•2H₂O)

Method A: diammonium 5,5'-bistetrazole-1,1'-diolate (0.04 g; 0.2 mmol) and **(1)** (0.135 g; 0.4 mmol; 2 eqv.) were dissolved in water (15 mL) at 80 °C and let cool to room temperature producing dark brown crystals (65 mg; 65 %) which were collected by filtration.

Method B: disodium 5,5'-bistetrazole-1,1'-diolate was synthesized from diammonium 5,5'-bistetrazole-1,1'-diolate by boiling in water with excess sodium hydroxide for 12 hours. The disodium 5,5'-bistetrazole-1,1'-diolate (64.9 mg; 0.3 mmol) dissolved in water (10 mL) and added to a solution of **(4•**H_2O**)** (153 mg; 0.6 mmol; 2 eqv.) in water (5 mL). The combined solutions were stirred for 1 hour before the olive-green precipitate was collected by filtration. The solvent volume was then reduced to half by evaporation and filtered again; yielding 87 mg (57 %) product.

^{13}C NMR (CD_3CN): δ 154, 150, 135, 133; LRMS: 169 m/z (ESI-), 172 m/z (ESI+); IR: 3413 (m), 3377 (m), 3250 (m), 3132 (m), 2971 (m), 1650 (m), 1624 (m), 1534 (m), 1513 (m), 1482 (m), 1453 (m), 1397 (m), 1335 (m), 1317 (m), 1277 (m), 1222 (m), 1168 (m), 1111 (m), 1060 (m), 1036 (m), 991 (m), 933 (m), 882 (m), 793 (m), 771 (m), 762 (m), 728 (m), 677 (m), 645 (m), 613 (m), 574 (m), 499 (m), 461 (m); Elemental Analysis (%) for $2C_3N_7H_6O_2•C_2N_8O_2•2H_2O$ (548.35 $gmol^{-1}$): Calcd. C 17.52; H 2.94; N 56.20; O 23.34; TGA: T_{dec}: 130 °C; Impact Sensitivity: < 1 J; Friction Sensitivity: < 5 N.

2,3,5-triamino-6-nitro-1,2,4-triazinium nitrate monohydrate (TANT•NO₃•H₂O) (4•H₂O)

To a solution of **(2•**H_2O**)** (201 mg; 0.9 mmol) in water (15 mL) was added silver nitrate (153 mg; 0.9 mmol; 1 eqv.). After stirring in the dark for 30 minutes, the precipitated silver chloride was removed by syringe filtration (0.45 μm) and the solvent removed under high vacuum yielding a gray solid (187 mg; 83 %).

LRMS: 172 m/z (ESI+); IR: 3371 (m), 3321 (m), 3140 (m), 1688 (m), 1644 (s), 1604 (m), 1531 (m), 1504 (m), 1396 (s), 1360 (s), 1306 (s), 1272 (s), 1205 (s), 1168 (s), 1102 (m), 1050 (m), 1011 (m), 911 (m), 885 (s), 800 (m), 770 (s), 761 (s), 720 (m), 652 (s), 628 (s), 527 (m), 458 (s); Elemental Analysis (%) for $C_3N_7H_6O_2 \bullet NO_3 \bullet H_2O$ (252.15 $gmol^{-1}$): Calcd. C 14.29; H 3.20; N 44.44; O 38.07; TGA: T_{dec}: 150 °C; Impact Sensitivity: < 1 J; Friction Sensitivity: 48 - 54 N.

2,3,5-triamino-6-nitro-1,2,4-triazinium perchlorate salt (TANT•ClO_4) (5)

To a solution of **(2**•H_2O**)** (201 mg; 0.9 mmol) in water (15 mL) was added silver perchlorate (185 mg; 0.9 mmol; 1 eqv.). After stirring in the dark for 30 minutes, the precipitated silver chloride was removed by syringe filtration (0.45 µm) and the solvent removed under high vacuum yielding a pale-purple solid (170 mg; 70 %).

LRMS: 99 m/z (ESI-), 101m/z (ESI-), 172 m/z (ESI+); IR: 3351 (w), 3443 (w), 3311 (m), 3275 (m), 1669 (m), 1621 (m), 1545 (m), 1495 (m), 1415 (m), 1344 (m), 1323 (w), 1276 (m), 1239 (w), 1215 (m), 1163 (w), 1120 (m), 1065 (s) 991 (m), 924 (m), 882 (s), 799 (m), 773 (m), 762 (m), 724 (m), 679 (m), 656 (m), 633 (s), 519 (s), 459 (s); Elemental Analysis (%) for $C_3N_7H_6O_2 \bullet ClO_4$ (271.58 $gmol^{-1}$): Calcd. C 13.27; H 2.23; N 36.10; O 35.35; TGA: T_{dec}: 180 °C; Impact Sensitivity: 5 J; Friction Sensitivity: 40 – 48 N.

2,3,5-triamino-6-nitro-1,2,4-triazinium 5-nitro-tetrazolate salt (TANT•5NT) (6)

To a solution of **(2**•H_2O**)** (200 mg; 0.9 mmol) in water (15 mL) was added silver 5-nitrotetrazolate (197 mg; 0.9 mmol; 1 eqv.). After stirring in the dark for 30 minutes, the precipitated silver chloride was removed by syringe filtration (0.45 µm) and the solvent removed under high vacuum yielding a gray solid (242 mg; 96 %).

^{13}C NMR: δ 167, 154, 150, 135; LRMS: 114 m/z (ESI-), 172 m/z (ESI+); IR: 3399 (w), 3361 (m), 3139 (m), 2980 (m), 2485 (vw), 1675 (m), 1629 (s), 1538 (m), 1499 (m), 1464 (m), 1442 (m), 1423 (m), 1399 (m), 1354 (m), 1319 (m), 1280 (m), 1214 (m), 1177 (m), 1154 (m), 1061 (w), 1047 (w), 1030 (w), 1004 (m), 938 (w), 885 (m), 835 (m), 762 (m), 723 (m), 707 (m), 670 (m), 648 (m), 608 (s), 591 (s), 535 (m), 518 (m), 463 (s); Elemental Analysis (%) for $C_3N_7H_6O_2 \bullet CN_5O_2$ (286.17

$gmol^{-1}$): Calcd. C 16.79; H 2.11; N 58.73; O 22.36; TGA: T_{dec}.: 158 °C; Impact Sensitivity: < 1 J; Friction Sensitivity: 40 – 48 N.

BNTM AND METAL SALTS

Experimental Section

General

All reagents and solvents were used as received unless otherwise stated. 5,5´-diamino-3,3'-methylene-1H-1,2,4-triazole (DABTM) [9] and titanium superoxide were prepared according to literature procedures [10]. ^{1}H and ^{13}C NMR spectra were recorded with a Bruker Avance-III-800 (5mm QCI Z-gradient cryoprobe) NMR spectrometer. All chemical shifts are quoted in ppm relative to TMS (^{1}H, ^{13}C). Infrared spectra were recorded with a PerkinElmer Spectrum Two spectrometer with UATR (Universal Attenuated Total Reflectance) accessory. Transmittance values are described as "strong" (s), "medium" (m), and "weak" (w). Melting and decomposition points were measured with a TA Instruments Q50 TGA using heating rates of 5 °C min^{-1}. Low resolution mass spectra were measured with an Agilent 1260 Infinity II Quaternary LC instrument. Sensitivity data were determined using a BAM friction tester and BAM Drop-hammer (OZM research). Elemental analysis was performed using an Elementar vario EL cube elemental analyzer. Single crystal XRD data were collected on Bruker Quest instruments (refer to Appendix B for details).

Synthesis

BNTM

Method A: Sodium nitrite (30.634 g; 444 mmol) was dissolved in water (42.5 mL) and heated to 60 °C. While stirring vigorously a solution of DABTM (2 g; 11.1 mmol) in water (42.7 mL) and 20% sulfuric acid (21.6 mL) was added dropwise maintaining a temperature less than 70 °C. The mixture was stirred for 2 hrs. and then cooled to room temperature and acidified with 20% sulfuric acid to a pH of 1. The acidic solution was extracted with ethyl acetate and the solvent removed with a rotary evaporator. The yellow solid was purified by recrystallization from water as needle-like pale yellow crystals (2.117 g; 79% yield).

Method B: In 30-minute intervals freshly prepared titanium superoxide (2 g) was added in portions [Caution! Foam] to a solution of DABTM (2 g; 11.1 mmol) in water (100 mL) and 50% hydrogen peroxide (100 mL). The mixture was stirred for 3-days and extracted with ethyl acetate. Evaporation of the solvent resulted in a pale-yellow solid, 2.091 g (79%).

^{1}H (800 MHz, DMSO-d6): δ4.59 ppm (s, 2H, CH_2). ^{13}C NMR (DMSO-d6): δ= 162.94 (C-NO_2), 153.72 (C-CH_2), 25.08 (CH_2) ppm. LRMS: [M-H] 239 m/z, [2M-H] 479 m/z. EA ($C_5H_4N_8O_4$, 240.14) calcd.: C, 25.01; N, 46.66; H, 1.68 %; Found: C, 25.1; N, 46.7; H, 1.7 %. IR $\tilde{\nu}$: 3576.6 (w) 2974.7 (w) 1579.4 (w), 1537.9 (w), 1487.1 (w), 1400.2 (w), 1346 (w), 1302.4 (w), 1205.3 (w), 1160.3 (w), 1069.8 (w), 921.2 (w), 841.7 (w), 808.7 (w), 763.6 (w), 673.6 (w), 651.9 (w), 457 (w) cm^{-1}.

General Alkali Metal Salt Synthesis

To a cooled (T <10 °C) vigorously stirred mixture of BNTM in water was added dropwise a solution of the metal hydroxide in water. Additional water was added during the addition to maintain a pale-yellow coloring. After addition the solution stirred for 1 hour before the solvent was evaporated by airline overnight yielding hydrated salts.

Potassium Salt of BNTM: 503 mg (2.09 mmol) BNTM in 15 mL H_2O, 237 mg (4.22 mmol; 2.01 eqv.) KOH in 10.5 mL H_2O; yield 748 mg; EA ($C_5H_2N_8O_4K_2$•H_2O) calcd.: C, 17.96; N, 33.53; H, 1.21 %; Found C, 17.51; N, 33.22; H, 1.87 %. IR $\tilde{\nu}$: 3590.7 (w), 3343.2 (w), 3270 (w), 1708.8 (w), 1669.4 (w), 1512.2 (m), 1470 (m) 1440.6 (m), 1387.9 (m), 1351 (w), 1325.6 (m), 1295.3 (m), 1085.4 (m), 980 (w), 912 (w), 843.8 (m), 758 (w), 724.3 (w), 696.1 (w), 657.8 (m), 583.6 (w), 558.3 (m) cm^{-1}.

Sodium Salt of BNTM: 502 mg (2.09 mmol) BNTM in 15 mL H_2O, 168 mg (4.2 mmol; 2 eqv.) NaOH in 6 mL H_2O; yield 777 mg; EA ($C_5H_2N_8O_4Na_2$•$3H_2O$) calcd.: C, 17.76; N, 33.14; H, 2.38 %; Found: C, 17; N, 32.28; H, 2.3 %. IR $\tilde{\nu}$: 3593.5 (w), 3437.9 (w), 3205.3 (w), 2181.4 (w), 1673 (w), 1627 (w), 1537.2 (s), 1496.4 (m), 12476 (m), 1461.8 (m), 1444.4 (m), 1396.8 (s), 1360 (w), 1336.6 (m), 1300.5 (m), 1223.9 (m), 1191 (w), 1094.2 (s), 1060.5 (m), 1025.3 (w), 918.4 (w), 851.6 (s), 777.7 (m), 755.2 (m), 698.8 (m), 656.8 (m), 582.9 (s), 563.77 (s), 460.4 (m) cm^{-1}.

Lithium Salt of BNTM: 502 mg (2.09 mmol) BNTM in 15 mL H_2O, 175 mg (4.2 mmol; 2 eqv.) LiOH in 9 mL H_2O; yield 736 mg; EA ($C_5H_2N_8O_4Li_2 \cdot 3H_2O$) calcd.: C, 16.68; N, 31.12; H, 3.92 %; Found: C, 16.43; N, 30.58; H, 3.52 %. IR $\tilde{\nu}$: 3613.5 (w), 2992.9 (w), 2226.4 (w), 1652.6 (w), 1547.2 (m), 1480.5 (m), 1447.2 (w), 1402 (s), 1348.8 (m), 1304.9 (m), 1251.6 (w), 1187 (w), 1116.1 (s), 1066.1 (w), 985.8 (w), 923.9 (w), 851 (s), 815.6 (m), 780.2 (s), 761.7 (m), 701.8 (m), 658.7 (m), 628.6 (w), 592.1 (w), 558.1 (m), 488.5 (s) cm^{-1}.

Cesium Salt of BNTM: 501 mg (2.09 mmol) BNTM in 10 mL H_2O, 880 mg (5.24 mmol; 2.5 eqv.) cesium hydroxide monohydrate in 5 mL H_2O; yield 1.287 g; EA ($C_5H_2N_8O_4Cs_2 \cdot 2H_2O$) calcd.: C, 11.12; N, 20.75; H, 1.12 %; Found: C, 11.42; N, 20.44; H, 1.44 %. IR $\tilde{\nu}$: 3337.9 (m), 3241.9 (w), 3002.8 (w), 2805.9 (w), 2673.7 (w), 2237.7 (w), 2170.1 (w), 1655.5 (w), 1519.7 (s), 1472.2 (m), 1447.2 (m), 1439.8 (s), 1388.4 (s), 1352.2 (m), 1323.3 (s), 1303.6 (m), 1285.9 (m), 1091.1 (s), 1058.7 (m), 1022.4 (w), 991.5 (w), 918.9 (w), 853.7 (w), 841.6 (s), 772.1 (w), 762.3 (m), 724.3 (w), 652.6 (s), 587.6 (s) cm^{-1}.

Rubidium Salt of BNTM: 500 mg (2.08 mmol) BNTM in 10 mL H_2O, 1.08 g (4.99 mmol; 2.5 eqv.) rubidium hydroxide in 5 mL H_2O; yield 854mg; EA ($C_5H_2N_8O_4Rb_2 \cdot 3H_2O$) calcd.: C, 12.97; N, 24.2; H, 1.74 %; Found: C, 13.18; N, 24.17; H,1.6 %. IR $\tilde{\nu}$: 3624.5 (w), 3334.7 (w), 1621.6 (w), 1542.8 (w), 1509.4 (m), 1470.1 (s), 1439.1 (s), 1380.9 (s), 1347.9 (m), 1322.1 (s), 1289.9 (m), 1077.1 (s), 1059 (m), 1019 (w), 915.6 (w), 840.67 (s), 756.2 (m), 721.5 (w), 660.3 (s), 552.6 (w), 471.4 (m) cm^{-1}.

Synthesis of BNTM Strontium Salt

A slurry of BNTM (702 mg; 2.9 mmol) and strontium nitrate (618 mg; 2.9 mmol) in water (20 mL) was stirred for 45 minutes at room temperature. A solution of sodium hydroxide (144.2 mg; 3.6 mmol; 1.23 eqv.) in water (10 mL) was added dropwise to the slurry and the mixture was stirred overnight. The solvent was removed and yellow solid recrystallized from water yielding 778 mg of hydrated material. The sample was dried in desiccator with Drierite® before elemental analysis was performed. EA ($C_5H_2N_8O_4Sr \cdot H_2O$) calcd.: C, 17.47; N, 32.6.40; H, 1.17 &; Found: C, 17.79; N, 32.67; H, 1.86 %. IR $\tilde{\nu}$: 3641.3 (w), 3613.2 (w), 3141 (w), 1627.2 (w), 1582.9 (w), 1536.9 (m), 1484.1 (m), 1455.7 (m) 1416.3 (m), 1388.2 (s), 1329 (m), 1303.5 (m), 1289.7 (m),

1227.8 (w), 1199.7 (w), 1171.5 (w), 1095.3 (m), 1070.9 (m), 1054.1 (m), 1036.5 (m), 1019.6 (m), 912.7 (w), 881.8 (w), 845 (s), 817.9 (m), 765. (m), 651.3 (s), 560 (m), 524 (m), 456.37 (s) cm^{-1}.

References for Appendix A

[1] E. K. Voinkov, E. N. Ulomskiy, V. L. Rusinov, K. V. Savateev, V. V. Fedotov, E. B. Gorbunov, M. L. Isenov, O. S. Eltsov, New stable form of nitroacetonitrile *Mendeleev Communications* **2016**, *26*, 172-173.https://doi.org/10.1016/j.mencom.2016.03.031

[2] S. Rozen, M. Brand, Epoxidation of Olefins with Elemental Fluorine in Water/Acetonitrile Mixtures *Angewandte Chemie International Edition in English* **1986**, *25*, 554-555.doi:10.1002/anie.198605541

[3] S. Rozen, S. Dayan, At Last, 1,10-Phenanthroline-N,N′-dioxide, A New Type of Helicene, has been Synthesized using HOF·CH3CN *Angewandte Chemie International Edition* **1999**, *38*, 3471-3473.doi:10.1002/(SICI)1521-3773(19991203)38:23<3471::AID-ANIE3471>3.0.CO;2-O

[4] S. E. Creegan, M. Zeller, E. F. C. Byrd, D. G. Piercey, Synthesis and Characterization of the Energetic 3-Azido-5-amino-6-nitro-1,2,4-triazine *Propellants, Explosives, Pyrotechnics* **2021**, *46*, 214-221.10.1002/prep.202000136

[5] S. E. Creegan, M. Zeller, E. F. C. Byrd, D. G. Piercey, Energetic 1,2,4-Triazines: 3,5-Diamino-6-nitro-1,2,4-triazine and Its Oxide *Crystal Growth & Design* **2021**, *21*, 3922-3927.10.1021/acs.cgd.1c00241

[6] E. E. Glover, K. T. Rowbottom, N-amination and subsequent oxidation of some fused imidazoles and triazoles *Journal of the Chemical Society, Perkin Transactions 1* **1976**, 367-371.10.1039/P19760000367

[7] T. M. Klapötke, C. M. Sabaté, Safe 5-nitrotetrazolate anion transfer reagents *Dalton Transactions* **2009**, 1835-1841.10.1039/B818900P

[8] N. Fischer, T. M. Klapötke, M. Reymann, J. Stierstorfer, Nitrogen-Rich Salts of 1H,1′H-5,5′-Bitetrazole-1,1′-diol: Energetic Materials with High Thermal Stability *European Journal of Inorganic Chemistry* **2013**, *2013*, 2167-2180.https://doi.org/10.1002/ejic.201201192

[9] M. F. Alexander A. Dippold, Thomas M. Klapotke, 5,5´-Dinitrimino-3,3´-methylene-1H-1,2,4-bistriazole – a Metal Free Primary Explosive Combining Excellent Thermal Stability and High Performance *Central European Journal of Energetic Materials* **2011**, *8*, 261 - 278

[10] R. Santhosh Reddy, T. M. Shaikh, V. Rawat, P. U. Karabal, G. Dewkar, G. Suryavanshi, A. Sudalai, A Novel Synthesis and Characterization of Titanium Superoxide and its Application in Organic Oxidative Processes *Catalysis Surveys from Asia* **2010**, *14*, 21-32.10.1007/s10563-010-9085-5

APPENDIX B. CRYSTALLOGRAPHIC DATA

AANT

Appendix B: Table 1-1. Experimental Crystallographic Data for Compounds (**1**●H_2O) and AANT.

Crystal	(**1**●H_2O)	AANT
Formula	$C_3H_4N_8O_3$● H_2O	$C_3H_2N_8O_2$
Formula Weight [g mol^{-1}]	218.16	182.13
Temperature [K]	150	150
Crystal System	triclinic	orthorhombic
Space Group	$P\bar{1}$	$P2_12_12_1$
a [Å]	5.1820 (4)	5.1049 (3)
b [Å]	8.5921 (7)	9.0235 (7)
c [Å]	9.3192 (7)	14.3979 (11)
α [°]	101.054 (2)	90
β [°]	96.040 (2)	90
γ [°]	96.920 (2)	90
V [$Å^3$]	400.74 (5)	663.23 (8)
Z	2	4
ρ(calc) [g cm^{-3}] [150 K]	1.808	1.824
R_1 /wR_2 (all data)	0.0504/0.1501	0.0298/0.0749
R_2/wR_2 (I>2σ)	0.0481/0.1457	0.0279/0.0732
S	1.15	1.05
No. of reflec.	1726	2510
Restraints	3	0
CCDC[a]	2004613	2004612

[a]These data can be obtained free of charge from The Cambridge Crystallographic Data Centre via www.ccdc.cam.ac.uk/data_request/cif.

DANT and DANTX

Single crystal X-ray diffraction data for DANT were collected on a Bruker Quest diffractometer with a fixed chi angle, a Mo Kα wavelength (λ = 0.71073 Å) sealed tube fine focus X-ray tube, single crystal curved graphite incident beam monochromator, and a Photon II area detector. Data for the DANTX samples were collected on a Bruker Quest diffractometer with kappa geometry, a Cu Kα wavelength (λ = 1.54178 Å) I-μ-S microsource X-ray tube, laterally graded multilayer (Goebel) mirror for monochromatization, and a Photon III C14 area detector. Both instruments were equipped with an Oxford Cryosystems low temperature device and examination and data collection were performed at 150 K. Data were collected, reflections were indexed and processed, and the files scaled and corrected for absorption using APEX3 [1] and SADABS [2]. The space groups were assigned using XPREP within the SHELXTL suite of programs [3-4] and solved by direct methods using ShelXS [4] and refined by full matrix least squares against F^2 with all reflections using Shelxl2018 [5-6] using the graphical interface Shelxle [7]. H atoms attached to carbon atoms were positioned geometrically and constrained to ride on their parent atoms. C-H bond distances were constrained to 0.98 Å for aliphatic CH_3 moieties and were allowed to rotate but not to tip to best fit the experimental electron density. The solvate molecule in the DANTX acetonitrile solvate is located on a two-fold axis and the methyl H-atoms are thus 1:1 disordered. N-H bond distances were either constrained to 0.88 Å and NH_2 groups were constrained to be planar (sp^2 hybridized) (for DANT, DANTX-DMSO solvate) or amine H atom positions were freely refined (DANTX low- and high-density polymorphs, DANTX-ACN solvate). U_{iso}(H) values were set to a multiple of U_{eq}(C) with 1.5 for CH_3 and 1.2 or 1.5 for NH_2 units, respectively.

[1] Bruker, Madison (WI), USA, **2019**.
[2] L. Krause, R. Herbst-Irmer, G. M. Sheldrick, D. Stalke, Comparison of silver and molybdenum microfocus X-ray sources for single-crystal structure determination *Journal of Applied Crystallography* **2015**, *48*, 3-10.doi:10.1107/S1600576714022985
[3] Bruker Advanced X-ray Solutions, Bruker AXS Inc., Madison, Wisconsin: USA **2000-2003**.
[4] G. Sheldrick, A short history of SHELX *Acta Crystallographica Section A* **2008**, *64*, 112-122.doi:10.1107/S0108767307043930
[5] G. Sheldrick, Crystal structure refinement with SHELXL *Acta Crystallographica Section C* **2015**, *71*, 3-8.doi:10.1107/S2053229614024218
[6] G. M. Sheldrick, *University of Göttingen, Germany* **2018**
[7] C. B. Hübschle, G. M. Sheldrick, B. Dittrich, ShelXle: a Qt graphical user interface for SHELXL *Journal of Applied Crystallography* **2011**, *44*, 1281-1284.10.1107/s0021889811043202

Appendix B: Table 6-1. Crystallographic Data for DANT and DANTX

	DANT	DANTX			
Name	DANT	Low density polymorph	High-density polymorph	Dimethyl sulfoxide solvate	Acetonitrile solvate
Formula	$C_3H_4N_6O_2$	$C_3H_4N_6O_3$	$C_3H_4N_6O_3$	$C_3H_4N_6O_3 \bullet C_2H_6OS$	$2(C_3H_4N_6O_3) \bullet C_2H_3N$
Formula Weight [g mol^{-1}]	156.12	172.12	172.12	250.25	385.30
Temperature [K]	150	150	150	150	150
Crystal System	monoclinic	triclinic	monoclinic	triclinic	monoclinic
Space Group	$P\,2_1/c$	$P\bar{1}$	$P\,2_1/c$	$P\bar{1}$	$C2/c$
a [Å]	4.6115 (11)	6.6850 (5)	5.0535 (3)	5.4545 (2)	16.754 (4)
b [Å]	16.953 (4)	8.7556 (6)	5.3907 (3)	9.4042 (3)	12.645 (2)
c [Å]	7.4329 (19)	11.9207 (8)	22.3375 (11)	10.8334 (5)	7.1381 (15)
α [°]	90	79.812 (3)	90	98.907 (2)	90
β [°]	100.679 (10)	81.840 (3)	93.131 (4)	102.005 (2)	95.214 (11)
γ [°]	90	69.876 (3)	90	99.824 (1)	90
V [Å3]	571.0 (2)	642.32 (8)	607.61 (6)	525.03 (4)	1506.0 (5)
Z	4	4	4	2	4
ρ [g cm^{-3}] [150 K]	1.816	1.780	1.882	1.583	1.699
R1 /wR2 (all data)	0.1265/0.1858	0.0463/0.1373	0.0376/0.1043	0.0476/0.1215	0.0383/0.1019
R2/wR2 (I>2σ)	0.0707/0.1612	0.0430/0.1337	0.0359/0.1024	0.0442/0.1181	0.0355/0.0990
S	1.01	1.12	1.14	1.07	1.04
No. of reflec.	1408	2587	1308	2140	1455
Restraints	0	0	0	0	0
CCDC[a]	2057283	2057287	2057284	2057286	2057285

[a]These data can be obtained free of charge from The Cambridge Crystallographic Data Centre via www.ccdc.cam.ac.uk/data_request/cif.

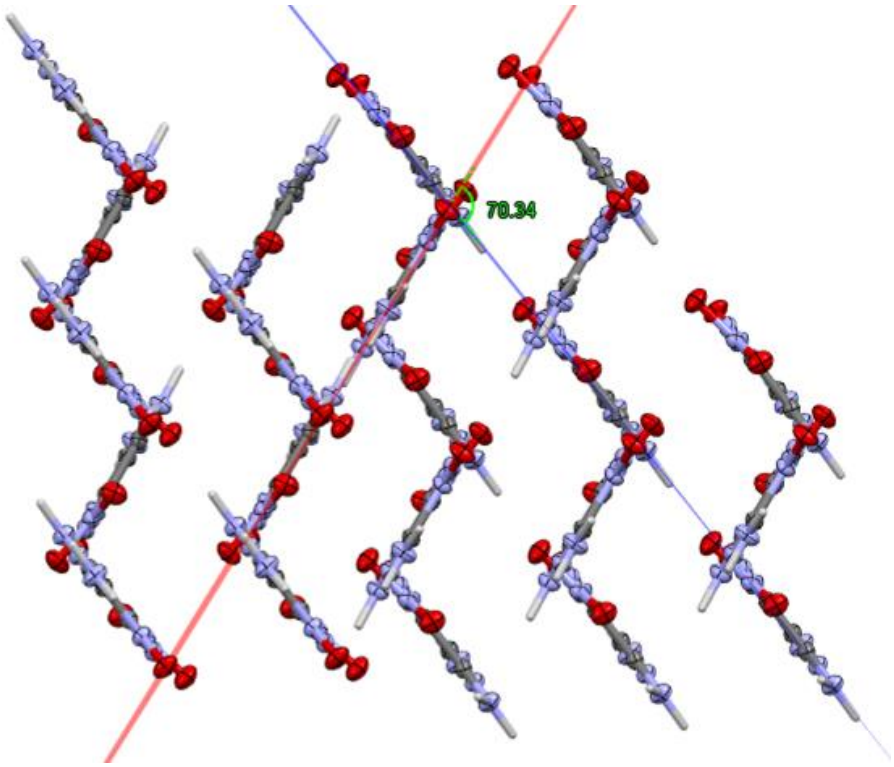

Appendix B: Figure 6-1. Ribbon rotation for mixed crystal structure of high-density DANTX

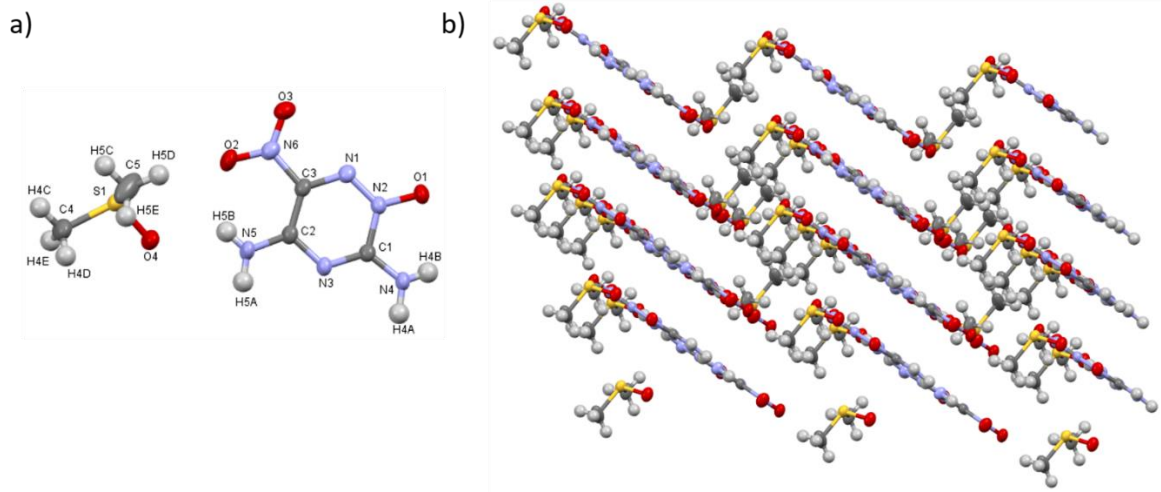

Appendix B: Figure 6-2. a) DMSO solvated-crystal X-ray structure of DANTX; b) Packing diagram of DANTX●DMSO solvated crystal

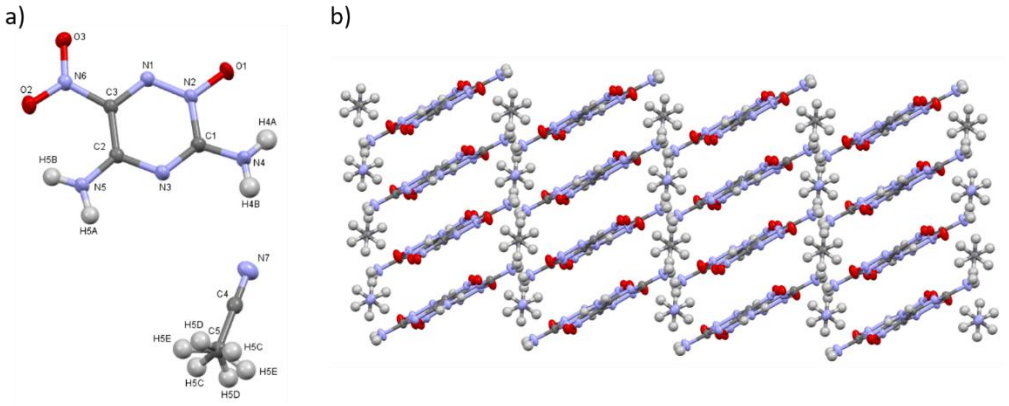

Appendix B: Figure 6-3 . a) MeCN solvated-crystal X-ray structure of DANTX; b) Packing diagram of DANTX●1/2MeCN solvated crystal

Crystals of **(1), (2•H_2O), (3•$2H_2O$), (4•H_2O), (5),** and **(6)** were analyzed with a Bruker Quest diffractometer with a fixed chi angle, a Mo Kα wavelength (λ=0.71073 Å) fine focus sealed X-ray tube, single-single crystal curved graphite incident beam monochromator, a PhontonII charge-integrating pixel array detector. The instrument was equipped with an Oxford Cryosystems low-temperature device and examination and data collection were performed at 150 K. Additional data was collected at room temperature for **(5)** due to structural rearrangement upon cooling. After data collection, reflections were indexed and processed, and the files scaled and corrected for absorption using APEX3 [1] and SADABS [2]. The space groups were assigned using XPREP within the SHELXTL suite of programs[3-4] and solved by direct methods using ShelXS [4] or ShelXT [5] and refined by full matrix least squares against F^2 with all reflections using Shelxl2018 [6-7] using the graphical interface Shelxle [8]. H atoms were treated by a mixture of independent and constrained refinement. C-H bond distances were constrained to 0.95 Å for aromatic C-H moieties, and to 0.98 Å for CH_3 moieties, respectively. Amine N-H bond distances were refined. For **(5)** the N-H distances were restrained to a target value of 0.88(2) Å. Water H atom positions were refined and O-H distances were restrained to 0.84(2) Å. U_{iso}(H) values were set to 1.2 or 1.5 times U_{eq}(C/O/N).

For **(5)** at room temperature, the perchlorate ion was refined as disordered by rotation. It was refined with two moieties. Apparent additional minor disorder was not modelled. The two disordered moieties were restrained to have similar geometries. U^{ij} components of ADPs for disordered atoms closer to each other than 2.0 Å were restrained to be similar. Subject to these conditions the occupancy ratio refined to 0.577(18) to 0.423(18).

Upon cooling to 150 K the structure undergoes a reversible single crystal to single crystal phase transformation with quadrupling of the shortest axis (the b-axis in the room temperature setting) and reduction in symmetry to monoclinic space group *Pc* (the glide plane along the 15 Angstrom axis is retained). The structure is then modulated, being based on the orthorhombic room temperature structure with a quarter of the volume (space group $Pna2_1$, a = 15.3040(6), b = 6.6472(3), c = 9.7259(4)). The monoclinic structure was found to be twinned by pseudomerohedry, emulating the orthorhombic setting. Application of the twin transformation matrix 1 0 0, 0 -1 0, 0 0 -1 yielded close to perfect twinning (twin ratio 0.503(2) to 0.497(2)). One of the eight

independent ion pairs was refined as disordered (cation E and anion B). A common occupancy ratio was used. The perchlorate ion was refined as disordered by rotation. The two disordered moieties were restrained to have similar geometries as another not disordered anion (moiety A). Oxygen atom O5B/I was omitted from the disorder. U^{ij} components of ADPs for disordered atoms closer to each other than 2.0 Å were restrained to be similar.

The cation perchlorate ion was refined as disordered by a slight twist motion. The two disordered moieties were restrained to have similar geometries as another not disordered cation (moiety A). ADPs of the minor moiety were constrained to be identical to those of another cation related to the minor moiety by close to perfect translation (cation H). U^{ij} components of ADPs for disordered atoms closer to each other than 2.0 Å were restrained to be similar, and ADPs were restrained to be close to isotropic. Subject to these conditions the occupancy ratio refined to 0.649(7) to 0.351(7).

Amine N-H bond distances were restrained to a target value of 0.88(2) Å. All H...H distances within amine moieties for each type of amine were restrained to be similar to each other (SADI restraint, esd 0.02 Å squared). Distances to the second next atom (i.e. H-N-C and H-N-N angles) were restrained to be similar for each type of amine (SADI restraint, esd 0.02 Å squared).

[1] Bruker, Madison (WI), USA, **2019**.
[2] L. Krause, R. Herbst-Irmer, G. M. Sheldrick, D. Stalke, Comparison of silver and molybdenum microfocus X-ray sources for single-crystal structure determination *Journal of Applied Crystallography* **2015**, *48*, 3-10.doi:10.1107/S1600576714022985
[3] Bruker Advanced X-ray Solutions, Bruker AXS Inc., Madison, Wisconsin: USA **2000-2003**.
[4] G. Sheldrick, A short history of SHELX *Acta Crystallographica Section A* **2008**, *64*, 112-122.doi:10.1107/S0108767307043930
[5] G. Sheldrick, SHELXT - Integrated space-group and crystal-structure determination *Acta Crystallographica Section A* **2015**, *71*, 3-8.doi:10.1107/S2053273314026370
[6] G. Sheldrick, Crystal structure refinement with SHELXL *Acta Crystallographica Section C* **2015**, *71*, 3-8.doi:10.1107/S2053229614024218
[7] G. M. Sheldrick, *University of Göttingen, Germany* **2018**
[8] C. B. Hübschle, G. M. Sheldrick, B. Dittrich, ShelXle: a Qt graphical user interface for SHELXL *Journal of Applied Crystallography* **2011**, *44*, 1281-1284.10.1107/s0021889811043202

Appendix B: Table 6-2 . Crystallographic data for DANTA triazinium salts

Crystal	**(1)**	**(2)**	**(3)**	**(4)**	**(6)**	**(5)**	
Formula	$C_3H_6N_7O_2$• $C_7H_7O_3S$	$C_3H_6N_7O_2$• Cl•H_2O	$2(C_3H_6N_7O_2)$• $C_2N_8O_2$•$2(H_2O)$	$C_3H_6N_7O_2$• NO_3•H_2O	$C_3H_6N_7O_2$• CN_5O_2	$C_3H_6N_7O_2$•ClO_4	
Formula Weight	343.33	225.61	548.43	252.17	286.21	271.6	
Temperature [K]	150	150	150	150	150	150	294
Crystal System	monoclinic	monoclinic	triclinic	monoclinic	monoclinic	monoclinic	orthorhombic
Space Group	$P2_1/c$	$P2_1/n$	$P\bar{1}$	$P2_1$	$P2_1/c$	Pc	$Pna2_1$
a [Å]	6.0873 (13)	6.6155(7)	6.5709(5)	7.0074(4)	7.1930(2)	9.736(3)	15.3040(6)
b [Å]	32.140 (9)	8.5919(9)	8.7936(6)	8.8221(7)	8.3499(3)	26.348(7)	6.6472(3)
c [Å]	8.0134 (10)	15.2366(14)	8.9143(7)	15.6773(12)	18.2515(6)	15.010(2)	9.7259(4)
α [°]	90	90	89.982(4)	90	90	90	90
β [°]	111.742 (13)	98.324(6)	84.843(4)	99.353(3)	100.8545(13)	90.039(16)	90
γ [°]	90	90	87.448(4)	90	90	90	90
V [Å^3]	1456.3 (5)	856.92(15)	512.49(7)	956.29(12)	1076.59(6)	3850.7(16)	989.40(7)
Z	4	4	1	4	4	16	4
ρ(calc) [g cm^{-3}]	1.566	1.749	1.777	1.752	1.766	1.874	1.823
R_1 /wR_2 (all data)	0.0559/0.1078	0.0859/0.1005	0.0517/0.1054	0.0692/0.1009	0.0362/0.0904	0.0761/0.0965	0.0507/0.1014
R_2/wR_2 (I>2σ)	0.0383/0.0992	0.0472/0.0887	0.0353/0.0970	0.0417/0.0908	0.0317/0.0876	0.0412/0.0818	0.0342/0.0916
S	1.047	1.034	1.036	1.031	1.041	1.001	1.078
No. of reflec.	4600	2622	3694	6461	4068	27575	3902
Restraints	0	0	0	1	0	1412	161
CCDC	2157073	2157069	2157068	2157072	2157067	2157070	2157071

TITANIUM SUPEROXIDE FOR THE OXIDATION OF AMINES: SYNTHESIS OF BIS(3-NITRO-1H-1,2,4-TRIAZOL-5-YL)METHANE AND ITS METAL SALTS

Single crystal X-ray data for the sodium salt had been collected on a Bruker Quest diffractometer with kappa geometry, an I-μ-S microsource X-ray tube, laterally graded multilayer (Goebel) mirror single crystal for monochromatization, a Photon-III C14 area detector. Examination and data collection were performed with Cu Kα radiation (λ = 1.54178 Å). Single crystal X-ray data for all other compounds analyzed were collected on a Bruker Quest diffractometer with a fixed chi angle, a sealed tube fine focus X-ray tube, single crystal curved graphite incident beam monochromator, a Photon II area detector. Examination and data collection were performed with Mo Kα radiation (λ = 0.71073 Å). Both instruments were equipped with an Oxford Cryosystems low temperature device and examination and data collection were performed at 150 K. Data were collected, reflections were indexed and processed, and the files scaled and corrected for absorption using APEX3 [1] and SADABS [2]. The space groups were assigned using XPREP within the SHELXTL suite of programs [3-4] and solved by direct methods using ShelXS [4] or ShelXT [5] and refined by full matrix least squares against F^2 with all reflections using Shelxl2018 [6-7] using the graphical interface Shelxle [8]. H atoms attached to carbon atoms were positioned geometrically and constrained to ride on their parent atoms.

In the structure of the strontium complex, an area of not-metal coordinated water molecules is extensively disordered. Water molecules are located in an elongated cylindrically shaped space surrounded by metal coordinated well defined water molecules and nitro groups that act as hydrogen bonding acceptors. The center of the water occupied space hosts a crystallographic inversion center. The partially occupied water molecule at the terminal end of the cylinder is associated with another water molecule close to the center of inversion (O14 and O15, respectively), and they are hydrogen bonded to each other. The other water molecules were refined as disordered over three mutually incompatible positions (O11, O12 and O13) hydrogen bonded to nitro and coordinated water molecules, but not to each other. U^{ij} components of ADPs for disordered atoms closer to each other than 2.0 Å were restrained to be similar. Occupancies were constrained to full occupancy for the disordered site. One well defined metal coordinated water molecule (O8) is hydrogen bonded to its own symmetry equivalent across an inversion center, thus inducing 1:1 disorder of one of its H atoms. All water H atom positions were initially refined and

O-H and H...H distances were restrained to 0.84(2) and 1.36(2) Å, respectively, while a damping factor was applied. Some water H atom positions were further restrained based on hydrogen bonding considerations. In the final refinement cycles H atoms attached to disordered water molecules were set to ride on their carrier atoms and the damping factor was removed. Subject to these conditions the occupancy rates for the disordered water molecules refined to 0.338(3) (O11), 0.360(3) (O12), 0.133(3) (O13), and 0.169(3) (O14 and O15).

Densities at room temperature were determined using the same instruments and crystals as for the whole data collection at 150 K. For accurate unit cell determinations one 180° phi scan at theta = 0° (Mo Kα radition) or at theta = 55° (Cu Kα) were collected for each single crystalline compound. Data were indexed and integrated using APEX3 and the obtained unit cell parameter were used to determine the crystal density.

Appendix B: Table 6-3. Crystallographic data for BNTM and the cesium, sodium, and strontium salts

Crystal	BNTM	Cesium Salt	Sodium Salt	Strontium Salt
Formula	$C_5H_4N_8O_4$	$C_5H_6Cs_2N_8O_6$	$C_5H_8N_8Na_2O_7$	$C_5H_{12}N_8O_9Sr{\cdot}2.169(H_2O)$
Formula Weight [g mol^{-1}]	240.16	540.00	338.17	454.93
Temperature [K]	150	150	150	150
Crystal System	orthorhombic	monoclinic	monoclinic	triclinic
Space Group	*Fdd*2	*C*2/*c*	*C*2/*c*	$P\bar{1}$
a [Å]	10.1167 (5)	15.6648(7)	14.1217(7)	6.7354(7)
b [Å]	13.6132 (6)	7.4707(3)	9.4525(5)	9.2547(8)
c [Å]	13.6274 (7)	13.6087(6)	11.0697(6)	13.5219(12)
α [°]	90	90	90	95.192(4)
β [°]	90	121.5680(12)	122.3730(11)	100.151(4)
γ [°]	90	90	90	97.299(4)
V [Å^3]	1876.77(16)	1356.91(10)	1247.99(11)	817.44(13)
Z	8	4	4	2
ρ [g cm^{-3}] [150 K]	1.7	1.643	1.8	1.848
R1 /wR2 (all data)	0.0517/0.1156	0.0205/0.0460	0.0402/0.1102	0.0496/0.0730
R2/wR2 (I>2σ)	0.0426/0.1069	0.0200/0.0458	0.0397/0.1100	0.0352/0.0682
S	1.032	1.224	1.199	1.068
No. of reflec.	2074	2588	1340	6272
Restraints	1	0	0	125
CCDC[a]		2132933	2132934	2132935

[a]These data can be obtained free of charge from The Cambridge Crystallographic Data Centre via www.ccdc.cam.ac.uk/data_request/cif.

References for Appendix B

[1] Bruker, Madison (WI), USA, **2019**.

[2] L. Krause, R. Herbst-Irmer, G. M. Sheldrick, D. Stalke, Comparison of silver and molybdenum microfocus X-ray sources for single-crystal structure determination *Journal of Applied Crystallography* **2015**, *48*, 3-10.doi:10.1107/S1600576714022985

[3] Bruker Advanced X-ray Solutions, Bruker AXS Inc., Madison, Wisconsin: USA **2000-2003**.

[4] G. Sheldrick, A short history of SHELX *Acta Crystallographica Section A* **2008**, *64*, 112-122.doi:10.1107/S0108767307043930

[5] G. Sheldrick, SHELXT - Integrated space-group and crystal-structure determination *Acta Crystallographica Section A* **2015**, *71*, 3-8.doi:10.1107/S2053273314026370

[6] G. Sheldrick, Crystal structure refinement with SHELXL *Acta Crystallographica Section C* **2015**, *71*, 3-8.doi:10.1107/S2053229614024218

[7] G. M. Sheldrick, *University of Göttingen, Germany* **2018**

[8] C. B. Hübschle, G. M. Sheldrick, B. Dittrich, ShelXle: a Qt graphical user interface for SHELXL *Journal of Applied Crystallography* **2011**, *44*, 1281-1284.10.1107/s0021889811043202